The PHILOSOPHICAL MAGAZINE

FIRST PUBLISHED IN 1798

1 Eighth Series No. 6 June 1956

A Journal of Theoretical Experimental and Applied Physics

PRICE 15s. 0d.

Annual Subscription £8 0s. 0d. payable in advance

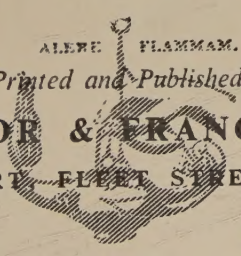

Printed and Published by

TAYLOR & FRANCIS LTD.

RED LION COURT, FLEET STREET, LONDON, E.C.4

Journal of Fluid Mechanics

Contents of July, 1956

Price per part £1

Price per annum £5 10s. post free

Printed and Published by

TAYLOR & FRANCIS LTD

RED LION COURT, FLEET STREET, LONDON, E.C.4

CONTENTS OF No. 6.

**All communications for the Philosophical Magazine should be addressed, post-paid, to the Editors, c/o Messrs. Taylor and Francis, Ltd., Red Lion Court, Fleet Street, London, England.

LI. *The Strength of Lomer–Cottrell Sessile Dislocations*

By A. N. Stroh
Cavendish Laboratory, Cambridge† ‡

[Received December 21, 1955]

A Lomer–Cottrell sessile dislocation at the head of a piled-up group of dislocations may give way under the combined action of stress and temperature. Depending on its orientation relative to the group, the dislocation may yield either by recombining and slipping on a (100) plane or by dissociating into the two dislocations from which it was formed. The size of the group required for both these mechanisms is obtained as a function of stress, but the results depend rather sensitively on the structure of the dislocation core.

§ 1. Introduction

Lomer (1951) has pointed out that, in a face-centred cubic crystal, two dislocations in different slip planes can attract one another and combine ; thus the dislocation with Burgers vector $\frac{1}{2}a\,[10\bar{1}]$ in the plane (111) can react with the dislocation $\frac{1}{2}a\,[011]$ in $(11\bar{1})$ giving

$$\tfrac{1}{2}a\,[10\bar{1}]+\tfrac{1}{2}a\,[011]\rightarrow\tfrac{1}{2}a\,[110]. \quad . \quad . \quad . \quad . \quad . \quad (1)$$

The dislocations must all be parallel to the line of intersection of the slip planes, i.e. to the line $[1\bar{1}0]$, and so the resulting dislocation $\frac{1}{2}a\,[110]$ has as slip plane, the plane (001). Cottrell (1952) then remarked that the dislocation $\frac{1}{2}a\,[110]$ could dissociate :

$$\tfrac{1}{2}a\,[110]\rightarrow\tfrac{1}{6}a\,[11\bar{2}]+\tfrac{1}{6}a\,[110]+\tfrac{1}{6}a\,[112]\,; \quad . \quad . \quad . \quad (2)$$

these three dislocations are all imperfect and when they separate they will be linked by two strips of stacking fault. This group of three dislocations will be unable to glide and will form an obstacle in the slip plane against which further dislocations can pile-up. If the original dislocations were dissociated into partial dislocations,

$$\left.\begin{aligned}\tfrac{1}{2}a\,[10\bar{1}]&\rightarrow\tfrac{1}{6}a\,[11\bar{2}]+\tfrac{1}{6}a\,[2\bar{1}\bar{1}],\\ \tfrac{1}{2}a\,[011]&\rightarrow\tfrac{1}{6}a\,[112]+\tfrac{1}{6}a\,[\bar{1}21],\end{aligned}\right\} \quad . \quad . \quad . \quad . \quad . \quad (3)$$

the sessile dislocation may be formed by the direct combination of the second dislocation of each pair

$$\tfrac{1}{6}a\,[2\bar{1}\bar{1}]+\tfrac{1}{6}a\,[\bar{1}21]\rightarrow\tfrac{1}{6}a\,[110]\,; \quad . \quad . \quad . \quad . \quad . \quad (4)$$

† Now at Department of Physics, University of Sheffield.
‡ Communicated by the Author.

the two remaining partial dislocations are linked to this by strips of stacking fault giving the same set of three dislocations as before. We note that all three dislocations making up the sessile are of pure edge type.

Other possible combinations of dislocations have been considered by Friedel (1955) who finds, however, that either the short range interaction is not such as to lead to a stable complex, or there is no long range attraction so that the dislocations are unlikely to meet. Thus the reaction discussed above appears to be the only one of importance.

The observation of work softening in aluminium single crystals, that is a decrease in the flow stress when a specimen first deformed at one temperature is further strained at a higher temperature, has led Cottrell and Stokes (1955) to suggest that the sessile dislocation may give way under the combined action of stress and temperature. There will then be a limit to the size of the piled-up group of dislocations which can be formed against a sessile dislocation at any temperature, and raising the temperature will cause piled-up groups formed at the lower temperature to break up so that their contribution to the work hardening is lost. Friedel (1955) has also

Fig. 1

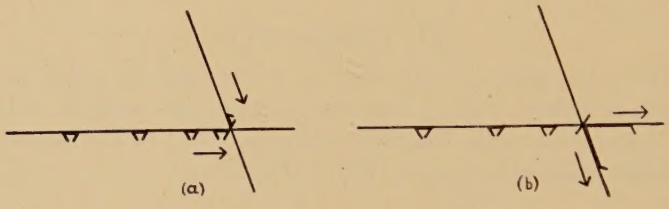

Sessile with its apex (*a*) away from the pile-up (narrow stacking fault) and (*b*) towards the pile-up (broad stacking fault).

suggested that the sessile dislocation may give way, and has interpreted the change from linear to parabolic hardening observed in copper single crystals by Blewitt *et al.* (1955) in terms of this. In the present paper an attempt is made to estimate the size of the piled-up group which the sessile dislocation can withstand.

§ 2. General Considerations

The piled-up group may be formed on either side of the sessile dislocation, so that the latter may have its apex pointing either away from the group as in fig. 1 (*a*), or towards the group as in fig. 1 (*b*). The arrows indicate the directions in which the stresses tend to move the partial dislocations forming the sessile dislocation ; thus the stacking fault will be narrow in the first case, wide in the second.

If the dislocations are recombined by the reverse of reaction (2), and then allowed to dissociate again, the sessile dislocation may be converted from one arrangement to the other ; the stress will clearly favour the dislocation's pointing towards the group. The large activation energy

needed to combine the dislocations over a finite length can be avoided by the sequence shown in fig. 2. This represents successive positions of two of the three partial dislocations forming the sessile dislocation, the stacking fault between them being shaded. Of the dislocations, one, that with Burgers vector $\frac{1}{6}a$ [110], is constrained to lie along the line of intersection of the two slip planes ; the other, $\frac{1}{6}a$ [11$\bar{2}$] or $\frac{1}{6}a$ [112], then crosses over it as shown. By repeating this process on the other slip plane the sessile dislocation can turn its apex towards the group. It is easily seen that the activation energy needed is less than twice the energy of a constriction W_{constr}. For dislocations of this type, the latter has been estimated by Stroh (1954) to be

$$W_{\text{constr}} = 2{\cdot}5 \times 10^{-2}\, \mu a^2 d\, (\log d/r_0)^{1/2}, \qquad (5)$$

where μ is the rigidity modulus and r_0 the radius of the dislocation core ; d is the distance between the dislocations and depends on the stress. This activation energy will be found to be small compared with that required for the sessile dislocation to give way ; hence before this happens the dislocation should have turned its apex towards the piled-up group.

Fig. 2

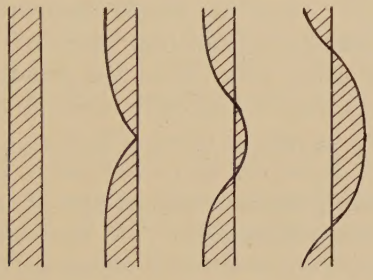

In the initial uniform ribbon of stacking fault (*a*), a constriction is formed (*b*) ; this develops into a small loop where the dislocations have crossed over (*c*), and the length of this portion increases (*d*).

When the partial dislocations cross over, the stacking fault will change from intrinsic (with the sequence of close packed planes abc ¦ bcabc . . . .) to extrinsic (abc ¦ b ¦ abca . . . .) or vice versa (Frank 1951, Frank and Nicholas 1953). These both have all nearest neighbour relationships correct, and the same number of incorrect second nearest neighbour relationships ; thus they may be expected to differ only slightly in energy. Since the stress due to the piled-up group will be found comparable to that required to extend the stacking fault by widely separating the partial dislocations, it should be quite great enough to overcome any small difference in stacking fault energies. Also any possible change in the core energy of the dislocations should be unimportant. On the other hand, the intrinsic stacking fault involves a break in the correct stacking sequence

across one plane, the extrinsic across two, and the possibility that the conversion is more difficult than energy considerations alone suggest cannot be entirely ruled out. In this case the sessile dislocation may give way from either position.

Summing up, we may say that if the change from intrinsic to extrinsic stacking fault can take place with reasonable ease, the sessile dislocations should all turn their apices towards the piled-up group and give way from this position ; but if the change in stacking fault cannot occur there will be two types of dislocation lock, which we may expect to be of different strengths.

The sessile dislocation may give way in either of two ways. First, the dislocations may recombine, the reverse of reaction (2), giving a perfect dislocation with Burgers vector $\frac{1}{2}a$ [110] which can then glide away on the (001) plane.† Though this is not the slip-plane usually observed, Boas and Schmid (1931) have reported slip on it in aluminium at high temperatures. This mechanism will be easier when the sessile dislocation points away from the piled-up group, as then the partial dislocations are close together and their energy of recombination is less.

Secondly, the sessile dislocation may dissociate into the two dislocations from which it was originally formed, which can then glide away on their respective slip planes. When the sessile dislocation points towards the piled-up group the dissociation can take place by the reverse of reaction (4) ; but if it should point away from the group the dislocations must first be recombined (by the reverse of 2) and then dissociated (the reverse of 1), and so the break up will be more difficult.

Failure by recombination will be considered in § 4, and by dissociation in § 5. In the following section, the energy of recombination per unit length of the dislocation is found.

§ 3. Energy of Recombination

To obtain this we must first find the stresses due to the piled-up group. We shall need only the stresses at the position of the sessile dislocation ; these are readily found by a simple argument. Take y axis normal to the plane of the group, the (111) plane, and z axis parallel to the dislocation lines, the [1$\bar{1}$0] direction. The Burgers vectors **b** of the dislocations may be resolved into edge components b_x, and screw components b_z. All the components of stress at a point in the slip plane due to any one dislocation are zero except σ_{xy} and σ_{yz} ; and these are in the ratio

$$\sigma_{xy}/\sigma_{yz}=b_x/(1-\nu)\,b_z, \qquad \ldots\ldots\ldots \quad (6)$$

where ν is Poisson's ratio. This must also be true for the resultant stress due to the whole group. For the purpose of calculating the stress, suppose the sessile dislocation to be replaced by a dislocation similar to those of the group ; the group produces on it a force $b_x\,\sigma_{xy}+b_z\,\sigma_{yz}$. If there are

† This was suggested by Professor F. C. Frank.

n dislocations piled up under a resolved shear stress σ_0 then according to Cottrell (1949), this force is $nb\sigma_0$, or

$$b_x \sigma_{xy}+b_z \sigma_{yz}=nb\sigma_0. \quad \ldots\ldots\ldots \quad (7)$$

Solving (6) and (7) we obtain

$$\left.\begin{aligned}\sigma_{xy}&=\frac{b_x bn\sigma_0}{b_x^2+(1-\nu)\,b_z^2},\\ \sigma_{yz}&=\frac{(1-\nu)\,b_z\,bn\sigma}{b_x^2+(1-\nu)\,b_z^2}.\end{aligned}\right\} \quad \ldots\ldots\ldots \quad (8)$$

With $\mathbf{b}=\frac{1}{2}a\,[10\bar{1}]=\frac{1}{4}a\,[11\bar{2}]+\frac{1}{4}a\,[1\bar{1}0]$, eqns. (8) reduce to

$$\sigma_{xy}=2\sqrt{3}n\sigma_0/(4-\nu), \quad \sigma_{yz}=2(1-\nu)n\sigma_0/(4-\nu). \quad \ldots \quad (9)$$

We also need the stresses on the $(11\bar{1})$ plane ; using dashes to denote corresponding quantities for this plane, we obtain by the usual transformation

$$\sigma_{x'y'}=\tfrac{7}{9}\sigma_{xy}, \quad \sigma_{y'z}=\tfrac{1}{3}\sigma_{yz}. \quad \ldots\ldots \quad (10)$$

The stresses (9) lead to a force per unit length on the dislocation $\frac{1}{6}a\,[11\bar{2}]$ of $\sqrt{2}\,n\sigma_0\,a/(4-\nu)$, while (10) gives a force $7\sqrt{2}n\sigma_0 a/9(4-\nu)$ on $\frac{1}{6}a\,[11\bar{2}]$. If the widths of the two ribbons of stacking fault are $d(1-\xi)$ and $d(1+\xi)$, so that d is the mean width, then the energy per unit length due to the stress and to the stacking fault energy γ is

$$2\gamma d \pm 16\sqrt{2}\,n\,\sigma_0\,ad\,(1-\tfrac{1}{8}\xi)/9\,(4-\nu)\,, \quad \ldots\ldots \quad (11)$$

where the positive or negative sign must be taken according as the stress tends to decrease or increase the width of the stacking fault, that is according as the apex of the sessile dislocation points away from or towards the piled-up group. To (11) we must add the energy of interaction of the dislocations.

Now according to Nabarro (1952) the energy per unit length of two edge dislocations with Burgers vectors $\mathbf{b}'$ and $\mathbf{b}''$ separated by a vector $\mathbf{r}$ is

$$-\frac{\mu}{2\pi\,(1-\nu)}\left\{\mathbf{b}'\,.\,\mathbf{b}''\log\frac{r}{r_0}-\frac{(\mathbf{b}'\,.\,\mathbf{r})(\mathbf{b}''\,.\,\mathbf{r})}{r^2}\right\}. \quad \ldots \quad (12)$$

Summing contributions of this form, we find the energy of interaction of the three partial dislocations of the sessile dislocation is,

$$-\frac{\mu a^2}{36\pi\,(1-\nu)}\left\{\log\frac{d}{r_0}+\tfrac{1}{2}\log\frac{1+2\xi^2}{(1-\xi^2)^2}-\frac{6\xi^2}{1+2\xi^2}\right\}, \quad \ldots \quad (13)$$

where a constant has been added so that the energy is zero when the dislocations are recombined. If $\xi \ll 1$, (13) becomes

$$-\frac{\mu a^2}{36\pi\,(1-\nu)}\left\{\log\frac{d}{r_0}+4\xi^2+O(\xi^4)\right\}. \quad \ldots \quad (14)$$

The total energy is the sum of (11) and (14); differentiating this sum with respect to d, we find the energy to be a minimum when

$$d=\frac{\mu a^2}{36\pi\,(1-\nu)}\left\{2\gamma\pm\frac{16\sqrt{2}}{9\,(4-\nu)}n\sigma_0\,a\,(1-\tfrac{1}{8}\,\xi)\right\}^{-1}. \quad . \quad . \quad (15)$$

The corresponding value of the energy is

$$-T'=-\frac{\mu a^2}{36\pi\,(1-\nu)}\left(\log\frac{d}{r_0}+4\xi^2-1\right). \quad . \quad . \quad . \quad . \quad (16)$$

We have now to vary ξ so as to minimize (16). When the upper sign in (15) is taken we find that for all values of $n\sigma_0$, $\xi\leqslant 1/64$; thus not only is our original assumption that $\xi\ll 1$ justified, but we may also to a good approximation neglect all terms in ξ. Terms in ξ may also be neglected, though to a less good approximation, when the lower sign in (14) is taken provided $n\sigma_0 a$ is small compared with γ. Since the stacking fault on (111) becomes infinitely wide (or rather the dislocation $\frac{1}{6}a$ [11$\bar{2}$] is displaced a large distance from the piled-up group to where the stress is less than the value (9)), when

$$\sqrt{2}n\sigma_0 a/(4-\nu)=\gamma, \quad . \quad . \quad . \quad . \quad . \quad . \quad . \quad (17)$$

the condition implies that the dislocations must not be too widely separated by the stress of the group if it is not fulfilled the energy of recombination becomes so large that the process is no longer of interest. Neglecting ξ, we may write the energy of recombination

$$T'=\{\mu a^2/36\pi\,(1-\nu)\}\,L_1, \quad . \quad . \quad . \quad . \quad . \quad . \quad (18)$$

where

$$L_1=\log\,(d/r_0)-1\,.$$

When the stress is so large that d is comparable to the radius of the core r_0, this expression cannot hold, as T' must always be positive if the extended state is stable. The difficulty arises because the interaction between the dislocations is no longer given correctly by elastic theory at short distances. If, to ensure that the force between two dislocations remains finite, we assume it varies as $(r^2+\zeta^2)^{-1/2}$ where ζ is a constant length (the *width* of the dislocation), instead of as r^{-1}, then in the expression for the energy (12), we must replace $\log\,(r/r_0)$ by $\log\,\{r+(r^2+\zeta^2)^{1/2}\}/\zeta$. With this the width of the stacking fault is given by

$$(d^2+\zeta^2)^{1/2}=\{\mu a^2/72\pi\,(1-\nu)\}\,(\gamma\pm 0{\cdot}343n\,\sigma_0\,a)^{-1}\,,$$

and the energy of recombination per unit length is still given by (18), but where now

$$L_1=\log\,\{d+(d^2+\zeta^2)^{1/2}\}/\zeta-d/(d^2+\zeta^2)^{1/2}\,;$$

if η is defined by

$$\cosh\eta=(d^2+\zeta^2)^{1/2}/\zeta=\frac{0{\cdot}066\,a/\zeta}{(\gamma/\mu a)\pm 0{\cdot}343\,(n\sigma_0/\mu)}, \quad . \quad . \quad . \quad (19)$$

then

$$L_1=\eta-\tanh\eta. \quad . \quad . \quad . \quad . \quad . \quad . \quad . \quad . \quad (20)$$

The stacking fault energy γ has according to Seeger and Schoeck (1953) the values 200 erg/cm^2 for aluminium, and 40 erg/cm^2 for copper ; the dimensionless quantity $\gamma/\mu a$ then becomes $1{\cdot}86\times10^{-2}$ for aluminium, and $0{\cdot}24\times10^{-2}$ for copper. On account of the high value for aluminium, the width of the stacking fault will be narrow ; if the dislocation width ζ is greater than $0{\cdot}35a$, (19) indicates that the dislocation will be completely recombined even in the absence of any applied stress. As the dislocation will not then be sessile, we must suppose $\zeta<0{\cdot}35a$. On the other hand it seems unlikely that ζ will be much smaller than the Burgers vector which is $a/\sqrt{6}=0{\cdot}41a$. These considerations suggest that $0{\cdot}2a$ or $0{\cdot}3a$ are suitable choices for ζ. For copper larger values of ζ would still lead to an extended dislocation ; nevertheless in numerical calculations the same values will be used so that the results may more readily be compared.

Fig. 3

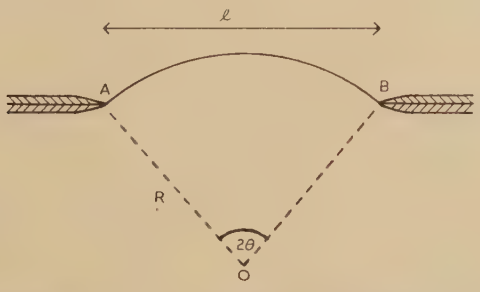

A dislocation recombined over a length l, and bowing out on a (100) plane.

§ 4. Failure by Recombination

Suppose that the dislocations are recombined over a length l ; this length of dislocation can then bow out on its slip plane, the (100) plane, in a manner reminiscent of a Frank–Read source. If σ' is the resolved shear stress on this plane, the radius of curvature R is given by

$$\sigma' a/\sqrt{2}=T/R \quad . \quad . \quad . \quad . \quad . \quad . \quad . \quad . \quad (21)$$

where $a/\sqrt{2}$ is the Burgers vector and T the line tension of the recombined dislocation. If the dislocation subtends an angle 2θ at its centre of curvature, the energy required to bow it out is made up of the following contributions :

(i) Twice the energy of a constriction, the factor 2 occurring since W_{constr} from (5) is the energy of a constriction in only one of the stacking fault ribbons ;

(ii) The energy of recombination of a length l, $T'l$;

(iii) The energy due to increase in length of the dislocation line, $T\,(2R\theta-l)$;

and (iv) minus the work done by the stress $(a/\sqrt{2})\sigma'\ (R^2\theta-\frac{1}{2}R^2\sin 2\theta)$.

Hence the total energy is

$$W_1 = 2W_{\text{constr}} + T'l + T\,(2R\theta - l) - (a/\sqrt{2})\,\sigma' R^2\,(\theta - \tfrac{1}{2}\sin 2\theta)$$
$$= 2W_{\text{constr}} + 2T'R\sin\theta + TR\,(\theta - 2\sin\theta + \tfrac{1}{2}\sin 2\theta), \quad . \quad . \quad . \quad . \quad . \quad (22)$$

on using (21) and $l = 2R\sin\theta$.

W_1 is a maximum for variations of θ when

$$\cos\theta = 1 - T'/T\,; \quad . \quad . \quad . \quad . \quad . \quad . \quad . \quad (23)$$

this gives a configuration of unstable equilibrium, and from this position the loop can grow without requiring further help from thermal fluctuations. Now the line tension T is

$$T = \{\mu a^2/8\pi\,(1-\nu)\}\log\,(R/r_0), \quad . \quad . \quad . \quad . \quad . \quad . \quad (24)$$

and comparing this with (18) we see $T'/T \ll 1$; then (23) gives approximately $\theta = (2T'/T)^{1/2}$. Substituting this in (22) we obtain the activation energy

$$W_1 = 2W_{\text{constr}} + 8T'^{3/2}\,T^{1/2}/3\sigma' a. \quad . \quad . \quad . \quad . \quad . \quad (25)$$

From the stresses (9) we obtain $\sigma' = \tfrac{1}{3}\sigma_{xy} = 2n\sigma_0/\sqrt{3}\,(4-\nu)$; then (18), (24) and (25) give

$$W_1 = 2W_{\text{constr}} + \frac{(4-\nu)\,\mu^2 a^3\,L_1^{3/2}\,L_2^{1/2}}{108\sqrt{6}\,\pi^2\,(1-\nu)^2\,n\sigma}$$
$$= 2W_{\text{constr}} + 3{\cdot}16\times 10^{-2}\,\mu a^3\,(\mu/n\sigma_0)\,L_1^{3/2}\,L_2^{1/2}, \quad . \quad . \quad (26)$$

where $$L_2 = \log\ R/r_0 \simeq \log\,(\mu/n\sigma_0). \quad . \quad . \quad . \quad . \quad . \quad . \quad . \quad . \quad . \quad (27)$$

The probability of the sessile dislocation's failing in time t is

$$\nu t\,(l/a)\exp\,(-W_1/kT),$$

where ν is an atomic frequency of vibration, and l the length of the dislocation, so that l/a is the number of points at which the breakaway can start. Equating this probability to unity we find the dislocation will give way when

$$W_1 = kT\log\,(\nu t l/a)\,; \quad . \quad . \quad . \quad . \quad . \quad . \quad . \quad (28)$$

with $\nu \sim 10^{12}$ sec $^{-1}$, $t \sim 10^3$ sec, $l/a \sim 10^4$, this is $W_1 = 44\,kT$.

From (26) and (28) the stress at which the sessile dislocation gives way may be found as a function of temperature ; results are shown in fig. 4, for the case in which the dislocation points away from the piled-up group. As typical results we may note that under a stress of 1 kg/mm^2 the maximum number of dislocations in the group varies for copper from about 150 at 300°K to 220 at 100°K ; for aluminium at the same two temperatures the numbers are 25 and 45.

When the dislocation points towards the group, the activation energy will be large for large stresses because the stacking fault is wide, and also for small stresses because the size of the critical loop is then large ; thus

there will be a minimum activation energy for which the dislocation can give way. For aluminium this minimum is 2·6 ev if $\zeta=0{\cdot}2a$ and 0·80 ev if $\zeta=0{\cdot}3a$, the corresponding temperatures according to (28) being 680°K and 210°K ; the possibility of the sessile dislocation's failing in this way thus depends very sensitively on the structure of the dislocation core. For copper, the greater width of the stacking fault leads to so great a value for the energy (of the order of 100 ev) that this mechanism can be altogether ruled out.

Fig. 4

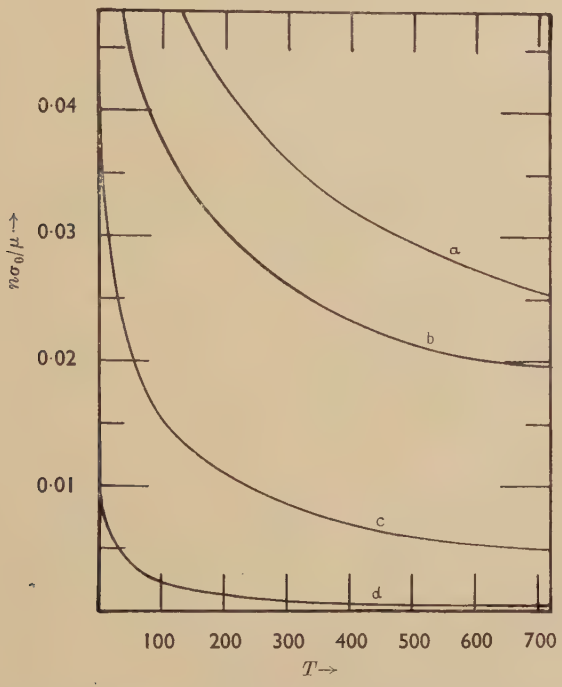

Stress at which the sessile gives way by recombination plotted as a function of temperature for two different values of the dislocation width ζ: (*a*) copper, $\zeta/a=0{\cdot}2$, (*b*) copper, $\zeta/a=0{\cdot}3$, (*c*) aluminium, $\zeta/a=0{\cdot}2$, (*d*) aluminium $\zeta/a=0{\cdot}3$.

§ 5. Failure by Dissociation

As was mentioned in § 2, the sessile dislocation can dissociate more easily when it points towards the piled-up group ; we shall suppose this to be the case. If the number of dislocations in the group is greater than indicated by eqn. (17), the dislocations $\frac{1}{6}a$ [11$\bar{2}$] and $\frac{1}{6}a$ [112] will be repelled to large distances, and so will not influence the dissociation of the dislocation $\frac{1}{6}a$ [110]. When this dissociates, by the reverse of reaction (4), work must be done in separating the two dislocations so formed, and the separation can take place most easily by first forming a small loop (fig. 5). Since forming such a loop involves doing work against the line tension, we expect the energy to be least when only one of the two dislocations deforms to any

great extent. The stress on $\frac{1}{6}a\,[2\bar{1}\bar{1}]$ is the greater, and so this is the dislocation which can deform more easily; the dislocation $\frac{1}{6}a\,[\bar{1}21]$ is assumed to remain straight and undeformed along the line $[1\bar{1}0]$, the z axis. The energy of the loop can be found by a method similar to that used by Stroh (1954) to obtain the energy of a constriction; this gave values of the constriction energy in good agreement with those obtained by Seeger and Schoeck (1955) by a variation method.

A small element of the dislocation $\frac{1}{6}a\,[2\bar{1}\bar{1}]$ of length δs at the point $P\,(x, z)$ is subjected to the following forces:

(i) A force due to the line tension $T\,(d^2x/dz^2)\delta s$ where

$$T=\frac{\mu a^2}{32\pi}\left\{1+\frac{1}{3\,(1-\nu)}\right\}\log\frac{R}{r_0}\;; \qquad \ldots\ldots \quad (29)$$

(ii) A force due to the attraction of the dislocation $\frac{1}{6}a\,[\bar{1}21]$ which we take to be $-A\delta s/(x^2+\zeta^2)^{1/2}$, where

$$A=(\mu a^2/16\pi)\{1+\tfrac{1}{9}\,(1-\nu)^{-1}\}\;; \qquad \ldots\ldots \quad (30)$$

and (iii) a force $F\delta s$ due to the stress and to the stacking fault where

$$F=\gamma+n\sigma_0 a\,(2-\nu)/\sqrt{2}(4-\nu), \qquad \ldots\ldots \quad (31)$$

and we have used the stresses (9).

The energy of the loop will be greatest when it is in a position of unstable equilibrium; for equilibrium the above forces give

$$T(d^2x/dz^2)-A(x^2+\zeta^2)^{-1/2}+F=0.$$

Integrating, we have

$$\tfrac{1}{2}T\,(dx/dz)^2=A\,\log\,\{x/\zeta+(1+x^2/\zeta^2)^{1/2}\}-Fx, \qquad \ldots \quad (32)$$

since $dx/dz=0$ when $x=0$. At the point $z=0$ at which the separation is greatest dx/dz is zero, so that the maximum separation x_m can be found by equating the right hand side of (32) to zero and solving for x; the result is plotted in fig. (6) as a function of $F\zeta/A$.

Now we have the following contributions to the energy of the loop:

(i) $\frac{1}{2}T\int(dx/dz)^2\,dz$ due to the line tension;

(ii) $A\int\log\,\{x/\zeta+(1+x^2/\zeta^2)^{1/2}\}\,dz$ due to the mutual attraction of the dislocations;

and (iii) $-F\int x\,dz$ due to the stress;

where in each case the integration extends over the whole length of dislocation which has dissociated. The total energy is then

$$W_2=\int[\tfrac{1}{2}T\,(dx/dz)^2+A\,\log\,\{x/\zeta+(1+x^2/\zeta^2)^{1/2}\}-Fx]\,dz$$

$$=2\,(2TA)^{1/2}\int_0^{x_m}[\log\,\{x/\zeta+(1+x^2/\zeta^2)^{1/2}\}-Fx/A]^{1/2}\,dx$$

on using (32). Substituting $x=\zeta\,\sinh\,u$ we obtain

$$W_2=2\,(2TA)^{1/2}\zeta\,f\,(F\zeta/A) \qquad \ldots\ldots \quad (33)$$

where

$$f\,(v)=\int_0^{u_m}(u-v\,\sinh\,u)^{1/2}\,\cosh\,u\,du$$

$$=\frac{1}{v}\int^{u_m}(u-v\,\sinh\,u)^{1/2}\,du, \qquad \ldots\ldots \quad (34)$$

and u_m is the positive value of u for which the integrand is zero ; the function $vf(v)$ is plotted in fig. 7. Equations (29), (30), (31) and (33) give, with $\nu = 1/3$,

$$W_2 = 5{\cdot}26 \times 10^{-2}\, \mu a^2 \zeta\, (\log x_m/\zeta)^{1/2}\, f(F\zeta/A), \quad . \; . \; . \quad (35)$$

and

$$F\zeta/A = \{43{\cdot}0\,(\gamma/\mu a) + 13{\cdot}8\,(n\sigma_0/\mu)\}(\zeta/a). \quad . \; . \; . \; . \; . \quad (36)$$

Fig. 5

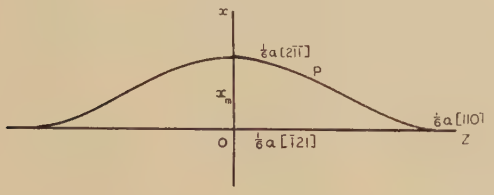

$\frac{1}{6}\,a$ [110] dislocation dissociated over a short length.

Fig. 6

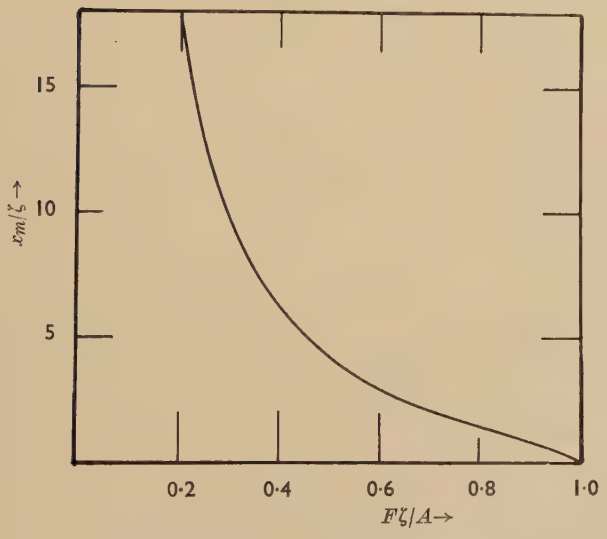

Size of critical loop as function of stress.

The above analysis holds provided the size of the critical loop is small compared with the width of the stacking fault. When numerical values are inserted, this is found to be so for copper for all stresses giving an activation energy of reasonable magnitude ; in this case we may determine the stress at which the sessile dislocation breaks down as a function of temperature from eqns. (28) and (35). For a metal with a high stacking fault energy such as aluminium this will only hold at high stresses (low temperatures) ; for lower stresses the size of the critical loop will be greater than the width of the stacking fault. If it is much greater than the

stacking fault width, we can neglect the dissociation into partial dislocations, and suppose the dislocation breaks up by the reverse of reaction (1). Then we may use the previous treatment and the energy is still given by eqn. (33) but where now

$$A=(\mu a^2/16\pi)\{1+1/(1-\nu)\}\,,$$
$$T=(\mu a^2/32\pi)\{1+3/(1-\nu)\}\log\,(x_m/\zeta'),$$
and $$F=n\sigma_0\,a/\sqrt{2}\,; \qquad \ldots\ldots\ldots\ldots \quad (37)$$

we do not assume ζ has the same value as before and so denote it now by ζ'. With $\nu=\frac{1}{3}$ we obtain the energy

$$W_2=0{\cdot}15\,\mu a^2\,\zeta'\,(\log x_m/\zeta')^{1/2}\,f\,(28{\cdot}4n\,\sigma_0\,\zeta/\mu a). \quad \ldots \quad (38)$$

Fig. 7

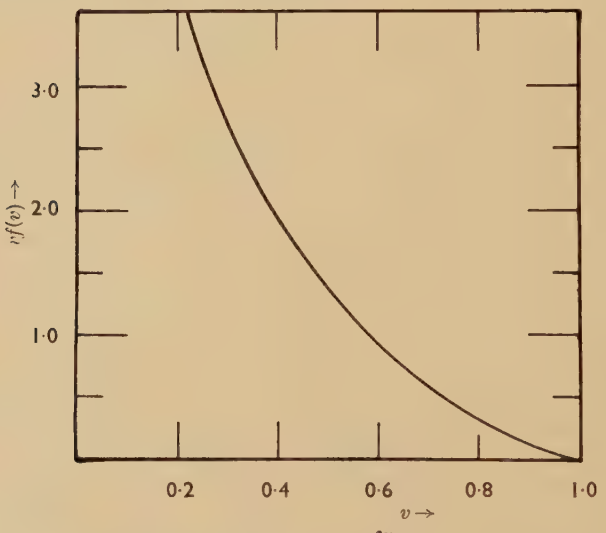

Value of the function $vf(v)=\int_0^{u_n}(u-v\sinh u)^{1/2}\,du$.

When the size of the critical loop and the width of the stacking fault are approximately equal neither eqns. (36) nor (38) apply. However, since both the size of the loop and the width of the stacking fault vary rapidly with stress at this point, the range of stress for which neither equation is valid is small and may be ignored. The curves for aluminium in fig. 8 have been obtained by using eqn. (36) when it is less than the width of the stacking fault and (38) when it is greater, and choosing ζ' so that the energy varies continuously. Under a stress of 1 kg/mm^2 the maximum number of dislocations in a piled-up group varies for copper from about 500 at 300°K to 750 at 100°K ; for aluminium at the same temperatures the numbers are 200 and 350. These numbers are several times those obtained in § 4, and illustrate the differences in strength of the sessile dislocation in the two situations,

When the sessile dislocation points away from the piled-up group, the activation energy for dissociation will be greater than if it pointed towards the group. Then comparing figs. 4 and 8 we see that the dislocation will give way by recombination before dissociation can occur. Accordingly there is no need to consider dissociation in detail in this case.

Fig. 8

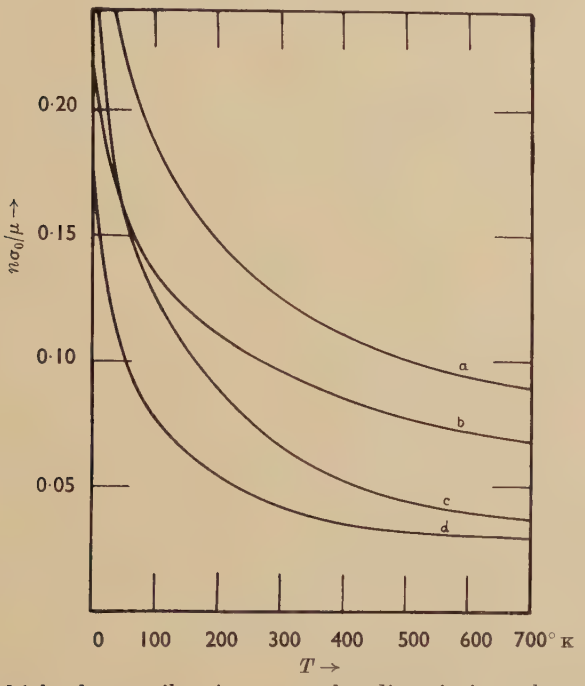

Stress at which the sessile gives way by dissociation plotted as a function of temperature for the different values of the dislocation width ζ: (*a*) copper, $\zeta/a=0{\cdot}2$; (*b*) copper, $\zeta/a=0{\cdot}3$; (*c*) aluminium, $\zeta/a=0{\cdot}2$; (*d*) aluminium, $\zeta/a=0{\cdot}3$.

§6. Discussion

As we have seen the results depend somewhat sensitively on the structure of the dislocation core, and accordingly not too much weight can be attached to the exact numerical values obtained. We can, however, draw some general conclusions. When the sessile dislocation points away from the piled-up group it will give way most easily by recombination and slip on (100); in this position it provides a rather weak obstacle, and in aluminium especially only a very small group would be needed to raise the stress sufficiently to overcome the sessile dislocation. If the dislocation can change its orientation it will strengthen itself considerably by pointing towards the group. If it cannot so change we will have two types of obstacles of rather different strengths; sessile dislocations pointing towards the piled-up group, being the stronger, will be the more important. From

this position the dislocation will give way by dissociation, except at high temperatures in metals with high stacking fault energy, such as aluminium, when recombination will be easier. At the temperature at which the latter begins there will be a marked drop in the size of the pile-up which can form.

Finally, we note that in no case can particularly large piled-up groups be formed. For comparison we may use the result of Stroh (1954 b) that to initiate a crack we require a piled-up group of magnitude given by $n\sigma_0/\mu \simeq 1{\cdot}5$, and this is greater by a factor of 10 or more than the groups which the sessile can withstand. We suggest that the reason why single crystals of face-centred cubic metals never fracture but always draw down to a point is that there are no obstacles which will withstand a sufficiently great piled-up group ; in polycrystals, on the other hand, grain boundaries can act as the barriers.

Acknowledgments

It is a pleasure to thank Dr. A. H. Cottrell for suggesting the problem, and Dr. J. Friedel for a number of stimulating discussions. The work was done during the tenure of a D.S.I.R. senior award.

References

Blewitt, T. H., Coltman, R. R., and Redman, J. K., 1955, *Defects in Crystalline Solids* (London : The Physical Society), p. 369.

Boas, W., and Schmid, E., 1931, *Z. Physik*, **71**, 703.

Cottrell, A. H., 1949, *Progress in Metal Physics* I ; 1952, *Phil. Mag.*, **43**, 645.

Cottrell, A. H., and Stokes, R. J., 1955, *Proc. Roy. Soc.* A, **233**, 17.

Frank, F. C., 1951, *Phil. Mag.*, **43**, 1224.

Frank, F. C., and Nicholas, J. F., 1953, *Phil. Mag.*, **44**, 1213.

Friedel, J., 1955, *Phil. Mag.*, **46**, 1169.

Lomer, W. M., 1951, *Phil. Mag.*, **42**, 1327.

Nabarro, F. R. N., 1952, *Advances in Physics*, **1**, 271.

Schoeck, G., and Seeger, A., 1955, *Defects in Crystalline Solids* (London : The Physical Society), p. 340.

Seeger, A., and Schoeck, G., 1953, *Acta Met.*, **1**, 519.

Stroh, A. N., 1954a, *Proc. Phys. Soc.* B, **67**, 427; 1954b, *Proc. Roy. Soc.* A, **223**, 404.

LII. *The Long β-Lifetime of* ^{14}C *and the* ^{14}N *Spectrum*

By J. P. Elliott
Atomic Energy Research Establishment, Harwell†

[Received November 28, 1955]

Abstract

The long β-lifetime of ^{14}C and the spectrum of ^{14}N are explained using a small tensor force in addition to the usual central and spin–orbit forces. The γ-decay branching ratio of the 3·95 Mev level of ^{14}N is predicted and also the nucleon reduced widths for the low levels of ^{14}N and ^{15}N.

§ 1. Introduction

The intermediate coupling shell model has met with such success (Inglis 1953, Zeldes 1953, Lane 1953, Elliott and Flowers 1955) in explaining the positions and properties of low levels in light nuclei that one welcomes any violent disagreement between theory and experiment as a means of learning more details of the model. The β-decay of ^{14}C to ^{14}N is such an apparent disagreement. According to the selection rules and the shape of the spectrum the transition is an allowed one, but the decay constant is such that log $ft=9{\cdot}03$. Thus we have a transition which, although formally allowed, is hindered by a factor of the order of 10^4.

Bouchez (1950) suggested that the large ft value results from a change in the orbital angular momentum which breaks the selection rules for an allowed transition (L-forbiddeness) but, on its own, this would demand a degree of L–S coupling quite incompatible with that of neighbouring nuclei. The explanation by Inglis (1953) depending on strong admixtures of higher configurations is also hard to accept in view of the overall success of the theory based on the lowest configuration.

Inglis (1953) showed that no mixture of central and spin–orbit forces could produce the cancellation in the matrix element necessary to give such a large ft value, but his remark that the introduction of a tensor force also failed to give cancellation was incorrect. Jancovici and Talmi (1954) showed that the inclusion of a tensor force with the central and spin–orbit forces of intermediate coupling gave the desired cancellation but that one needed such a large tensor force that the resulting spectrum of ^{14}N was in violent disagreement with experiment. In particular it gave a ground state with total angular momentum $J=2$ instead of the observed $J=1$.

† Communicated by B. H. Flowers.

The purpose of this paper is to show that the trouble which Jancovici and Talmi experienced with the spectrum arose from the ratio of two tensor force radial integrals which they calculated. This ratio turns out to be very sensitive to the radial dependence of the interaction and of the wave functions, both of which are uncertain. We treat this ratio as a parameter and show later that the value necessary to give the observed spectrum is a very reasonable one. Having determined wave functions which give the correct spectrum we go on to calculate relative reduced widths for the reactions ^{14}N(d, p)^{15}N and ^{13}C(d, n)^{14}N and the branching ratio for the γ-decay of the second excited state in ^{14}N at 3·95 Mev. If these also agree with experiment our procedure is largely vindicated.

§ 2. The Interaction Matrix Elements

A general two-body interaction consisting of a central force together with spin–orbit and tensor terms may be written

$$\sum_{i<j}(W+MP_{ij}^{x}-HP_{ij}^{\tau}+BP_{ij}^{\sigma})V_c(r_{ij})+\sum_i \xi(\mathbf{s}_i\cdot\mathbf{l}_i)$$
$$+\sum_{i<j}T(ij)\left\{\frac{(\boldsymbol{\sigma}_i\cdot\mathbf{r}_{ij})(\boldsymbol{\sigma}_j\cdot\mathbf{r}_{ij})}{r_{ij}^{2}}-\frac{\boldsymbol{\sigma}_i\cdot\boldsymbol{\sigma}_j}{3}\right\}V_t(r_{ij}). \quad . \quad . \quad (1)$$

The matrices of this interaction in the configuration p^{10} appropriate to mass 14 may be worked out by the standard processes described, for example, by Elliott (1953). They are given below for each value of J and of T, the isotopic spin :—

$T=0$

	$^{13}S_1$	$^{13}D_1$	$^{11}P_1$
$J=1$	$(L+2K)$	$-3\sqrt{5}\,C$ $(L-K)+\frac{3}{2}\xi-21A$	$\sqrt{\frac{2}{3}}\,\xi$ $-\sqrt{\frac{5}{6}}\,\xi$ $(L-3k)\,s$

$T=1$

	$^{31}S_0$	$^{33}P_0$
$J=0$	$(L+2K)q$	$\sqrt{2}\,\xi$ $(L-3K)t+\xi+10B$

	$^{13}D_2$		$^{33}P_1$
$J=2$	$(L-K)+\frac{1}{2}\,\xi+21A$	$J=1$	$(L-3K)t+\frac{1}{2}\xi-5B$

	$^{13}D_3$		$^{31}D_2$	$^{33}P_2$
$J=3$	$(L-K)-\xi-6A$	$J=2$	$(L-K)q$	$-\sqrt{\frac{1}{2}}\xi$ $(L-3K)t-\frac{1}{2}\xi+B$

Here L and K are the usual central force radial integrals for the p shell, A, B and C are similar tensor force integrals which we shall discuss later, and q, s and t describe the exchange character of the central force, viz. :—

$$q=W+M-H-B,\ s=W-M+H-B,\ t=W-M-H+B,\ \text{with}$$
$$W+M+H+B=1.$$

The factor $T(ij)$ in (1) describes the isotopic spin dependence of the tensor force and is of course contained in the parameters A, B and C. We write $[\alpha, \beta, \gamma]$ for the vector corresponding to the lowest root of the $J=1$, $T=0$ matrix, and similarly $[\mu, \nu]$ and $[\theta, \phi]$ for the (0, 1) and (2, 1) matrices respectively.†

§ 3. The β-Decay Matrix Elements

Since the ^{14}C$(\beta^-)^{14}$N transition involves a change of spin the Fermi matrix element vanishes. Calling the Gamow–Teller matrix element G, one finds

$$G \propto (\alpha\mu\sqrt{3}+\gamma\nu). \quad . \quad . \quad . \quad . \quad . \quad . \quad . \quad . \quad (2)$$

In order to obtain $\log ft \gtrsim 9$, this expression must be so small that we can assume it to vanish. Now, to produce the right sign of the doublet splitting in ^{15}N we must have $\xi<0$; hence from the (0, 1) matrix it follows that $(\mu/\nu)>0$ for the lowest root. A necessary condition for the vanishing of G is therefore that $(\alpha/\gamma)<0$; and precisely,

$$(\gamma/\alpha)=-\sqrt{3}(\mu/\nu). \quad . \quad . \quad . \quad . \quad . \quad . \quad . \quad . \quad (3)$$

If $C=0$, as in the absence of a tensor force, it can be seen from the (1, 0) matrix that $(\alpha/\gamma)>0$ for the lowest root and so G cannot vanish. Further, it can be seen that the vanishing of G depends sensitively on the value of C.

§ 4. General Restrictions on the Parameters

The general matrices written down in § 2 contain a large number of parameters but there are two at least that can be estimated with some certainty. They are the ratios $(L/K)=6$ and $(\xi/K)=4$. The first is a slowly varying function of range and potential shape ; the latter follows both from the intermediate coupling work of Lane (1953) on the neighbouring nucleus ^{13}C on the one side, and from the doublet splitting of ^{15}N on the other.

If we now write

$$3C=-xK \quad \text{and} \quad 21A=yxK$$

we can treat K as an energy unit, leaving only three parameters, x, y and s in the $T=0$ matrices. Instead of s we find it convenient to use the parameter Δ, being the excitation in units of K of the (2, 0) level

† We use the notation (J, T) to indicate spin and isotopic spin of a level.

above the lowest (1, 0) level. This has the added advantage that we can set a lower limit $\Delta K > 6$ from the observed spectrum. Let us now consider the (1, 0) matrix, making the condition that $(\alpha/\gamma) < 0$. This is a necessary, but insufficient, condition that the matrix element G should vanish. For each value of y we can then find regions of the (x, Δ) plane which satisfy this condition by drawing the curves of $\alpha = 0$ and of $\gamma = 0$. The regions are shown cross-hatched in figs. 1, 2 and 3 for values of y of 1, 2 and 4 respectively. Furthermore it can be shown that the double-hatched region labelled A is the only one allowed because that is the only region in which the negative value of (α/γ) corresponds to the lowest root of the matrix. It must be remembered that for each point x, Δ the exchange parameter s is determined and so there will be a further restriction if we have *a priori* knowledge of s.

Fig. 1

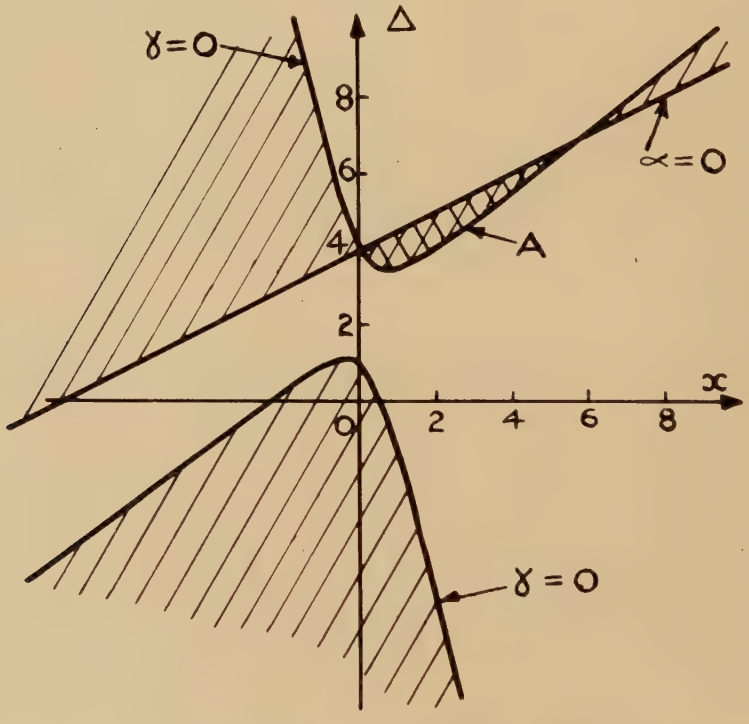

Allowed region A of (x, Δ) plane for $y = 1$.

The figures show that x must be positive, which gives a tensor force of the same sign as that needed for the deuteron. For small y there is a large range of x for which Δ is reasonable in the allowed region, while for larger y one has to come to very small x to get a large enough Δ.

Such a small value of x is hardly acceptable since it entails a large negative value of s, incompatible with the usual exchange mixtures suggested by Rosenfeld ($s = -1{\cdot}8$) and Serber ($s = 0$). It follows that for a large

Fig. 2

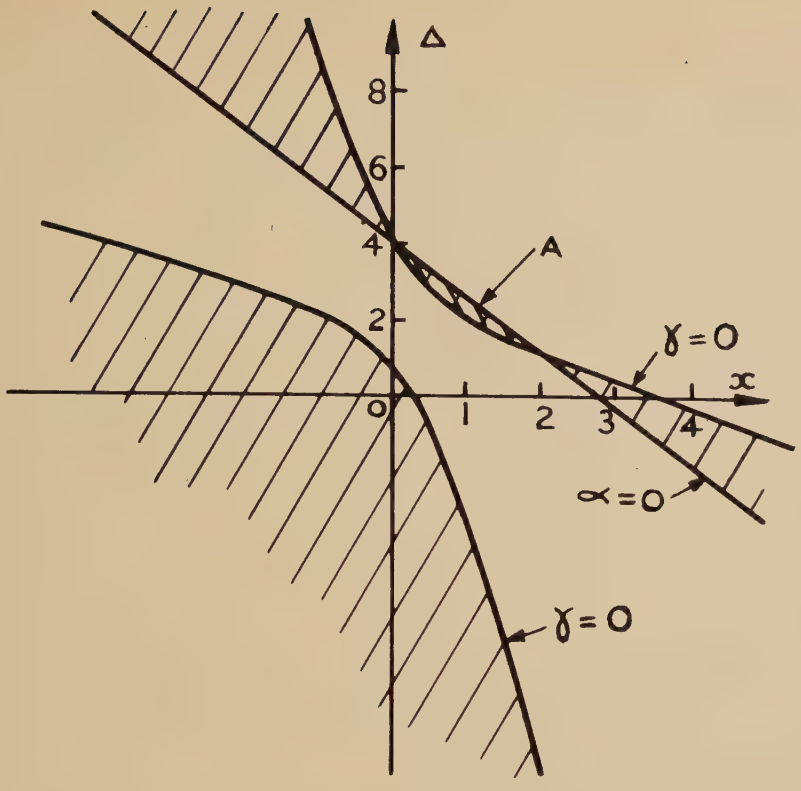

Allowed region A of (x, Δ) plane for y=2.

Fig. 3

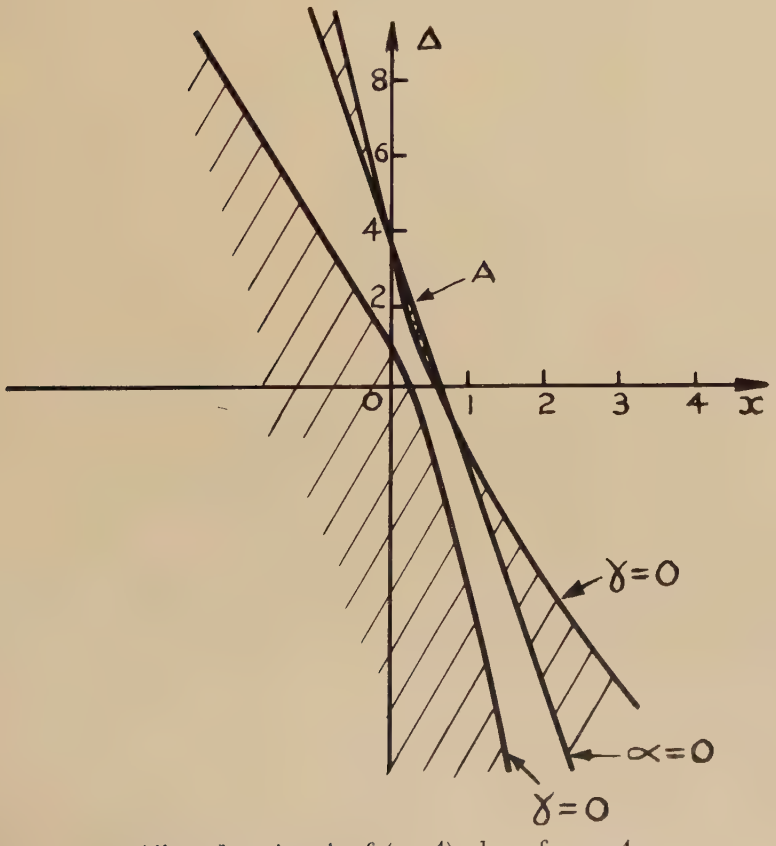

Allowed region A of (x, Δ) plane for y=4.

enough Δ and reasonable s we must look to the small values of y. Jancovici and Talmi (1953) used a large value of y with a reasonable s resulting in a low (even negative) value of Δ, and this gave the (2, 0) level as ground state in disagreement with observation.

§ 5. Assumption of Charge Symmetric Interaction, Leading to Spectrum Determination

In order to insert the precise condition (3) for the vanishing of G one must solve the (0, 1) matrix as well as the (1, 0) matrix, involving three new parameters q, t and B. It is fortunate that they can be related to those parameters already considered if we introduce the single assumption of charge symmetric forces, i.e., $M=2B$, $H=2W$ and $T(ij)=(\tau_i . \tau_j)$. For the remainder of the paper we make this assumption, whereupon†

$$q=-\tfrac{1}{3}s,\ t=-\tfrac{1}{3} \quad \text{and} \quad 3B=C-7A.$$

If we include the precise condition (3) we are able to plot the spectrum in units of K against x, the measure of strength of the tensor force ; and this can be done for each value of y we consider. Figures 4, 5 and 6 show all the calculated levels of the configuration p^{10} in the first $6K$ of energy excitation, which are to be compared with the observed spectrum in fig. 7, from Ajzenberg and Lauritsen (1955).

Above 4 Mev the observed spectrum is uncertain but we can be reasonably sure of the properties of the ground and lowest two excited levels. The calculated levels fit it very well with this pattern if we take x close to 0·4 in each figure. Fitting the first two excited levels determines x and K for each y, and q and ΔK then follow in table 1.

Table 1. Parameter Values Deduced from Fitting Spectrum

	y	x	K (Mev)	q	ΔK (Mev)
Fig. 4	1	0·400	−1·5	0·70	6·0
Fig. 5	2	0·395	−1·8	0·70	5·8
Fig. 6	4	0·384	−2·5	0·70	4·5

The calculated excitation ΔK of the (2, 0) level is seen to decrease as y increases, and since no (2, 0) level is observed in the first 5 Mev we must keep y small. It is probable that the (2, 0) level lies in the group observed between 4·9 and 6·4 Mev which would be consistent with $y=1$ or 2. The (2, 1) level, probably the analogue of the 6·7 Mev level in ^{14}C, lies in a reasonable position around 10 Mev. The scarcity of calculated levels near 6 Mev implies that all but one of the even parity levels observed there

† In the alternative notation for the central force, $a_{\sigma\tau}a_{\tau}=(1+3q)(3-3q)$.

Fig. 4

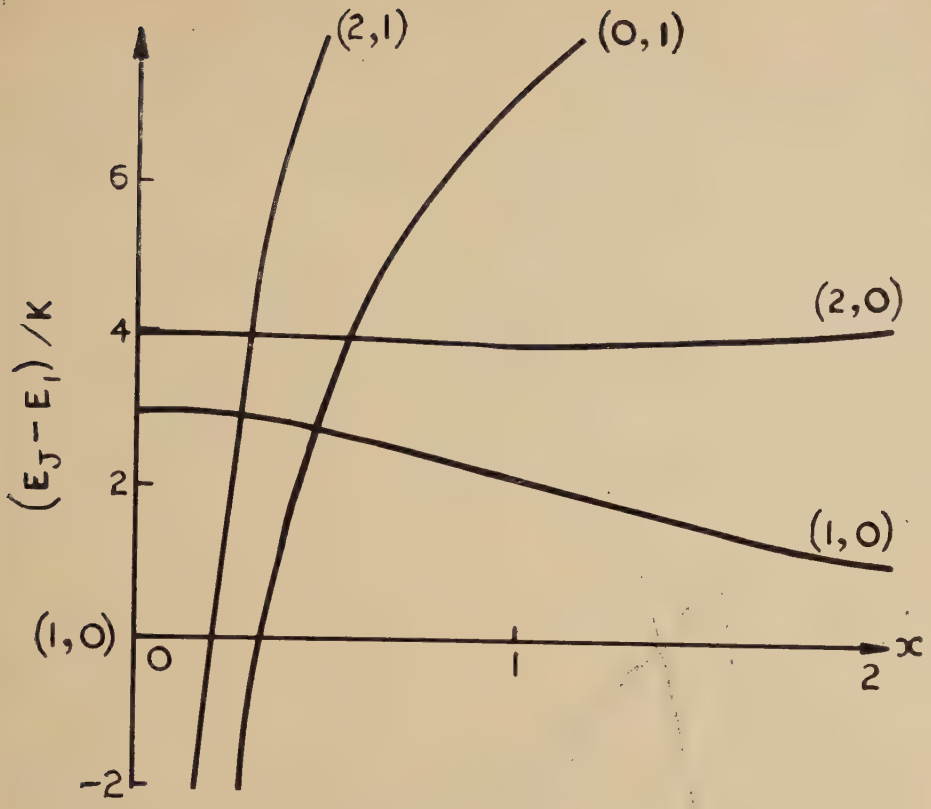

Calculated ^{14}N spectrum relative to lowest (1, 0) state as zero, with $y=1$.

Fig. 5

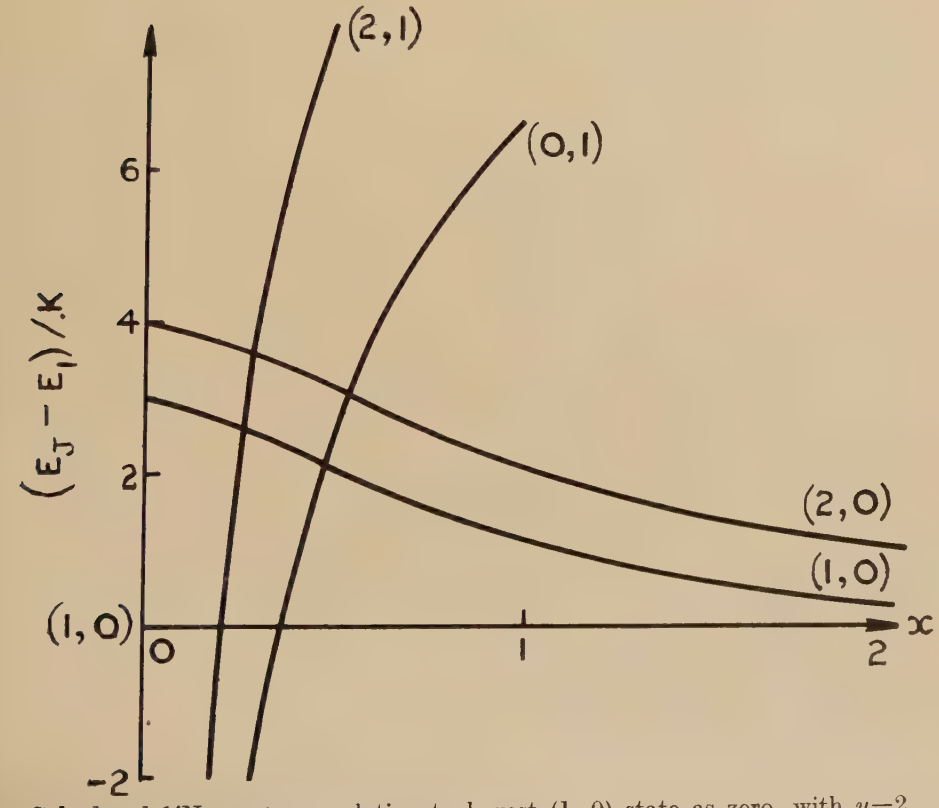

Calculated ^{14}N spectrum relative to lowest (1, 0) state as zero, with $y=2$.

Fig. 6

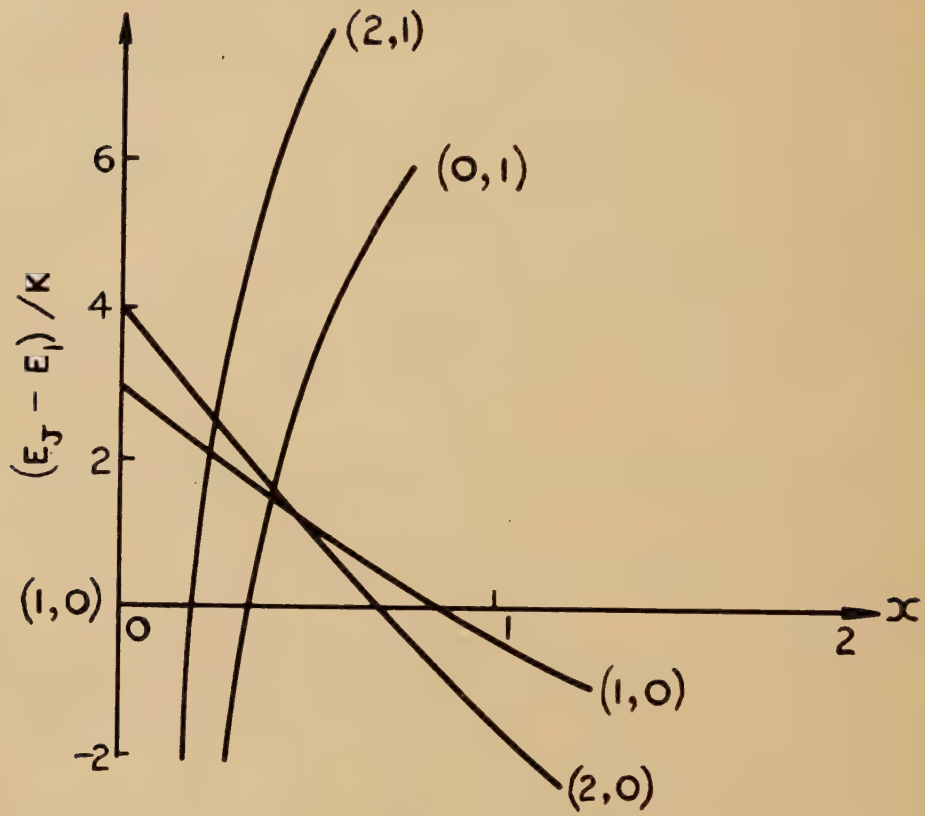

Calculated ^{41}N spectrum relative to lowest (1, 0) state as zero, with $y=4$.

Fig. 7

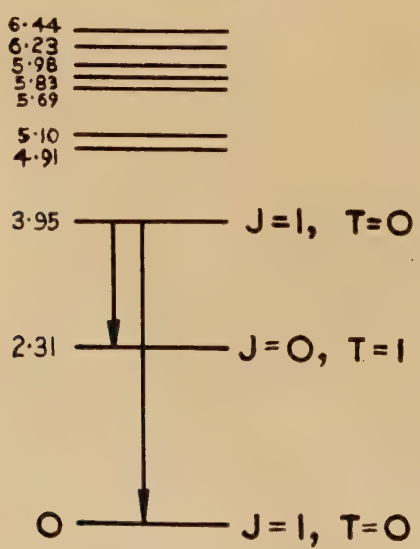

Observed ^{14}N spectrum.

must come from some higher configurations, but this is to be expected at such an excitation. The odd parity levels cannot of course come from the lowest configuration p^{10} considered here.

§ 6. Discussion of Deduced Parameter Values

We must now ask whether the parameter values of table 1 are reasonable. The value $q=0{\cdot}7$ which comes out for each value of y is in good agreement with the value $q=0{\cdot}6$ of the Rosenfeld central force based on the deuteron singlet-to-triplet strength ratio. It is found to be so constant here because we have fitted the (0, 1) level excitation above the ground state (1, 0), and this is sensitive to q. In his review, Inglis (1953) favoured a value of

Fig. 8

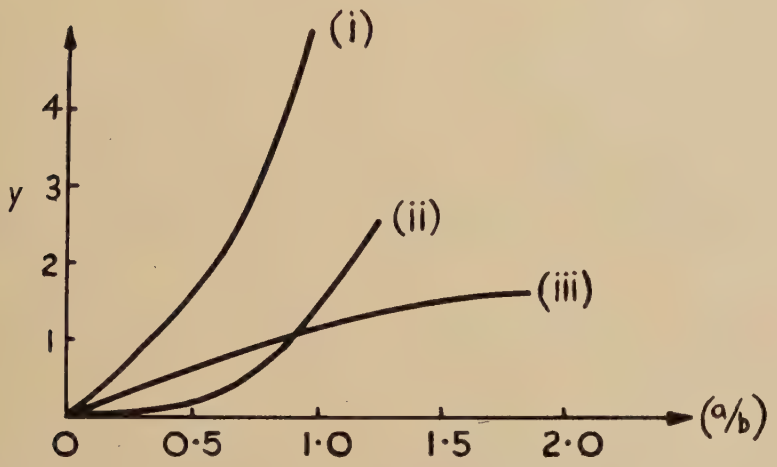

The ratio $y=-7A/C$ for various interactions and oscillator wave functions $\propto r\,e^{-r^2/2b^2}$.

(i) Yukawa $e^{-r/a}/(r/a)$.

(ii) Gauss e^{-r^2/a^2}.

(iii) Field theoretic $\dfrac{e^{-r/a}}{r/a}\left[1+3\dfrac{a}{r}+3\dfrac{a^2}{r^2}\right]$.

$K=-1{\cdot}3$ Mev which is in agreement with that found here for small y values. It is not simple to discuss the values of x and y because they both depend on the integral C which we find to be very sensitive to our choice of the radial dependence of the interaction and wave functions. With a Yukawa interaction of the usual range, and oscillator wave functions, C comes out as a difference of two nearly equal integrals and is therefore small. Thus in order to get a sufficiently large C with such assumptions one must take a very strong tensor force. making the integral A, which does not involve a cancellation, very large. This disrupts the spectrum as in the work of Jancovici and Talmi (1953). The key to the

problem therefore appears to lie in a larger value of (C/A), i.e. in a smaller y. The ratio

$$y=\frac{-7A}{C}$$

is plotted against a/b in fig. 8 for various interaction shapes, where a is the range of interaction and b the wave function parameter. Although a and b are uncertain we can make rough estimates of $a=1{\cdot}37$ and $b=1{\cdot}64$ (in units of 10^{-13} cm) from the π-meson mass and nuclear size respectively.

It is seen that although the Yukawa force gives a large y for reasonable a/b values, both the Gauss and the singular field theoretic forms give smaller y. However, y varies so much with a and b that one can say little more than that a small value of y such as is needed here is not unreasonable.

The strength of the tensor force is best illustrated by saying that the largest diagonal matrix element in this problem is $21A=-0{\cdot}6$ MEV for $y=1$, while the coupling term is $3\sqrt{5}\,C=1{\cdot}3$ MEV. The spin–orbit coupling terms are of the order of $\xi=6$ MEV, while the central force differences between diagonal terms is of the order of $3K=4{\cdot}5$ MEV. It can therefore be said that the tensor force in this problem is only a perturbation on the intermediate coupling result. The reason why a perturbation has such a large effect on the β-lifetime for this nucleus is discussed in § 10.

Although, as we have said above, it is difficult to relate the values of these parameters to the interaction constants because of the arbitrariness of the radial shapes, we can nevertheless obtain rough estimates. Let us assume the functions

$$V_c(r_{ij})=V_c\frac{\exp(-r_{ij}/a)}{r_{ij}/a}, \quad V_t(r_{ij})=V_t\frac{\exp(-r_{ij}/a)}{r_{ij}/a}$$

with oscillator wave functions $u(r)\propto r\exp(-r^2/2b^2)$, and set $a=b$. Since C is so sensitive, we use A and K to obtain the estimate; and taking the parameter values from the $y=1$ set of table 1 we find

$$V_c\sim-60 \text{ MEV}, \quad V_t\sim 20 \text{ MEV}.$$

We have already commented that the tensor force needed here has the same sign as that needed for the deuteron. The strength may be compared with the figures given by Pease and Feshbach (1952) who fitted the low energy, two-body data and the triton binding energy. For their best fit they found

$$V_c=-47 \text{ MEV}, \quad V_t=24 \text{ MEV};$$

and although these are based on ranges different from those used here the general agreement in sign and magnitude is encouraging.

Our value of V_t is proportional to y and depends sensitively on the position of the (2, 0) level which has not yet been assigned experimentally. It is therefore of great interest to know where this level lies.

§ 7. The Magnetic and Quadrupole Moments

Having determined the wave functions for the (1, 0) ground state in § 5 it is a simple matter to calculate the magnetic and quadrupole moments (see for example Elliott and Flowers 1955). They are found to vary very slowly with x and y, and using the $y=1$ set of parameter values from table 1 the results are compared with experiment in table 2. The agreement is

Table 2. Magnetic and Quadrupole Moments of ^{14}N

	Calculated	Observed
μ(n.m)	0·32	0·40
$Q(10^{-26}$ cm$^2)$	1·2	1·1

as good as is meaningful in view of the uncertainty in these quantities which arise from exchange currents, etc. It is pertinent to point out that because the magnetic moment is so insensitive to changes in the parameters an approach such as that of Sherr *et al.* (1955) which determines the wave function from an exact fit to the magnetic moment is open to large errors. A small correction to the magnetic moment due to exchange moments or collective effects could produce a large change in the deduced wave functions.

§ 8. The γ-Decay of the 3·95 and 2·31 Mev Levels of ^{14}N

The (1, 0) level at 3·95 Mev (see fig. 7) can decay by an M1 transition either to the ground state (1, 0) or to the (0, 1) level at 2·31 Mev. In addition it can decay to the ground state by an E2 transition. Let us first consider therefore the branching ratio for pure M1 radiation

$$\lambda_{\mathrm{M1}}=\frac{\Gamma(1^*\rightarrow 1)}{\Gamma(1^*\rightarrow 0)}$$

where Γ is the width of the level for such a transition. From energy arguments alone one might expect $\lambda_{\mathrm{M1}}>1$. However, it is a simple matter (cf. Elliott and Flowers 1955) to calculate λ_{M1} correctly from the wave functions deduced in § 5, with the striking result that $\lambda_{\mathrm{M1}}<0{\cdot}04$ for all values of x and y considered. Those values for $y=1$ in table 1 give $\lambda_{\mathrm{M1}}=0{\cdot}003$. Although for low energies an M1 process is generally more probable than an E2, the inhibition of the $1^*\rightarrow 1$ transition is so great that the two processes are comparable. In fact, calculating the E2 width for the $1^*\rightarrow 1$ transition in a similar way we find it to be twice as great as the M1 width. The combined branching ratio is then

$$\lambda_{\mathrm{M1+E2}}\approx 0{\cdot}01$$

where the $1^*\rightarrow 1$ transition is predominantly E2. Any collective motion, not considered here, would enhance this E2 transition and so increase λ.

Experimentally the situation is uncertain. Thomas and Lauritsen (1952) using the $^{13}C(d, n)^{14}N$ reaction found no definite 3·95 Mev gamma-ray. Woodbury, Day and Tollestrop (1953) using $^{13}C(p, \gamma)^{14}N$ estimated $\lambda=0{\cdot}5$, but the complex nature of the spectrum makes this rather uncertain. Clegg and Wilkinson (1953) from the same reaction did not see the 3·95 Mev gamma-ray and set an upper limit of rather less than 0·5. Mackin, Mims and Mills (1955) using $^{13}C(d, n)^{14}N$ assigned a gamma-ray to this transition with a branching ratio consistent with Woodbury *et al.* Clearly it would be of interest to have some more definite information on this decay which would then throw light on collective effects.

Sherr, Gerhart, Horie and Hornyak (1955) have given an upper limit of $3{\cdot}5\times10^{-13}$ sec for the half-life of the (0, 1) level at 2·31 Mev in ^{14}N. For the $y=1$ set of parameters from table 1 we find a half-life of $2{\cdot}6\times10^{-14}$ sec which is consistent with their limit. Again, an actual determination of this lifetime would be valuable.

§ 9. The Nucleon Reduced Widths of Low Levels of ^{14}N and ^{15}N

Consider the nucleon reduced width for the break up of a state Ψ into a state $\overline{\Psi}$ of one less particle and a nucleon of orbital angular momentum l. For simplicity in writing, and since it will be sufficient for our present purpose, we assume that both Ψ and $\overline{\Psi}$ belong to definite configurations. Then the width is non-zero only if the configuration of Ψ is that of $\overline{\Psi}$ with one extra l-particle. Suppose that in Ψ there are a number of closed shells and n equivalent l-particles. Then, in the notation of Lane and Thomas (1955), the nucleon reduced width, in units of the single particle width is

$$A^2=n\,|\,C^{\mathrm{TM}}_{\overline{\mathrm{TM}}\,\pm\frac{1}{2}}\,|^2(2\bar{\mathrm{J}}+1)\sum_x(2x+1)\Bigg[\sum_{\psi,\bar{\psi}}\{(2\mathrm{S}+1)(2\mathrm{L}+1)\}^{1/2}$$

$$\times\langle\Psi\,|\psi\rangle\,\langle\psi\{|\,\bar{\psi}\rangle\,\langle\bar{\psi}\,|\overline{\Psi}\rangle\begin{Bmatrix}\mathrm{S} & \bar{\mathrm{L}} & x\\ \bar{\mathrm{J}} & \frac{1}{2} & \bar{\mathrm{S}}\end{Bmatrix}\begin{Bmatrix}\mathrm{S} & \bar{\mathrm{L}} & x\\ l & \mathrm{J} & \mathrm{L}\end{Bmatrix}\Bigg]^2. \quad . \quad . \quad . \quad (4)$$

Here $\langle\Psi\,|\psi\rangle$ are expansion coefficients of the initial state in terms of the complete L–S coupled set ψ ; $\langle\psi\{\,|\,\bar{\psi}\rangle$ are the fractional parentage coefficients for the reduction $l^n\rightarrow l^{n-1}+l$; and $\langle\bar{\psi}\,|\,\overline{\Psi}\rangle$ are expansion coefficients for the final state in terms of the complete L–S coupled set $\bar{\psi}$. The $\pm$ sign refers to neutron or proton respectively which are treated as equivalent particles in the isotopic spin formalism. The Wigner 6–j symbol is defined, for example, by Elliott and Flowers (1955). Although the absolute values of widths extracted from stripping theory are not reliable, the relative widths of various levels of the final nucleus should be meaningful.

If we interpret the ground and 6·3 Mev levels of ^{15}N as the $1/2^-$ and $3/2^-$ doublet of the configuration p^{11} the wave functions are unique. In

table 3 we give the ratio of the reduced width of these two levels for break up to the ground state of ^{14}N using (4). The first three columns give values for the ratio which follow from ^{14}N wave functions corresponding to extreme coupling models, while the fourth gives the value resulting from the parameters of the $y=1$ set in table 1.

This value is not sensitive to changes in y and corresponds to an absolute value of $A^2(1/2^-)=1{\cdot}4$. Experimentally no figure is available although it could be found from the reaction $^{14}N(d, p)^{15}N$.

Table 3. $A^2(\frac{3}{2})/A^2(\frac{1}{2})$ for ^{15}N with Various Wave Functions

L–S extreme ^{13}S	L–S extreme ^{13}D	j–j extreme	Wave function from § 5
1·00	0·10	0	0·05

If we take the ^{13}C ground state wave function from the work of Lane (1953) we can similarly calculate the relative widths of various levels in ^{14}N for the reaction $^{13}C(d, n)^{14}N$. The widths relative to the ground state are given in table 4 together with the extreme coupling values. The absolute value of A^2(gs) corresponding to column 7 is 0·68. To our knowledge, experimental results are not yet available for these widths.

Table 4. A^2/A^2 (Ground State) for ^{14}N with Various Wave Functions

$(J\ T)$	Excitation (MEV)	L–S extreme		j–j extreme		Wave function from § 4
		State	A^2/A^2 (gs)	State	A^2/A^2 (gs)	A^2/A^2 (gs)
(0, 1)	2·31	^{31}S	2·50	$(3/2)^8\ (1/2)^2$	1·00	1·27
(1, 0)	3·95	^{13}S	2·50	$(3/2)^7\ (1/2)^3$	0	0·40
(2, 0)	~6 ?	^{13}D	0·60	$(3/2)^7\ (1/2)^3$	0	0·04
(2, 1)	~10 ?	^{31}D	0·40	$(3/2)^7\ (1/2)^3$	0	0·04

§ 10. Discussion

We have shown how the long β-lifetime of ^{14}C can be reconciled with the spectrum of ^{14}N by using a tensor force which turns out to be small compared with the central and spin–orbit forces and in general agreement with that deduced from deuteron and triton data. Having done this in detail it is always instructive to look back in general terms at the solution. The wave function of the ground state emerged as 96% $^{13}D_1$ state, and the 2·31 MEV level and ground state of ^{14}C are strong mixtures of $^{31}S_0$ and $^{33}P_0$ states. Hence the $^{14}C \rightarrow {}^{14}N$ β-decay can take place only through the small part (4%) of the ground state wave function, which is in the

$^{13}S_1$ or $^{11}P_1$ states. In making the matrix cancellation of § 3 we are setting conditions only on the small part of the wave function and we therefore need only a small tensor force. So far as the large part of the wave function is concerned the β-decay is L-forbidden, so that with no tensor force we should obtain log $ft \sim 5$. The effect of this small tensor force on everything but the sensitive lifetime is therefore a perturbation on the usual intermediate coupling calculation and its inclusion in other nuclei will, in most cases, cause no sensible change in the intermediate coupling result. There may however be a few isolated cases, such as that considered here, where the tensor force is important.

The inhibition of the M1 transition giving small λ, which was discussed in § 8, comes from a similar source since the large part of the wave function involves an S→D transition which is forbidden for M1 radiation.

Jancovici and Talmi (1953) pointed out that some confirmation that the large ft-value is produced by accidental cancellation is furnished by the much smaller value of log $ft=7{\cdot}3$ reported by Sherr *et al.* (1955) for the $^{14}O \rightarrow {}^{14}N$ decay which differs from the $^{14}C \rightarrow {}^{14}N$ decay only in the Coulomb correction if we assume charge independence of nuclear forces. They showed that the Coulomb correction is just sufficient to destroy the cancellation, increasing the matrix element by a factor 10 and so reducing log ft from 9 to 7. A similar argument would apply to the calculations of this paper.

Acknowledgments

I am grateful to Dr. A. M. Lane for stimulating this investigation and to Dr. B. H. Flowers and Dr. F. C. Barker for helpful discussions. Mrs. E. C. Ridley helped with the computation.

Note added in proof.—It has been brought to the author's notice that Hird, Whitehead, Butler and Collie (1954) measured the branching ratio for the decay of the 3·95 Mev level in ^{14}N finding $\lambda = 5 \pm 5\%$. This is in good agreement with the small value $\sim 1\%$ ' predicted ' in § 8 of this paper.

Further note added in proof.—Very recently Gove, Litherland, Almqvist and Bromley have also determined λ through the reaction $C^{12}(He^3, p\gamma)N^{14}$ finding $\lambda = 4{\cdot}3 \pm 0{\cdot}8\%$ in agreement with Hird *et al.* and with these calculations. The fact that this value, although small, is about four times larger than the calculated value is consistent with the enhancement to be expected for an E.2 transition in this mass region from some weak surface coupling, see Elliott and Flowers (1955).

References

Ajzenberg, F., and Lauritsen, T., 1955, *Rev. Mod. Phys.*, **27**, 77.
Bouchez, R., 1950, *Compt. Rend.*, **231**, 225.
Clegg, A. B., and Wilkinson, D. H., 1953, *Phil. Mag.*, **44**, 1269.
Elliott, J. P., 1953, *Proc. Roy. Soc.* A, **218**, 345.
Elliott, J. P., and Flowers, B. H., 1955, *Proc. Roy. Soc* A, **229**, 536.
Hird, B., Whitehead, C., Butler, J., and Collie, C. H., 1954, *Phys. Rev.*, **96**, 702.

Inglis, D. R., 1953, *Rev. Mod. Phys.*, **25,** 390.
Jancovici, B., and Talmi, I., 1954, *Phys. Rev.*, **95,** 289.
Lane, A. M., 1953, *Proc. Phys. Soc.* A, **66,** 977.
Lane, A. M., and Thomas, R. G., *Rev. Mod. Phys.* (to be published).
Mackin, R. J., Mims, W. B., and Mills, W. R., 1955, *Phys. Rev.*, **98,** 43.
Pease, R. L., and Feshbach, H., 1952, *Phys. Rev.*, **88,** 945.
Sherr, R., Gerhart, J. B., Horie, H., and Hornyak, W. F., 1955, private communication N.Y.O.—7326.
Thomas, R. G., and Lauritsen, T., 1952, *Phys. Rev.*, **88,** 977.
Woodbury, H. H., Day, R. B., and Tollestrop, A. V., 1953, *Phys. Rev.*, **92,** 1199.
Zeldes, N., 1953, *Phys. Rev.*, **90,** 416.

LIII. *Correlation Effects in Diffusion in Crystals*

By A. D. LeClaire and A. B. Lidiard
Atomic Energy Research Establishment, Harwell †

[Received December 10, 1955]

Abstract

It is a feature of many atomic diffusion jump mechanisms that successive jumps of an atom are 'correlated' in the sense that the direction of a jump is not completely at random but is influenced to some extent by the direction of the preceding jump or jumps. General formulae are derived for the diffusion coefficient which take account of this correlation. The theory is applied to a calculation of the diffusion coefficient of solute atoms by the Johnson mechanism.

§1. Introduction

The starting point for a descriptive treatment of diffusion is the assumption of Fick's law, which for one dimensional diffusion reads

$$J=-D\frac{dc}{dx}, \quad . \quad . \quad . \quad . \quad . \quad . \quad . \quad . \quad . \quad (1.1)$$

where J is the current density, dc/dx is the concentration gradient and D is the diffusion coefficient. The purpose of this paper is to discuss an assumption which is frequently made in the derivation of the theoretical expression for D in terms of atomic quantities. We begin by summarizing the general steps in such a derivation to the point where this assumption is made.

It is accepted that the fundamental process responsible for diffusion in crystalline solids is the continual migration of each of the atoms by an endless succession of jumps from site to site throughout the lattice. This entails a mixing of the atoms and so leads to the final effect of diffusion, viz., the removal of differences in composition. It is easily shown that a continual migration on the part of each atom does in fact produce a directed net flow down a concentration gradient at a rate proportional to it as required by the macroscopic eqn. (1.1).

The usual and simplest way of doing this is to consider only those jumps that occur between two adjacent lattice planes (1 and 2) normal to the direction of the concentration gradient (see e.g. Cottrell 1955). J, which is simply the difference in the numbers of atoms jumping per

† Communicated by the Authors.

unit time in opposite directions between unit area of 1 and 2, is then found to be given by an expression of the form (1.1) with

$$D=\tfrac{1}{2}\Gamma' s^2,$$

where Γ' is the probability per unit time that an atom will make any one of the possible jumps which take it out of the plane (1 or 2) and s is the interplanar spacing. The factor $\frac{1}{2}$ arises because it is assumed that the jumps are random, in the sense that *whenever* an atom on one of the considered planes makes a jump the probability is $\frac{1}{2}$ that it does so towards and on to the other plane and $\frac{1}{2}$ that it jumps in the opposite direction.

Now for a number of atomic jump mechanisms this is *not* true for every individual atom jump, and it is this assumption and the manner in which the problem is to be handled when it is not valid that forms the subject of this paper.

As a typical example consider diffusion by the vacancy mechanism. An atom which has just arrived on plane 1 from plane 2 by exchanging places with a vacancy, of necessity has this vacancy immediately adjacent to it on plane 2. This makes the probability greater than $\frac{1}{2}$ that its next jump is back to 2, in which event the net contribution to J of these two jumps would be zero. If it arrived on plane 1 from the plane before 1, the probability is less than $\frac{1}{2}$ that it contributes to J by jumping to 2. In either case the effect is to reduce J and hence D. To assume that the jump probabilities are always $\frac{1}{2}$ would be to assume that immediately after a jump the vacancy responsible always migrated away from the atom and made further contact with it in only a random way, i.e., approaching from all directions with equal probability. In fact the probability of an atomic jump in one direction depends on the direction of the previous jump and the jump directions are said to be ' correlated '.

This correlation effect for vacancy self diffusion seems first to have been noticed by Herring (see Bardeen 1948, especially footnote p. 1404) and has been discussed by Bardeen and Herring (1952), who calculated for a quadratic layer lattice and for the body-centred cubic and face-centred cubic lattices, the decrease in D which it brings about. Since their treatment is rather condensed and since one of their equations (eqn. A.2) contains an elementary but important error we feel it worthwhile to discuss the topic again in simplified form. The corrected equations show that in both face-centred and body-centred cubic lattices D is reduced by about 20%.

There can be a much stronger correlation between successive jumps in the case of the diffusion of solute atoms, at low concentration, by the Johnson (1939) mechanism. When there is an appreciable attraction between solute atoms and vacancies, comparatively stable solute atom-vacancy pairs will be formed and these can migrate as entities through the lattice. A particular jump of a vacancy can be with either its associated solute atom (probability per unit time, w_2) or with any of the solvent atoms which are neighbours of both solute atom and vacancy

(probability per unit time for exchange with any one such solvent atom, w_1). If $w_2 \gg w_1$ then there is a high probability that a second jump of a solute atom will be the reverse of its first jump. On the other hand if $w_1 \gg w_2$, then after one jump of a solute atom the vacancy will make on the average a large number of moves around the shell of nearest neighbour solvent atoms surrounding the solute atom, before exchanging again with the solute atom. By this time its position among the sites neighbouring the solute atom will be practically random. The degree of correlation can then be very large ($w_2 \gg w_1$) or very small ($w_1 \gg w_2$) depending on the relative magnitudes of w_1 and w_2. We therefore expect D to contain the rate of jumping not only of solute atoms but also of those of the solvent, so that the correlation here produces a qualitative change in the expression for D as distinct from the small quantitative correction that it makes in the vacancy self-diffusion case. Previous treatments of the Johnson mechanism are either incorrect or incomplete (Johnson 1939, Wyllie 1947) and we shall therefore in § 3 apply the general results of § 2 to a calculation of D for this case.

In the interstitialcy mechanism of diffusion an atom in an interstitial position migrates by pushing a neighbouring atom into another interstitial site, itself occupying the normal site vacated. The path of a particular atom is then a sequence of jumps between alternately normal (n) and interstitial (i) sites. A jump from an i-site to an n-site is clearly uncorrelated with previous jumps, the atom having an equal probability for jumping to any one of the allowed n-sites. However there is an appreciable probability that its next jump from the n-site will consist of being pushed back to its original i-site by the interstitial atom created by its previous jump. In this example then only alternate pairs of jumps are correlated (i.e. pairs of the type $i \rightarrow n \rightarrow i$).

There is clearly no correlation between successive jumps of a solute atom in an interstitial solid solution, for these jumps are from one interstitial site to another, each one completely at random.

From these few but important examples we see that correlation is a very frequent but not a universal feature of atomic jump processes in crystals.

§ 2. The General Formula for the Diffusion Coefficient

When correlation effects exist it is clearly inadequate to consider only those jumps that occur between two adjacent planes of atoms for we require to know the directions from which atoms arrive on these planes, and are therefore interested in jumps made from other planes on either side of them. This suggests that we could take account of correlation if we considered jumps between larger numbers of consecutive planes. One of us has in fact recently treated the Johnson mechanism by this method and the results agree with those of § 3 (Lidiard 1955, particularly § 4).

A more satisfactory method, yielding more readily to general treatment is to consider not merely jumps between a given number of planes but

the whole sequences of jumps that constitute the paths of atoms migrating through the lattice. Such an approach to diffusion problems is known as the 'random walk method'. In the present case it is more correct to speak of correlated random walks.

If successive jumps are of vector magnitude $\mathbf{r}_1$, $\mathbf{r}_2$, etc. then after a time t a total of $n=\Gamma t$ will have been made † and the atom will be a vector distance $\mathbf{R}(t)=\sum_{i=1}^{n}\mathbf{r}_i$ from its original position. $\overline{\mathbf{R}^2(t)}$, the average of $\mathbf{R}^2(t)$ over a large number of identical atoms is simply related to D; it can be shown that for one-dimensional diffusion

$$\frac{\partial c}{\partial t}=\frac{\overline{\mathbf{R}^2(t)}}{6t}\frac{\partial^2 c}{\partial x^2} \quad . \quad . \quad . \quad . \quad . \quad . \quad . \quad . \quad . \quad (2.1)$$

(see e.g. Joos 1934, § 7 of chapter XXXIV).

Whence,

$$D=\frac{\overline{\mathbf{R}^2(t)}}{6t} \quad . \quad . \quad . \quad . \quad . \quad . \quad . \quad . \quad . \quad . \quad (2.2)$$

The next step in the argument is to show that $\overline{\mathbf{R}^2(t)}$ is proportional to t and to relate it to the individual jumps which compose $\mathbf{R}$. We have

$$\begin{aligned}\overline{\mathbf{R}^2(t)} &= \overline{(\Sigma\mathbf{r}_i)^2}\\ &= \Sigma_i\overline{\mathbf{r}_i^2}+2\sum_{j=1}^{n-1}\sum_{i=1}^{n-j}\overline{\mathbf{r}_i.\mathbf{r}_{i+j}} \quad . \quad . \quad . \quad . \quad (2.3)\end{aligned}$$

We shall assume for simplicity that the individual jump vectors are of equal magnitude r. This is true for the commonly occurring face-centred and body-centred cubic lattices and also for the hexagonal close packed lattice. Since the average value of $\mathbf{r}_i.\mathbf{r}_{i+j}$ will be independent of i in the case of vacancy diffusion we can write (2.3) in the form

$$\overline{\mathbf{R}^2(t)}=nr^2+2r^2\sum_{j=1}^{n-1}(n-j)\,\overline{\cos\theta_j}\ \text{(vacancy)}. \quad . \quad . \quad . \quad . \quad (2.4)$$

where $\overline{\cos\theta_j}$ is the average value of the cosine of the angle between the i^{th} and the $(i+j)^{\text{th}}$ jump of an atom.

If the direction of one jump is completely independent of the direction of the preceding or earlier jumps the jumps are uncorrelated and $\overline{\cos\theta_j}=0$ for all j, since all possible values of θ_j are equally probable. $\overline{\mathbf{R}^2(t)}$ is then proportional to t, since $n=\Gamma t$, and D becomes

$$D=\tfrac{1}{6}\Gamma r^2. \quad . \quad . \quad . \quad . \quad . \quad . \quad . \quad . \quad . \quad (2.5)$$

This is identical with the previous expression for D when the relations between Γ and Γ' and between r and s are inserted.

† Γ is the *total* number of jumps which an atom makes per unit time and is not to be confused with Γ' introduced earlier. The relation between the two quantities is easily determined once the lattice is specified.

As we have noted in §1 (2.5) is applicable to interstitial diffusion in interstitial solid solutions, but is not exactly applicable to vacancy or to interstitialcy diffusion. However it is to be emphasized that so long as we are dealing with self diffusion in a pure crystal eqn. (2.5) is, as we shall see, in error only by a numerical factor not very different from unity, and is not qualitatively incorrect ; most of the theoretical analyses which have been made of D therefore still stand (see for example Zener 1952). In cases like that of the Johnson mechanism, (2.5) is considerably in error and the correct equation differs from it radically.

To discuss correlation effects we return to eqn. (2.4) and consider the quantities $\overline{\cos\theta_j}$. Firstly in order to see the relation between $\overline{\cos\theta_j}$ and $\overline{\cos\theta_{j-1}}$ consider the vectors $\mathbf{r}_i$, $\mathbf{r}_{i+j-1}$ and $\mathbf{r}_{i+j}$. Their poles in stereographic projection form the corners of a spherical triangle the sides of which are the angles θ_1, θ_{j-1} and θ_j. Writing down the standard relation† between these angles, and taking averages on both sides we get

$$\overline{\cos\theta_j} = \overline{\cos\theta_{j-1}\cos\theta_1} + \overline{\sin\theta_{j-1}\sin\theta_1\cos\phi} \quad . \quad . \quad . \quad . \quad . \quad (2.6)$$

where ϕ is the angle between the two planes defined by $\mathbf{r}_i$ and $\mathbf{r}_{i+j-1}$ and by $\mathbf{r}_{i+j-1}$ and $\mathbf{r}_{i+j}$. The averages of the product terms on the right-hand side can be replaced by the products of the averages of their separate factors, provided these factors are statistically independent of one another. This condition is satisfied for vacancy diffusion since $\overline{\cos\theta_1}$, the mean cosine of the angle between two successive jumps, is independent of the jumps which have gone before. In other words there is a direct correlation only between consecutive jumps, the correlation between one jump and a jump later than the next, being indirect and determined only by the direct correlations between successive intermediate jumps. Also the probability of a given angle θ between two jumps depends only on θ and not on the orientation of the plane of the jumps —at least for lattices where all atom jumps are of equal length and of equal probability, so that $\overline{\cos\phi}=0$. Thus (2.6) yields‡

$$\overline{\cos\theta_j} = \overline{\cos\theta_{j-1}} \cdot \overline{\cos\theta_1} = (\overline{\cos\theta_1})^j. \quad . \quad . \quad . \quad . \quad . \quad . \quad (2.7)$$

Substituting (2.7) into (2.4) and passing to the limit $n, t\to\infty$ we get

$$D=\tfrac{1}{6}\Gamma r^2\frac{(1+C)}{(1-C)}, \text{ (vacancy)} \quad . \quad . \quad . \quad . \quad . \quad . \quad (2.8)$$

† See e.g. *Introduction to Crystallography* by F. C. Phillips, p. 182.

‡ A more rigorous derivation of eqn. (2.7) is possible. It has been shown (R. Howard and A. B. Lidiard) that (2.7) is valid for vacancy diffusion in all lattices having one atom per unit cell and all jump vectors of the same magnitude. It is also true for the plane honeycomb layer and the diamond lattice. The apparent contradiction of (2.7) provided by Bardeen and Herring's eqns. (A.3) and (A.5) for the plane quadratic layer is not real since their eqn. (A.5) is incorrect.

where we have written C for $\overline{\cos\theta_1}$ the average of the cosine of the angle between consecutive jumps. The term $(1+C)/(1-C)$ we may refer to as the ' correlation factor '.

By a detailed calculation (the principles of which we illustrate in § 3 when we consider impurity diffusion by the Johnson mechanism) Bardeen and Herring obtained numerical values for C for self diffusion in body-centred and face-centred cubic lattices. Their results are respectively $C(\text{b-c.c.})=-0{\cdot}124$ and $C(\text{f-c.c.})=-0{\cdot}109$. Substituted into (2.8) these values give correlation factors of 0·78 and 0·80 respectively.

The derivation of (2.8) assumes that the direct correlation between a pair of consecutive jumps is the same for *any* such pair. We have already seen that this is not true for interstitialcy diffusion where only alternate pairs of jumps are correlated at all. This simplifies considerably the derivation of the correlation factor. Of the terms $\overline{\mathbf{r}_i.\mathbf{r}_{i+j}}$ in eqn. (2.3) all those with $j>1$ are zero, and of those for which $j=1$ only alternate ones are non-zero. For this case therefore

$$\overline{\mathbf{R}^2(t)}=nr^2(1+\overline{\cos\theta})$$

so that

$$D=\tfrac{1}{6}\Gamma r^2(1+\overline{\cos\theta}) \quad \text{(interstitialcy).} \qquad \ldots\ldots \quad (2.9)$$

Here $\overline{\cos\theta}$ is the mean value of the cosine of the angle between consecutive $i\rightarrow n$ and $n\rightarrow i$ jumps.

§ 3. Impurity Diffusion by the Johnson Mechanism

The Johnson mechanism of the diffusion of a solute in a dilute alloy assumes the existence of short range forces of attraction between a solute atom and a vacancy in the host lattice. In the following discussion we shall assume that we are dealing with a face-centred cubic lattice and that the attraction between an impurity atom and a vacancy may be neglected unless they are nearest neighbours. The average fraction of solute atoms with which a vacancy is associated will be denoted by p. The number of times that the associated vacancy and impurity change places with each other per unit time is w_2; w_1 is the frequency with which an associated vacancy will jump from one position to another particular nearest neighbour position of the impurity. (Each pair of nearest neighbours in a face-centred cubic lattice has four common neighbours). Hence $\frac{1}{6}\Gamma r^2$ is seen to be equal to $\frac{1}{3}a^2w_2p$ when the distance between nearest neighbours, r, is put equal to $\sqrt{2}a$.

It remains to calculate C. Let us do this first for the limiting case where the vacancy–solute pairs dissociate very much less frequently than they change their orientation. Suppose that the initial jump of the impurity was from position† (011) to (000) so that we start with the impurity at (000) and the vacancy at (011). We wish to calculate the average cosine of the angle between the vector (0−1−1) and the next impurity jump

† For convenience we omit the factor a.

vector. The first jump of the vacancy at (011) is back to (000) with probability $w_2/(4w_1+w_2)$. This means that the impurity jump vector is (011), i.e. opposite to (0−1−1) so that the cosine of the angle is −1. The contribution to the average cosine C from this possibility is thus $(-1)w_2/(4w_1+w_2)$. On the other hand it is easily verified that the first vacancy jump could have been to one of the positions (110), (101), (−110) and (−101) each with probability $w_1/(4w_1+w_2)$. We now consider the second vacancy jump. First we see that we can forget those systems in the ensemble where the vacancy went to (000) since we are interested only in calculating the mean cosine of the angle between *two consecutive* jumps of the impurity. Thus we consider that the second jump of the vacancy may be from any of the above four positions to (000), each with probability $w_2/(4w_1+w_2)$. The cosine of the angle is $-\frac{1}{2}$ for each of the four positions. There is therefore a contribution to C from the second vacancy jump of amount,

$$(-\tfrac{1}{2})\frac{w_2}{(4w_1+w_2)}\frac{4w_1}{(4w_1+w_2)}.$$

By following the vacancy around the twelve neighbouring sites to (000) in this way, we could write down a contribution to C coming from every vacancy jump. By induction we can then write down and prove the nature of the term in C coming from the n^{th} jump. Summation of the series for C so obtained gives

$$C=-w_2/(2w_1+w_2). \quad . \quad . \quad . \quad . \quad . \quad . \quad . \quad . \quad (3.1)$$

However a more elegant formulation is possible and is necessary for more complicated cases than the one we are considering in this section. After the n^{th} vacancy jump let the probability of occupation of the site s by the vacancy be $p_n(s)$. Thus with the above initial conditions $p_0(011)=1$ and all other $p_0(s)$ are zero, whilst $p_1(110)$, $p_1(101)$, $p_1(-110)$ and $p_1(-101)$ each equal $w_1(4w_1+w_2)$. By ordering the sites s in some suitable manner the various $p_n(s)$ coefficients can be written as a column matrix, p_n. The contribution of the $n+1^{\text{th}}$ jump to C can then be expressed as the matrix product τp_n, where τ is a row matrix each of whose elements is the probability, $w_2/(4w_1+w_2)$, that a vacancy will jump to (000) multiplied by the cosine of the angle for the appropriate site. If p_n has been contracted because some elements are always equal to one another by symmetry, then τ must also be contracted and each element in addition to the above two factors will contain a third factor which is the number of distinct sites which are represented by the single probability corresponding to that element of τ. We have then

$$C=\sum_{n=0}^{\infty}\tau p_n. \quad . \quad . \quad . \quad . \quad . \quad . \quad . \quad . \quad (3.2)$$

Also the probability coefficients $p_{n+1}(s)$ are related to the $p_n(s)$ by a set of linear equations. So we write

$$p_{n+1}=Pp_n$$

where P is the matrix of the coefficient in these equations. Hence

$$C=\tau \sum_{n=0}^{\infty} P^n p_0. \quad . \quad . \quad . \quad . \quad . \quad . \quad . \quad . \quad . \quad (3.3)$$

A glance at fig. 1 shows that in the present case, owing to the symmetry

Fig. 1

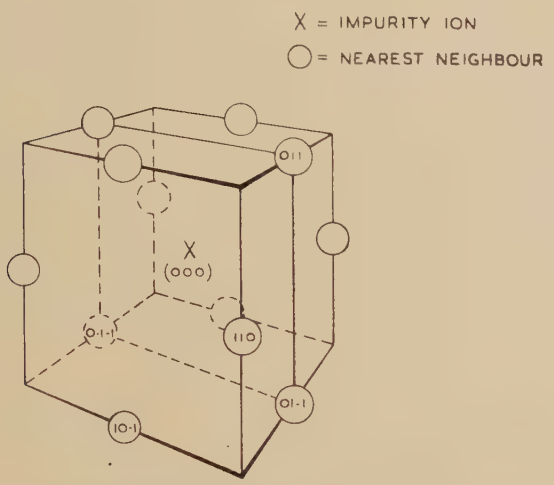

The twelve nearest neighbours to an impurity atom ($\times$) in the face-centred cubic lattice.

around the axis (011), there are only five distinct probability coefficients. These we take to be (1) $p_n(011)$, occurring once, (2) $p_n(110)$, occurring four times, (3) $p_n(01-1)$, occurring twice, (4) $p_n(10-1)$ occurring four times and (5) $p_n(0-1-1)$ occurring once. With these coefficients arranged in this order in a column matrix we easily find that τ must be the row matrix

$$\tau=g(-1\ -2\ 0\ 2\ 1), \quad . \quad . \quad . \quad . \quad . \quad . \quad (3.4)$$

where we have used g as an abbreviation for $w_2/(4w_1+w_2)$. By writing down the linear equations connecting p_{n+1} with p_n we easily find that P is

$$P=f\begin{bmatrix} 0 & 4 & 0 & 0 & 0 \\ 1 & 1 & 1 & 1 & 0 \\ 0 & 2 & 0 & 2 & 0 \\ 0 & 1 & 1 & 1 & 1 \\ 0 & 0 & 0 & 4 & 0 \end{bmatrix} \quad . \quad . \quad . \quad . \quad . \quad . \quad . \quad . \quad (3.5)$$

where $f=w_1/(4w_1+w_2)$. From (3.4) and (3.5) we find

$$\tau P=2f\tau,$$

whence

$$\tau P^n=(2f)^n\tau.$$

Finally, since p_0 is the column matrix

$$p_0=\{1\quad 0\quad 0\quad 0\quad 0\},$$

we see that (3.3) gives

$$C=\tau p_0 \sum_{n=0}^{\infty} (2f)^n = -g(1-2f)^{-1}, \quad . \quad . \quad . \quad . \quad . \quad (3.6)$$

which by insertion of the expressions for f and g leads to

$$C=-w_2/(2w_1+w_2), \quad . \quad . \quad . \quad . \quad . \quad . \quad . \quad . \quad (3.1)$$

as stated above.

Up to this point we have assumed that dissociation jumps by the vacancies attached to impurity ions are very rare. It is a simple matter to remove this restriction if we assume that the return probability of a dissociating vacancy may be neglected in calculating C. Let k_1 be the probability per unit time that an associated vacancy will make one particular dissociation jump, i.e. a jump to a particular site which is not a nearest neighbour of the impurity. An associated vacancy has seven such jumps open to it. The preceding calculation remains unaltered except that the relative probabilities f and g are now respectively $w_1/(w_2+4w_1+7k_1)$ and $w_2/(w_2+4w_1+7k_1)$. Use of eqn. (3.6) then gives

$$C=-w_2/(2w_1+w_2+7k_1). \quad . \quad . \quad . \quad . \quad . \quad . \quad (3.7)$$

If we pass to the limit when $w_1=w_2=k_1$, i.e. when the 'impurity' is a tracer atom, then (3·7) predicts that $C=-0{\cdot}10$. This may be compared with the Bardeen and Herring figure of 0·109 for a face-centred cubic lattice. The difference arises from the fact that we have neglected the return probability of a 'dissociating' vacancy. Bardeen and Herring included this probability by taking explicit account of the probability coefficients $p_n(s)$ for next nearest neighbour and more distant sites. The principles of the calculation are the same although the detailed computation becomes rapidly more involved as the order of P increases especially when τ is not an eigen vector of P as it is here. It is however certain that the error in (3.7) decreases as the binding between the impurity atom and the vacancy becomes stronger, i.e. as k_1 decreases relative to w_1 and w_2.

Insertion of (3.7) into (2.8) gives the final expression for the diffusion coefficient appropriate to the Johnson model in a face-centred cubic lattice,

$$D=\frac{a^2p}{3}\frac{w_2(w_1+7k_1/2)}{(w_1+w_2+7k_1/2)}, \quad . \quad . \quad . \quad . \quad . \quad (3.8)$$

—in agreement with the result which was previously obtained using kinetic theory (Lidiard 1955).

§ 4. Summary and Conclusion

In the present paper we have given a simplified account of the random walk method of dealing with correlation effects in atomic diffusion in crystals. The general formula (2.8) for the coefficient of diffusion by the vacancy mechanism in a lattice where the elementary jumps are of equal length, expresses the fact that *direct* correlations exist between

consecutive atom jumps and that they exist equally between every pair of consecutive jumps. When the institialcy mechanism is operative such correlations exist only between pairs of type $i \rightarrow n$ followed by $n \rightarrow i$, and the diffusion coefficient is then given by (2.9). In § 3 we illustrated the matrix formulation of the method of evaluating C by a calculation of the Johnson model of impurity diffusion in a face-centred cubic lattice. The results agreed with those obtained previously using a kinetic method. At present we are investigating by a random walk method the self diffusion of solvent atoms by vacancies which are strongly bound to impurity atoms. A practical example of this state of affairs is the diffusion of radioactive sodium in a crystal of sodium chloride containing divalent impurity cations, e.g. $CdCl_2$ (Etzel and Maurer 1950, Aschner 1954). A reliable kinetic treatment of this problem would be extremely cumbersome.

Note added in proof. The authors are indebted to Prof. C. A. Coulson for pointing out that equation (2.8), or rather the equation for $\overline{\mathbf{R}^2(t)}$ corresponding to it

$$\overline{\mathbf{R}^2(t)} = nr^2(1+C)/(1-C),$$

has been employed in the theory of rubber elasticity for a number of years. It gives the distribution of lengths of a chain of n carbon–carbon bonds when there is free rotation around each bond but the bond angle is constant (θ_1). See e.g. L. R. G. Treloar, *The Physics of Rubber Elasticity* (Oxford: Clarendon Press), 1949.

References

Aschner, J. F., 1954, *Thesis*, University of Illinois.

Bardeen, J., 1949, *Phys. Rev.*, **76**, 1403.

Bardeen, J., and Herring, C., 1952, *Imperfections in Nearly Perfect Crystals* (New York: Wiley), p. 261.

Cottrell, A. H., 1955, *Theoretical Structural Metallurgy*, 2nd Edn. (London: Arnold).

Etzel, H. W., and Maurer, R. J., 1950, *J. Chem. Phys.*, **18**, 1003.

Johnson, R. P., 1939, *Phys. Rev.*, **56**, 814.

Joos, G., 1934, *Theoretical Physics* (Glasgow: Blackie).

Lidiard, A. B., 1955, *Phil. Mag.*, **46**, 1218.

Wyllie, G., 1947, *Proc. Phys. Soc.*, **59**, 694.

Zener, C., 1952, *Imperfections in Nearly Perfect Crystals* (New York: Wiley), p. 289.

LIV. *Density Changes during the Annealing of Deformed Nickel*

By L. M. Clarebrough, M. E. Hargreaves and G. W. West
Division of Tribophysics, C.S.I.R.O., University of Melbourne, Australia†

[Received December 15, 1955]

Abstract

A differential method has been used to measure the changes in density which accompany the annealing of plastically deformed nickel. The results of these measurements are correlated with earlier measurements of stored energy, electrical resistivity and hardness for the same material. There are two sudden increments in density ; the first is attributed to the disappearance of vacancies and the second to recrystallization. These are superimposed on a gradual increase in density attributed to recovery. There is a considerable discrepancy between the densities of dislocations calculated from the stored energy measurements and from the density measurements.

§ 1. Introduction

In a recent paper (Clarebrough, Hargreaves and West 1955, hereinafter called I) the release of stored energy during the annealing of plastically deformed nickel was correlated with changes in hardness and electrical resistivity. The conclusion was reached that the disappearance of both vacancies and dislocations contributed to the release of energy. In an attempt to separate the contributions of these two types of defect, measurements have been made of the changes in macroscopic density which take place during annealing of plastically deformed nickel.

Preliminary results, given in I, were obtained by Mr. G. A. Bell of the National Standards Laboratory, C.S.I.R.O., Sydney. He measured the absolute density of a specimen as deformed, again after heating to a temperature considered high enough to allow the vacancies to disappear and again after further heating to a temperature in excess of the recrystallization temperature. The details of the method used will be published elsewhere (Bell 1956). These preliminary results did not give sufficient detail of the manner in which the change of density was related to the temperature of annealing, and more detailed experiments were required. These are described in the present paper. A differential method for measuring small changes in density was developed simultaneously by Mr. Bell and by the authors. This method has been employed in making the measurements described here.

† Communicated by W. Boas.

§ 2. Experimental

(*a*) *Preparation of Specimens*

The nickel used for the density measurements was of commercial purity (99 6% Ni) and from the same batch (K) as that used for the measurements of stored energy, electrical resistivity and hardness (I). Deformation in torsion and in compression was carried out on specimens of the same dimensions and in the same manner as described in I. The bars deformed in torsion were ground lightly to remove the roughened surface produced by the heavy deformation. Specimens for the measurement of density, $1\frac{5}{8}$ in. in length and $\frac{3}{4}$ in. in diameter, were then cut from the ground bars and the end faces ground flat. Since the bar deformed by compression was not in a suitable form for grinding, the specimen for the measurement of density was produced by turning. All cutting, grinding and turning operations were done under a copious flow of coolant.

One of the deformed specimens was annealed by heating at a rate of 6°C per min to 900°C and this specimen was used throughout the experiments as the standard to which all deformed specimens were referred. In each case the weight of the deformed specimen in air was made equal to the weight of the standard in air within 1 mg.

(*b*) *Procedure*

The differential method involved determination of the difference in upthrust between the standard specimen and a deformed specimen when both were immersed in a liquid of high density.

An analytical balance with a capacity of 200 g and a nominal sensitivity of 1/10 mg was used in the experiments. A concave mirror was attached to the beam of the balance to focus a beam of light onto a scale at a distance of 5 metres ; rest points were determined on this scale.

The balance was mounted rigidly above a water-bath and the temperature of this bath was controlled at $27 \pm 0{\cdot}01$°C. A glass vessel containing the working liquid (1, 1, 2, 2 tetrabromo-ethane) was supported centrally in the water-bath. This vessel is described elsewhere (Bell 1956) and the design allows the liquid to be stirred without introducing a mechanical stirrer. The stirring was stopped during weighing. For weighing in iquid the specimens were held in nickel wire cages, which in turn were suspended by fine nickel wires from hooks underneath the balance pans.

Before making a measurement the cages were suspended in the working liquid and sufficient time allowed for the cages and the liquid to reach the operating temperature. The rest point of the balance was then determined with the standard specimen and the deformed specimen on the pans and the cages in the liquid. The specimens were then transferred to the cages in the liquid and, after they had reached the temperature of the liquid, the rest point of the balance was determined again and adjustments made with a rider to restore the rest point to approximately that for the specimens in air. The specimens were then removed from the liquid, washed in alcohol, dried and the rest point in air was checked. In

this way the difference in upthrust between the deformed and the standard specimen was measured.

The difference in upthrust was measured for each specimen after deformation and after heating to various temperatures at a rate of 6°c per min. From the differences in upthrust measured before and after any heating the corresponding fractional change in density may be calculated knowing the density of the liquid. This was determined from time to time by weighing in air and in the liquid a standard nickel specimen whose absolute density was known accurately from Bell's measurements.

For heating, the specimens were placed in a nickel boat inside a silica tube which was evacuated and then heated in a furnace to a particular temperature, withdrawn and allowed to cool. The vacuum was then broken, the specimen removed and the measurement of density made. The specimen was then replaced in the tube which was again evacuated and then returned to the furnace held at the particular temperature and heated to the next temperature required.

The differential method has several advantages over the measurement of absolute densities for determining small changes in density. The change in density is measured directly instead of being obtained as a small difference between two large measured quantities. Since two specimens of very nearly the same volume are used any changes in the density of the working liquid only cause second order errors in the result. For this reason the temperature of the working liquid need not be controlled within the very close limits required for the measurement of absolute density. The results of the differential method are not sensitive to errors in the balance nor do complications arise from the precision of weights or the use of buoyancy corrections.

§ 3. Results

Figure 1 shows the fractional change in density $\Delta D/D$ and the power difference ΔP as functions of the temperature for specimens deformed in torsion ($nd/l = 2{\cdot}34$, where n = number of turns, d = diameter and l = gauge length) and heated at a rate of 6°c per min. The power difference ΔP represents the rate of release of stored energy (Clarebrough, Hargreaves, Michell and West 1952). The density results were obtained with five separate specimens and the ΔP curve is the mean of four separate determinations.

The influence of the degree of deformation on the changes in density is shown in fig. 2 where $\Delta D/D$ is plotted as a function of temperature for three deformations in torsion corresponding to nd/l values of 0·47, 1·41 and 2·34.

Figure 3 shows $\Delta D/D$ as a function of temperature for a specimen deformed approximately 80% in compression. It can be seen that this curve has the same form as the $\Delta D/D$ curves in fig. 2 for specimens deformed in torsion. Thus the type of result is not influenced to any extent by the inhomogeneous deformation in torsion, as was also found for the determinations of stored energy, so that the results should be generally applicable.

Fig. 1

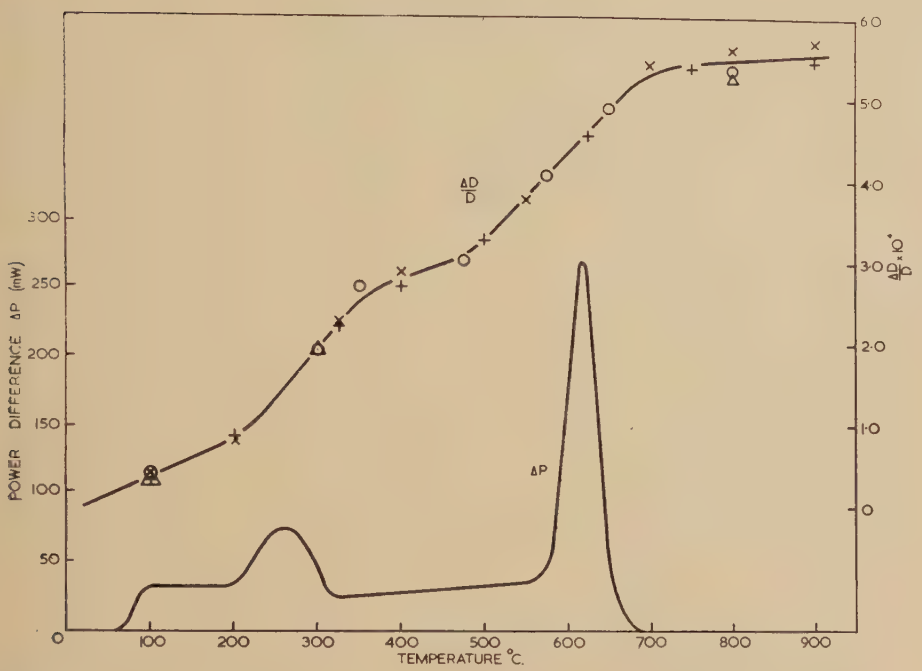

The rate of release of stored energy ΔP and the fractional change in density, measured at 27°C, $\Delta D/D$, as functions of temperature for nickel deformed in torsion to $nd/l=2{\cdot}34$.

Fig. 2

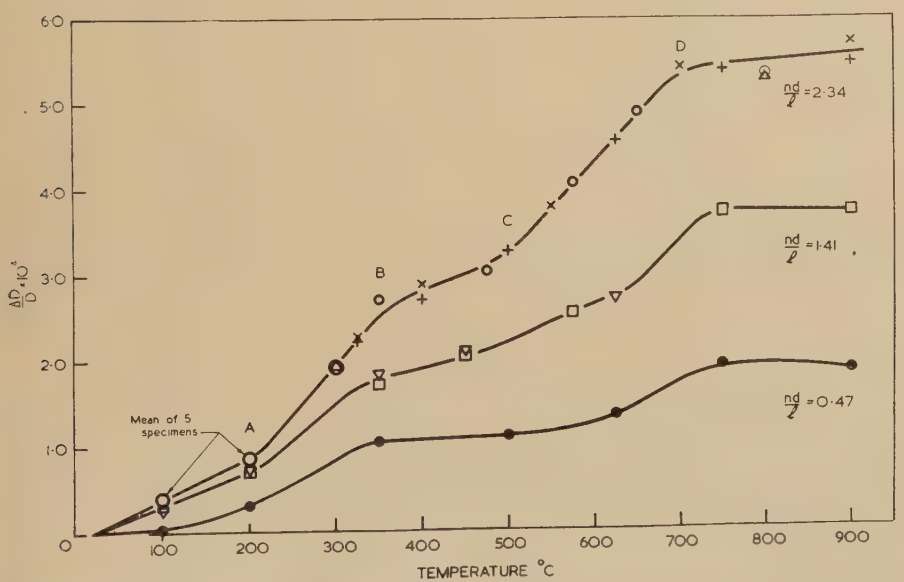

The fractional change in density, measured at 27°C, as a function of temperature for nickel deformed to various extents in torsion.

Fig. 3

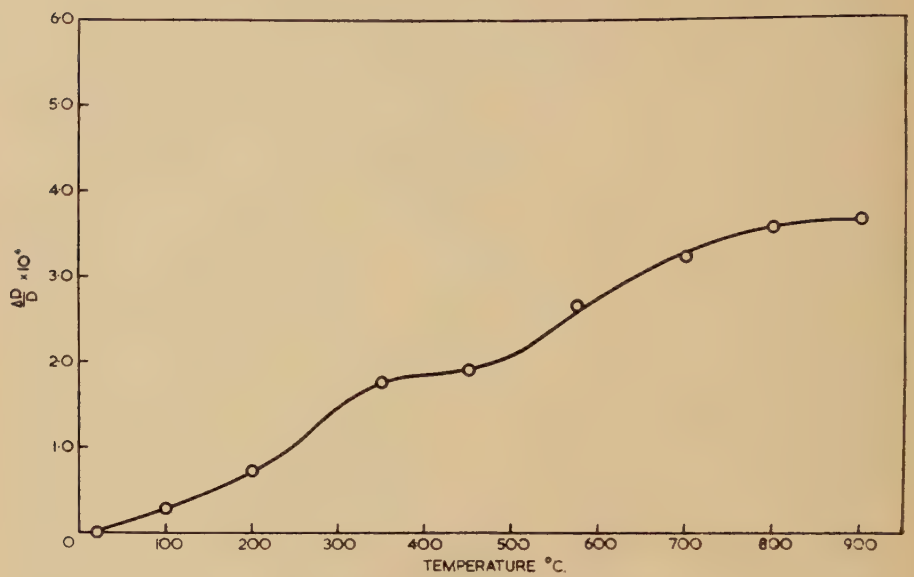

The fractional change in density, measured at 27°c, as a function of temperature for nickel deformed 80% in compression.

Fig. 4

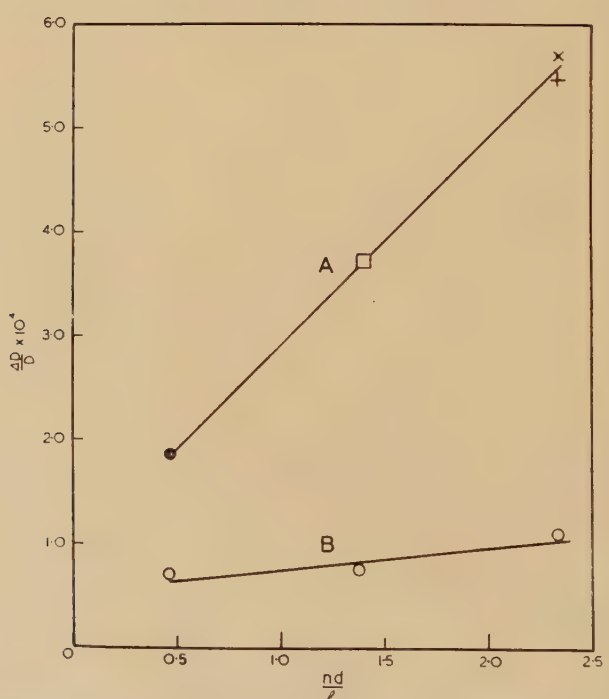

The total change in density, curve A, and the portion attributed to vacancies, curve B, as functions of the amount of deformation in torsion.

For all deformations the $\Delta D/D$ curve indicates a gradual rise in density on which two sudden increments in density (AB and CD in fig. 2) are superimposed. In fig. 4 the total fractional change in density together with the fractional change involved in the first increment, AB, are plotted against the torsional strain. The values for the first increment were obtained by extrapolating the portions BC of the curves back to 200°C. This procedure can only give a very approximate result for reasons discussed below, but the trend of the curve is clear.

Fig. 5

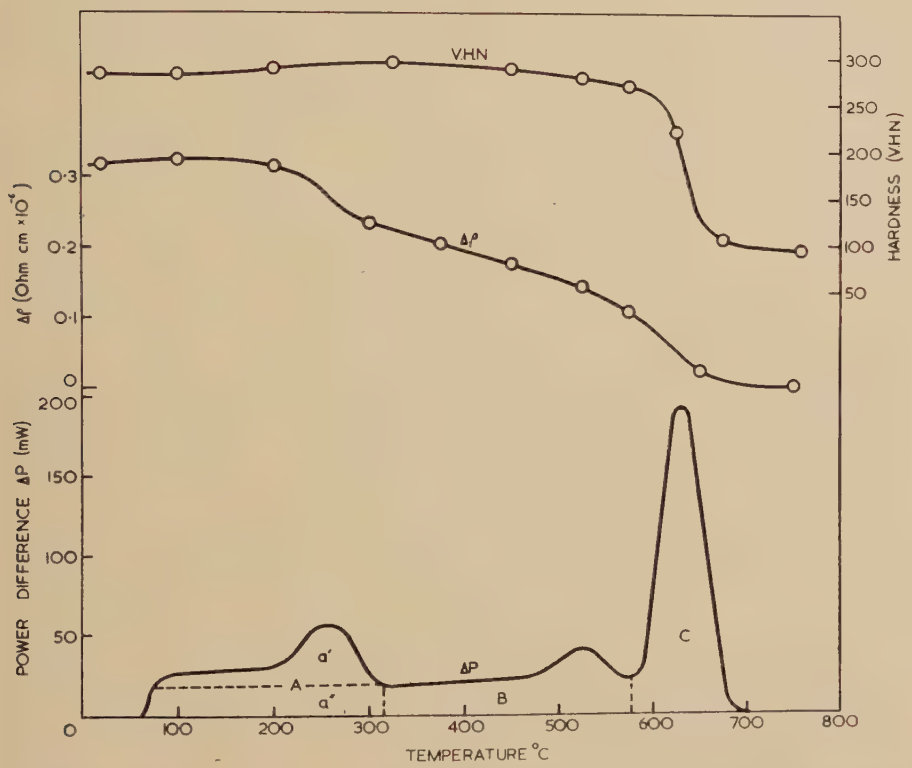

A typical result from (I). The rate of release of stored energy ΔP, the increment in electrical resistivity measured at 0°C, $\Delta\rho$, and the hardness measured at room temperature, V.H.N. as functions of the temperature for nickel deformed in torsion to $nd/l=1{\cdot}87$.

§ 4. Discussion

The changes in density observed should be considered in relation to the determinations of stored energy, hardness and electrical resistivity which had been made previously on the identical material. A typical set of these results from I is shown in fig. 5. The release of energy corresponding to the first peak in the ΔP curve, area a′, is accompanied by a decrement in the resistivity without any change in hardness and therefore has been attributed to the disappearance of vacancies produced by

deformation. On a vacancy model Nicholas (1955) obtained good agreement between calculated and experimental ΔP curves.

Now it is clear from fig. 1 that the first sudden increase in density AB takes place in the same range of temperature as the release of energy corresponding to area a′, the first peak in the ΔP curve. It was shown in I that this range of temperature was independent of the amount of deformation and the curves in fig. 2 show that this is also true for the range of temperature over which the first sudden increase in density occurs. Further, the amount of energy represented by area a′ (fig. 13 in I) and the magnitude of the first increment in density (curve B, fig. 4) are similarly almost independent of the amount of deformation. Thus the conclusion reached in I that vacancies created during deformation disappear during this range of temperature is supported by the present observations of the corresponding increase in density.

In estimating the energy of a vacancy it was assumed previously that the disappearance of vacancies was responsible for the whole of the increase in density observed, in the preliminary measurements, up to the temperature at which the release of energy represented by area a′ was complete. This assumption is not supported by the present results, as there appears to be a general upward trend in the $\Delta D/D$ curve on which the sudden increment is superimposed, and the extrapolation referred to in §3 must be carried out to find the change in density associated with area a′. The proportion of vacancies is therefore less than that calculated on this assumption and it now appears that the estimate of the energy of vacancy as 1·6 ev must be increased. However, the increment in density due to the disappearance of vacancies cannot be determined exactly from the present results for the following reasons.

Firstly, the necessary extrapolation cannot be made accurately without measuring the increase in density at smaller intervals of temperature. Secondly, the technique of annealing *in vacuo* adopted in this work requires an appreciable time for a specimen to reach the end point of the previous annealing, before heating through the next range of temperature, and also the rate of cooling after each heating is quite slow. A specimen on which the change in density is determined is therefore at elevated temperatures for a much longer period than a specimen used for a determination of the ΔP curve by uninterrupted heating in the calorimeter. As it has been found that the temperatures at which the peaks in the ΔP curve occur are somewhat dependent on the rate of heating, an exact correspondence of the ΔP and $\Delta D/D$ curves, with respect to temperature, is not to be expected. Further, the closer the intervals of temperature at which the increase in density is determined the more serious is this discrepancy likely to become.

It is hoped to resolve this difficulty by improving the technique of annealing and making experiments on a much purer grade of nickel. Preliminary experiments with this material indicate that the increase in density due to the disappearance of vacancies may be more clearly resolved.

The release of energy corresponding to area (a″+B) in fig. 5 is accompanied by only a slight decrease in hardness and a gradual decrease in electrical resistivity, on which is superimposed the more sudden decrease due to vacancies. This is very similar to the gradual increase in density, which takes place in the corresponding range of temperature, on which the increment due to vacancies is superimposed. The release of energy accompanying these changes has been attributed in I to recovery involving the annihilation and re-arrangement of dislocations. If it is accepted that the presence of dislocations in a metal reduces its density this gradual increase in density may be attributed to the operation of these same processes.

The second sudden increase in density, CD, takes place in approximately the range of temperature in which the second peak in the ΔP curve, area C, is observed. Measurements of hardness and resistivity such as those illustrated in fig. 5 together with metallographic and x-ray observations show that this peak corresponds to recrystallization (I). Thus, the second sudden increment in density may consistently be attributed to the decrease in the density of dislocations during recrystallization, assuming again that dislocations cause a reduction in density. The $\Delta D/D$ curve begins to rise at a temperature rather lower than that at which the peak, area C, in the ΔP curve begins. This is probably due to the deficiencies in the technique of annealing, which were pointed out above, since the total time during which the specimen has been at elevated temperatures has become considerable at this point in the experiment. Despite this effect it is clear from fig. 2 that the sudden increase in density, CD, attributed to recrystallization, occurs at higher temperatures for smaller amounts of deformation in the same way as do the relevant peak in the ΔP curve and the accompanying changes in properties.

It is of interest to compare the density of dislocations obtained from the results of the measurements of stored energy given in (I) and from the results of the present measurements of density. The appropriate values for two degrees of deformation are given in the table.

Deformation in torsion nd/l	Stored energy cal/g	Dislocation density from energy measurements lines cm^{-2}	Fractional change in density δ	Dislocation density from density measurements lines cm^{-2} N
1·41	0·40	$2{\cdot}1\times10^{11}$	$3{\cdot}0\times10^{-4}$	$1{\cdot}4\times10^{12}$
2·34	0·59	$3{\cdot}1\times10^{11}$	$4{\cdot}5\times10^{-4}$	$2{\cdot}0\times10^{12}$

In calculating the density of dislocations from the energy measurements it is assumed that the liberation of energy in area (a″+B+C) is due to a decrease in the density of dislocations and that the energy of a dislocation

in nickel is 7×10^{-4} erg cm^{-1}. As pointed out in (I) the first assumption is not fully justified as some interaction energy is almost certainly involved in the liberation of energy in area (a″+B+C). In addition, the value assumed for the energy of a dislocation is somewhat arbitrary and a value as low as $2{\cdot}5\times10^{-4}$ erg cm^{-1} might be taken for dislocations in heavily cold worked nickel. The corresponding densities of dislocations would then be $5{\cdot}9\times10^{11}$ and $8{\cdot}8\times10^{11}$ lines cm^{-2}.

In calculating the density of dislocations from the results of the present measurements of density, the total change in density, less the contribution due to vacancies, is assumed to be due to a decrease in the number of dislocations. It is assumed that an edge dislocation causes the same change in density as a row of vacancies of the same length, which is probably a reasonable upper limit, and that half of the dislocations are of the screw type, which make no contribution to the change in density. On this model, if the dislocation lines run between nearest neighbours, distant $a\sqrt{2}$, the total density of dislocations N which causes a fractional change in density δ is $N=4\sqrt{2}\delta/a^2$ lines cm^{-2}.

Taking the lower limit for the energy of a dislocation and this upper limit for the density change due to a dislocation there is still a considerable discrepancy between the densities of dislocations calculated from the energy measurements and from the density measurements. Thus it does not appear possible to explain the present results on the basis of the model suggested, involving only dislocations, without invoking still lower values for the energy of a dislocation and consequently densities of dislocations considerably greater than 10^{12} lines cm^{-2}. Such high densities of dislocations do not appear probable, on the available evidence, and thus it appears, that either the change in density due to a dislocation is higher than we have supposed, or that some other type of defect contributes to the change in density.

A similar anomaly has been found by Van Bueren (1955) for the increase in electrical resistivity due to deformation in copper and he has suggested that point defects are responsible for most of this increase, though it is not clear by what mechanism these are stabilized at relatively high temperatures.

Acknowledgments

We wish to thank Dr. W. Boas for his interest and encouragement during the course of this work. Thanks are also due to Mr. J. F. Nicholas for helpful discussions and to the staff of the workshop of this Division for the preparation of specimens.

References

Bell, G. A. (to be published).

Clarebrough, L. M., Hargreaves, M. E., Michell, D., and West, G. W., 1952, *Proc. Roy. Soc.* A, **215**, 507.

Clarebrough, L. M., Hargreaves, M. E., and West, G. W., 1955, *Proc. Roy. Soc.* A, **232**, 252 (referred to as I).

Nicholas, J. F., 1955, *Phil. Mag.*, **46**, 87.

van Bueren, H. G., 1955 *Z. Metall.*, **46**, 272.

LV. *Some Properties of Vacancies and Interstitials in* Cu_3Au

By R. A. Dugdale
Atomic Energy Research Establishment, Harwell, Berks†

[Received February 27, 1956]

Abstract

A series of experiments, based on electrical resistivity measurements, have resulted in the following conclusions: The activation energy for formation of vacancies is about 1·0 ev and for migration about 0·9 ev. The ordering process, involving the interaction of vacancies with wrong atoms, is complex; at least two relaxation processes are shown to operate. The decay time of an excess vacancy concentration appears to be limited by the presence of vacancy capturing impurities, the concentration of which can be varied by suitable heat treatment. Interstitials are more mobile than vacancies at a given temperature, but these too are probably trapped and can in turn contribute to the limitation of the vacancy decay time.

§ 1. Introduction

The present work on the alloy Cu_3Au originated as a study of the disordering effect of neutron bombardment. However, when an ordering effect was also discovered interest turned in this direction (for a review of these effects see Kinchin and Pease 1955). Ordering requires the microdiffusion of copper and gold atoms which, as with diffusion in face-centred cubic metals generally, is believed to occur through the migration of vacancies. Thus the objective has become, primarily, the study of the behaviour of vacancies in the alloy. Although it has not been possible to substantiate the vacancy mechanism directly the self consistency of the hypothesis is well supported.

The general technique was to study changes in the electrical resistivity (always measured at 0°C) brought about by various treatments including bombardments and quenches. By this technique the alloy appears to be so sensitive to small concentrations of vacancies that bombardments with γ-rays (discussed in the appendix) and low temperature quenches (from ~300°C) were convenient.

The description of the experimental work begins with preliminary experiments in support of the vacancy hypotheseis. Some plausible assumptions concerning the vacancy mechanism are then made and these are applied to determine E_f the activation energy of formation, to study the interaction with wrong atoms and to find the factors which control the decay time of excess vacancies. In addition, some attention is given to the behaviour of interstitials.

† Communicated by the Author.

§ 2. Experimental Technique

Much of the experimental technique has already been described (Dugdale and Green 1954—henceforth referred to as P1) and so only those aspects of particular relevance to the present work are mentioned here.

The alloy was made by Johnston, Matthey and Co., Ltd., in the form of wire of diameter 0·025 mm, from high purity copper and gold. An analysis, made by the Chemistry Division at Harwell, gave $25{\cdot}8 \pm 0{\cdot}2$ atomic % gold, with silver, iron and silicon as major impurities with concentrations between 0·01 and 0·1 atomic %.

Specimens were made from portions of the wire subjected to an initial heat treatment of 2 hours at 900°c, in an argon atmosphere, to remove coring. After suitably mounting on mica, they were given a further treatment at 600°c to remove any cold work effects. In the early stages a half hour treatment was given, but this was later increased to four hours. All the specimens mentioned in § 4 *et seq.* received the longer treatment.

The majority of the experiments were concerned with the state of long range order. Normally, specimens were prepared in this state by heating for periods of 5 to 8 days at 370°c, after which they were cooled to room temperature in a period of about 5 minutes giving a value of the electrical resistivity ρ, at 0°c, of about $6\,\mu\Omega$ cm (according to Siegel 1951 domain growth occurs most rapidly at $\sim$370°c). It was found that after such treatment (henceforth a specimen prepared in this manner will be termed 'partially ordered') equilibrium at lower temperatures ($\geqslant$250°c) could be closely approached in relatively short times; fig. 2.1 shows, for example, the relaxation towards equilibrium at 250°c and 290°c. Conversely, for specimens used in experiments during which the degree of order was increased, the partially ordered state could be recovereed by a short heat treatment at 370°c of only 2 hours.

Values of the equilibrium resistivity ρe have been obtained, by quenching, from several specimens during the experiments; these are plotted in fig. 2.2 as a function of temperature. Also shown are the values for a domain size of $\sim 10^{-5}$ cm deduced from the work of Sykes and Jones (1938) who used an alloy very close to the stoichiemetric composition. It can be seen that the values obtained from the present alloy are very reasonabie. ^{60}Co γ sources, giving uniform fluxes at the specimen of from 10^{14} to 10^{15} γ cm^{-2} hour^{-1}, were used for irradiations.

§ 3. Preliminary Experiments

The quenching in of vacancies is conveniently demonstrated on a tempering curve. For this purpose, a partially ordered specimen was quenched from 380°c and then heated at progressively increasing temperatures for 1 hour periods. The resistivity–temperature curve so obtained is shown in fig. 3.1 (*a*). The general shape of the curve, i.e., the passage through a minimum at $\sim$300°c, is characteristic of the alloy, but the important aspect, for the present purpose, is the inflection in the

Fig. 2.1

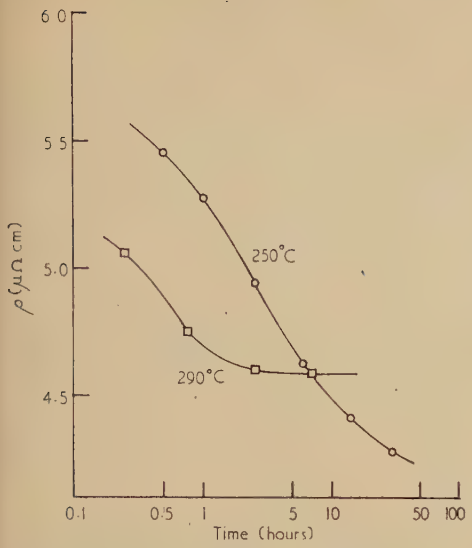

The relaxation towards equilibrium at 250°C and 290°C of the partially ordered state (initial resistivity $\sim 6\,\mu\Omega$ cm).

Fig. 2.2

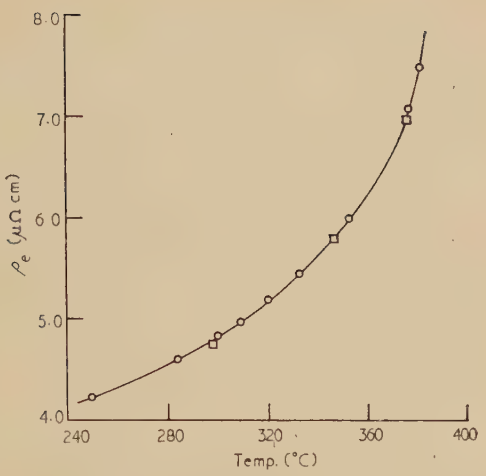

The equilibrium resistivity curve. The values marked by squares are from Sykes and Jones (1938), for a domain size of $\sim 10^{-5}$ cm.

Fig. 3.1

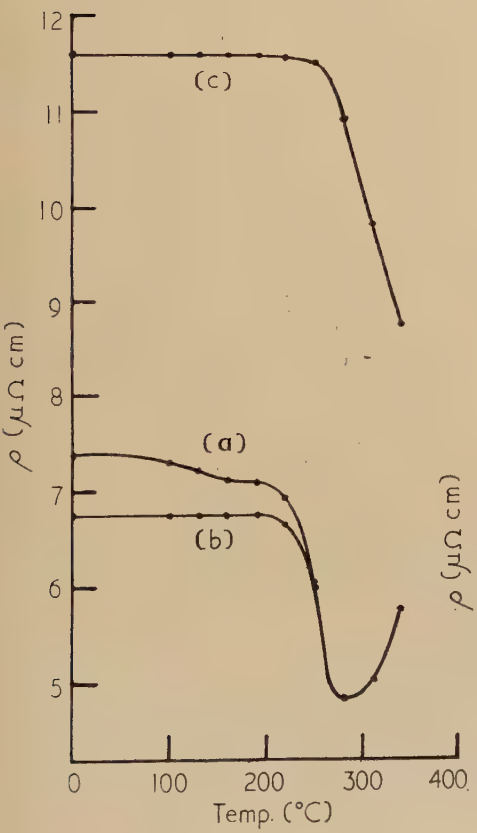

Tempering curves obtained after various initial heat treatments (see text).

Fig. 3.2

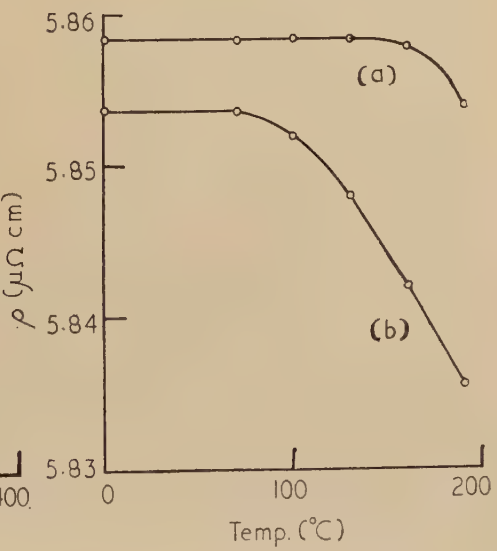

The effect of γ-bombardment on a tempering curve : (*a*) before, (*b*) after bombardment with $1{\cdot}5 \times 10^{16}\,\gamma\,\text{cm}^{-2}$.

neighbourhood of 170°C. The rate of ordering is noticeably greater just below this temperature than it is just above ; in fact, the ordering rate at 160°C is not again equalled until the temperature exceeds 200°C. This behaviour is just what might be expected if excess vacancies, frozen in by the quench, are mobile and decay to equilibrium at ~160°C. The higher ordering rates above 200°C are attributed to the thermal formation of sufficient vacancy concentrations.

Figure 3.1 (*b*) shows a similar tempering curve taken after the specimen was cooled from 380°C to room temperature relatively slowly (cooling time ~5 min) and then heated at 160°C for 16 hours. No ordering is noticeable until a temperature of ~200°C is reached, which is consistent with the above interpretation.

Quenching from lower temperatures gives smaller but similar inflexions in the neighbourhood of 170°C. Such quenches, of course, also result in a lower degree of order and initial resistivity. Quenching from 425°C (37°C above the critical temperature), on the other hand, results in the disordered state with a high resistivity. A tempering curve for this case (fig. 3.1 *c*) shows hardly any change in resistivity until ~250°C is reached. Although it has been shown by Skyes and Jones (1936) that considerable ordering does occur after such a quench it is evident that the resistivity is not sensitive to it. A state of long range order is therefore essential for the sensitive detection of excess vacancies at low temperatures.

Low temperature ordering may be induced in a slowly cooled specimen by means of a bombardment with ^{60}Co γ rays. The tempering curve (*a*) in fig. 3.2 shows the behaviour before bombardment (this time with half hour periods at each temperature), and curve (*b*) after bombardment with $1{\cdot}5\times10^{16}$ γ-rays cm^{-2}.

The isothermal decay of excess vacancies at 160°C and 190°C, after bombardement with $1{\cdot}5\times10^{16}$ γ-rays cm^{-2}, is shown in fig. 3.3. The first $2\frac{1}{2}$ hours of curve (*a*) shows the small but detectable thermal ordering at 160°C. The bombardment then produced an acceleration in ordering rate which decayed in about 3 hours. At 190°C (curve (*b*)) the thermal ordering rate is appreciably higher and the decay time of the excess vacancies is reduced to about 1 hour.

An attempt was made to observe the converse of this process at 190°C, i.e. the growth to equilibrium of an initially too small vacancy concentration. The previous experiment, involving an increase of temperature from 160°C to 190°C and hence an increase in the equilibrium vacancy concentration, suggested that it would be a very small effect. A partially ordered specimen was heated at 190°C for two hours to reach the equilibrium vacancy concentration. The ordering rate as a function of time during a subsequent hour is plotted in the first part of fig. 3.4. The specimen was then heated for long periods at 130°C and 100°C (respectively 24 and 134 hours) to reduce the vacancy concentration as much as possible. On returning to 190°C the second part of the curve was obtained. It will be seen that, in spite of the experimental errors, a time of about 10 min. appears to have elapsed before the initial ordering rate recovered.

The production of excess vacancies by cold working (Seitz 1952) can be expected to produce ordering at low temperatures. Figure 3.5 (*a*) shows the effect, at 100°C, of a series of light deformations performed on a partially ordered specimen initially quenched from 380°C. The first 500 min. allowed a decay of quenched in vacancies. At the end of this period a light deformation, at room temperature (for details of which see P1) produced an increase in ρ followed by further ordering and vacancy decay. Similar deformations at 500 min. intervals produced similar effects, although the ordering effect gradually diminished. The same experiment performed on a specimen initially quenched from 450°C produced no indication of ordering (curve (*b*)). This is consistent with the absence of domains of long range order noted above.

Fig. 3.3

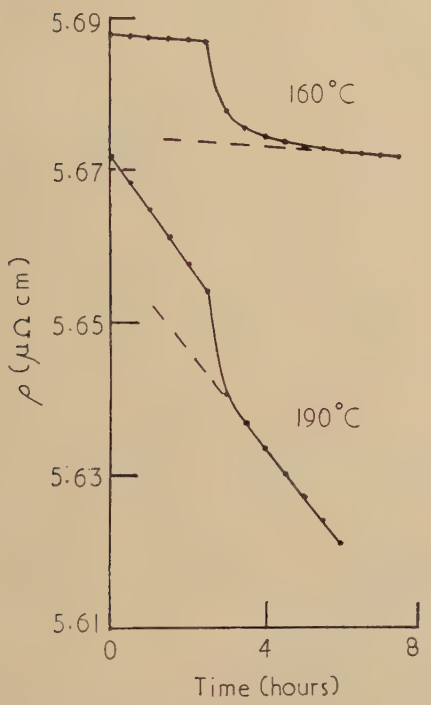

The isothermal decay at 160°C and 190°C of excess vacancies introduced by a bombardment of $1{\cdot}5\times10^{16}$ γ cm^{-2}.

Fig. 3.4

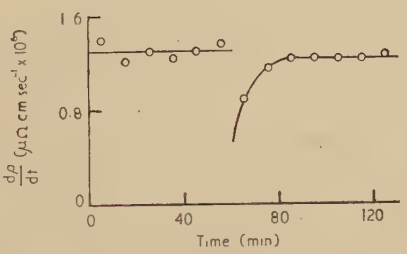

The growth to equilibrium at 190°C of an initially too small vacancy concentration.

Much of the data for the experiments described in § 4 *et seq.* was derived from the decay of excess vacancies at 130°C. This temperature was a convenient one practically and had the additional advantage that ordering due to the thermal equilibrium vacancy concentration was barely detectable. It was found that decay times were typically of the order of 10 hours and that the total drop in resistivity $\Delta\rho$, produced by an initial excess

vacancy concentration, was a reproducible quantity. As might be expected, the value of $\Delta\rho_b$ resulting from a constant bombardment was found to depend on the resistivity and, therefore, the degree of order. Figure 3.6 shows a plot of $\Delta\rho_b$ against ρ indicating that the ordering effect decreases as the equilibrium degree of order is approached. The partially ordered specimen used was heated between bombardments at 230°C to reduce ρ. It was noticed that, within experimental errors, the shape of the isotherms and hence the vacancy decay time was independent of ρ. Examples of these isotherms appear in later sections.

Fig. 3.5

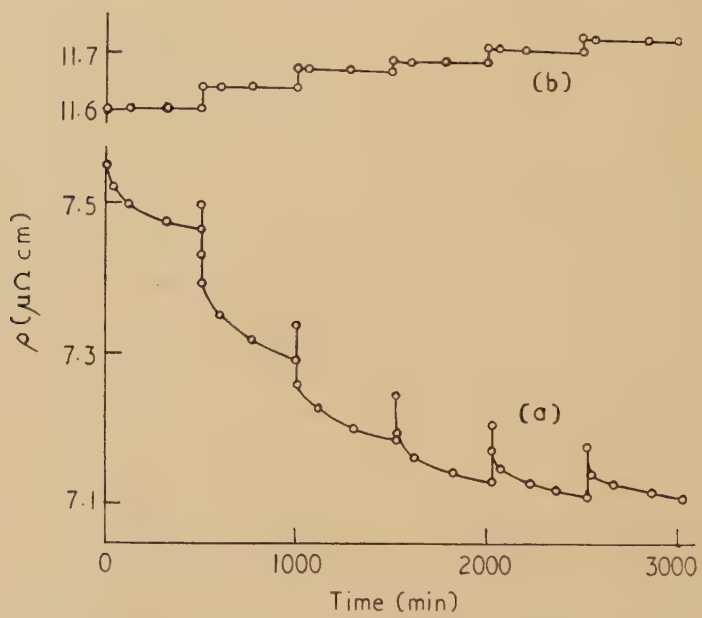

The effect on ordering at 100°C of a series of light deformations of (*a*) a partially ordered specimen, and (*b*) a disordered specimen.

In order to carry out a more detailed investigation of the properties of the vacancies the following assumptions were made : The vacancies are visualized as moving through the crystal sometimes putting wrong atoms right and sometimes putting right atoms wrong. When the degree of order S is below the equilibrium value S_e more are put right than wrong, and conversely if $S>S_e$. The ordering rate dW/dt (where W is the concentration of wrong atoms) is expected to be proportional to the vacancy concentration v and the hopping frequency ν_h, and also to be dependent on S. The rate of change of resistivity at constant temperature is therefore taken to be

$$\frac{d\rho}{dt}=\frac{d\rho}{dW}\frac{dW}{dt}=\frac{d\rho}{dW}v\nu_h f_T(S)=v\nu_h F_T(W). \quad . \; . \; . \quad (3.1)$$

in which $d\rho/dW$ and $f_T(S)$ have been combined into $F_T(W)$. On the usual simple models $\nu_h \sim \nu \exp(-E_m/kT)$ and the equilibrium value of $v \sim \exp(-E_f/kT)$ where ν is the atomic vibration frequency and E_m, E_f are, respectively, the activation energies for migration and formation of a vacancy.

Fig. 3.6

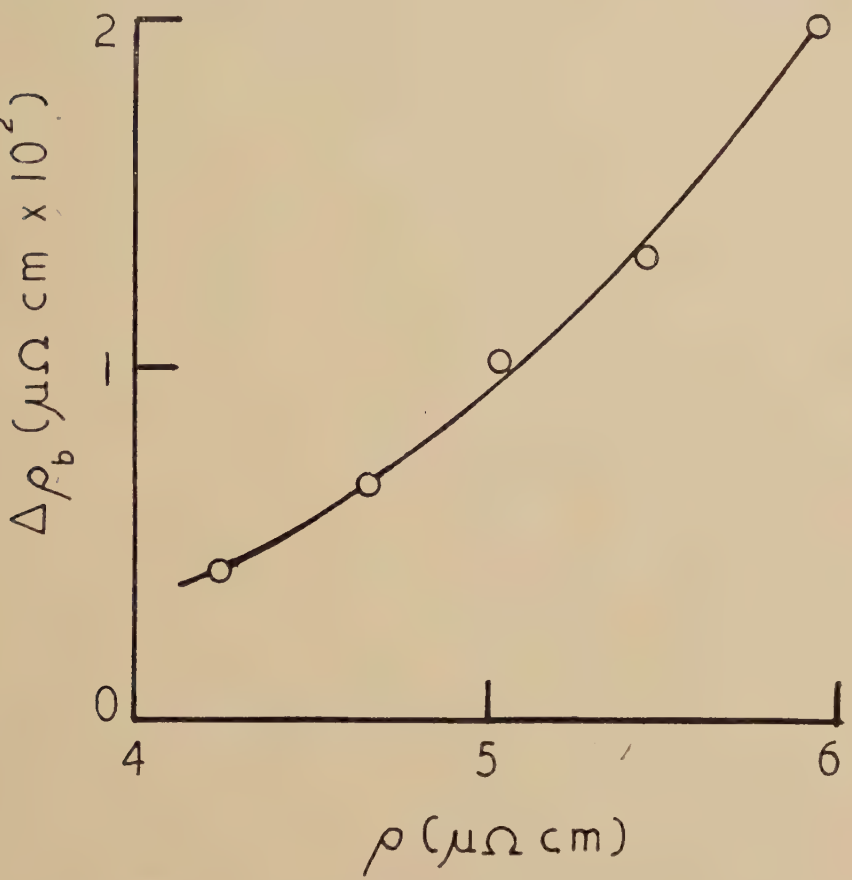

The ordering effect at 130°C due to bombardment with $1{\cdot}8 \times 10^{16}$ γ cm^{-2} as a function of resistivity.

It was shown in a previous paper (P1) that the ordering at low temperatures produced by an excess vacancy concentration is characterized by an activation energy of ~0·9 ev. This is now identified as the approximate value of E_m (a further discussion on this point occurs in § 5).

§ 4. E

From eqn. (3.1), the initial ordering rate at 130°C after quenching will be proportional to the frozen in vacancy concentration v and the function $F(W)$. If the latter can be eliminated it should be possible, by quenching, to obtain the temperature dependence of v and hence E_f. This was done

in the following manner: A partially ordered specimen was quenched from a series of temperatures. After each quench an isotherm at 130°C was taken, a fixed bombardment with γ-rays given and a further isotherm obtained. From the quench isotherms a set of values of the initial gradients g_q were obtained, and from the bombardment isotherms a set g_b. Plotting the latter as a function of resistivity allowed values of g_b at the beginning of the quench isotherms to be deduced by small extrapolations. Making the assumption that the bombardment induced vacancy concentration was independent of the degree of order then gave

$$\frac{g_q}{g_b} = \frac{u_q}{v_b} = \text{const. } \exp(-E_f/kT) \quad . \quad . \quad . \quad . \quad (4.1)$$

from which E_f was determined.

Fig. 4.1

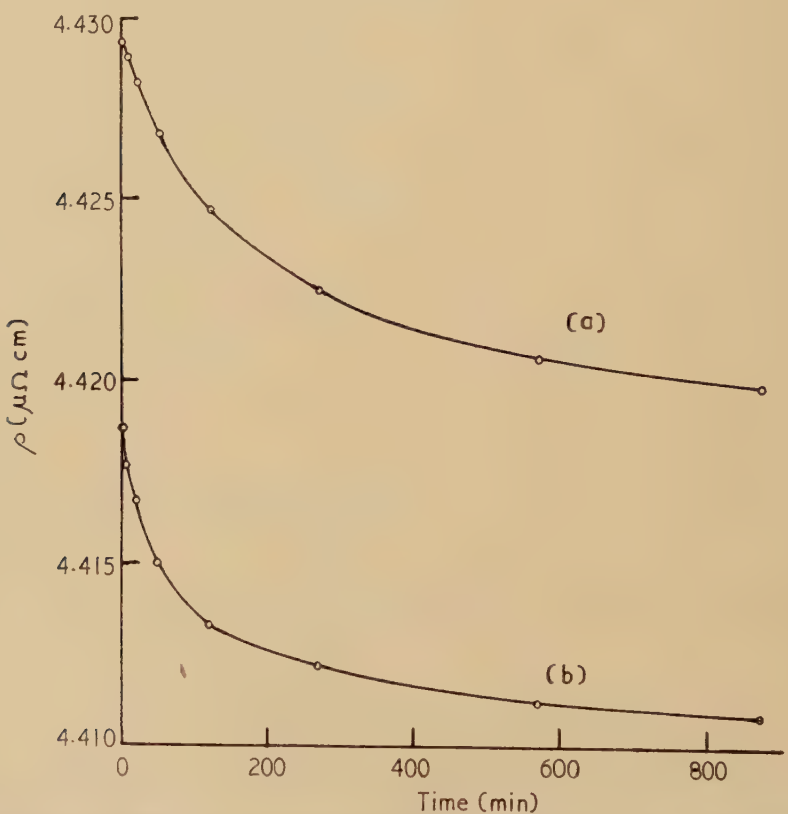

Isotherms at 130°C: (*a*) after quenching from 270·4°C, (*b*) after a subsequent bombardment with $1{\cdot}4 \times 10^{16}$ γ cm^{-2}.

In the actual experiment a partially ordered specimen was maintained at four temperatures in the range 250°C to 300°C for 17 hours and then water quenched. By way of example, the isotherms obtained after quenching from 270·4°C are shown in fig. 4.1 (the bombardment given was $1{\cdot}4 \times 10^{16}$ γ-cm ^{2}). It will be noticed that the shape of the curve is different in the two cases, the vacancies decaying more slowly after

quenching. This necessitated long heating at 130°C (not shown) before bombarding. On the other hand, it was found that all the isotherms of one type could be superimposed within the experimental error by normalizing the ordinates. This observation (discussed more fully in § 6) was of use since it allowed the values of g to be determined with a consistent rather than a variable error. The results obtained are given in the table. The final plot of $\log_{10}(g_a/g_b)$ against $10^3/T$ (using the corrected g_b) is shown in fig. 4.2 ; a good straight line results giving $E_f=1{\cdot}04$ ev.

T_a (°K)	ρ_a ($\mu\,\Omega$ cm)	$10^4\,g_a$ ($\mu\,\Omega$ cm min^{-1})	ρ_b ($\mu\,\Omega$ cm)	$10^4\,g_b$ ($\mu\,\Omega$ cm min^{-1})
573·2	4·831	4·4	4·777	2·6
557·6	4·611	2·0	4·587	2·0
543·6	4·429	0·85	4·419	1·7
529·7	4·310	0·42	4·306	1·4

Fig. 4.2

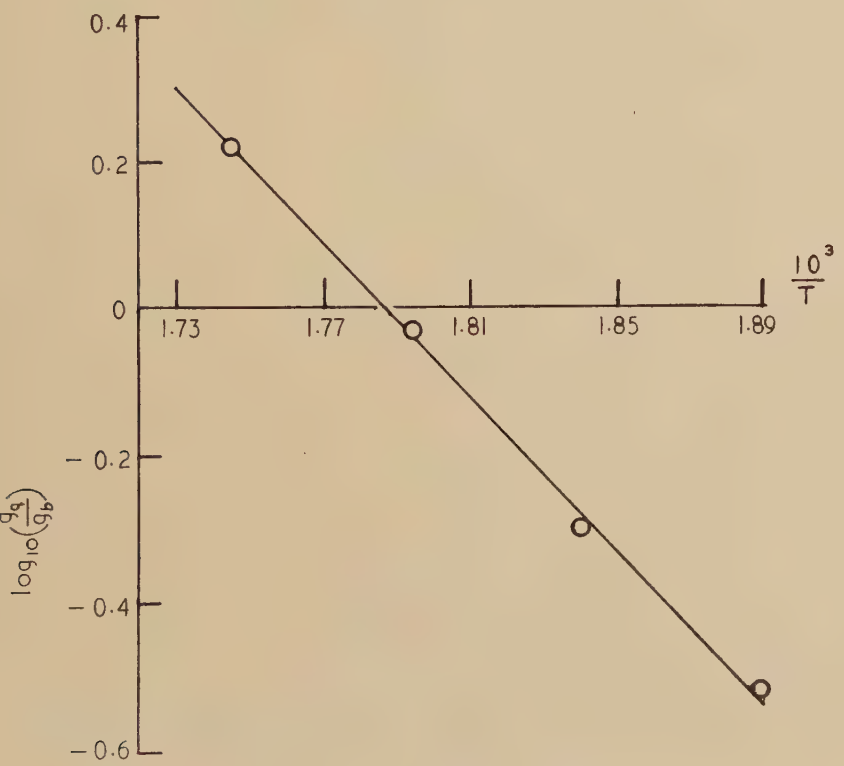

$\mathrm{Log}_{10}\,(g_a/g_b)$ as function of $10^3/T$.

The plot also gives $g_a/g_b=v_a/v_b=1$ at $T=560$°K. This allows a check on E_f to be made, for, using the value just quoted, $v_a\sim5\times10^{-10}$ at this

temperature, while, from the known γ flux and data given in the appendix, v_b is estimated to be $\sim 2\times 10^{-9}$ (this may actually be an over estimate as shown in § 7.)

A further rough check on E_f may be obtained in the following way: According to eqn. (3.1) the thermal ordering rate at high temperatures will be

$$\frac{d\rho}{dt} = \nu \exp(-(E_f+E_m)/kT)\, F_T(W).$$

Now it seems reasonable to suppose that the temperature dependence of the ordering rate lies mainly in $F(W)$ near to equilibrium and mainly in the exponential term when a long way from equilibrium. The ratio of the ordering rates at two temperatures T_1 and T_2 for the same value of W will be

$$\left(\frac{d\rho}{dt}\right)_1 \Big/ \left(\frac{d\rho}{dt}\right)_2 = \frac{F_1(W)}{F_2(W)} \exp\left[-(E_f+E_m)\left(\frac{T_2-T_1}{kT_1T_2}\right)\right]$$

from which a quantity Q may be obtained where

$$Q = E_f+E_m - \frac{kT_1T_2}{T_2T_1}\log\frac{F_1(W)}{F_2(W)} = \frac{kT_1T_2}{T_2-T_1}\log\left[\left(\frac{d\rho}{dt}\right)_2 \Big/ \left(\frac{d\rho}{dt}\right)_1\right]. \quad (4.2)$$

Putting in the values of E_f and E_m, Q should tend, therefore, towards $\sim 1{\cdot}9$ ev when a long way from equilibrium if the two temperatures are not very different.

Fig .4.3

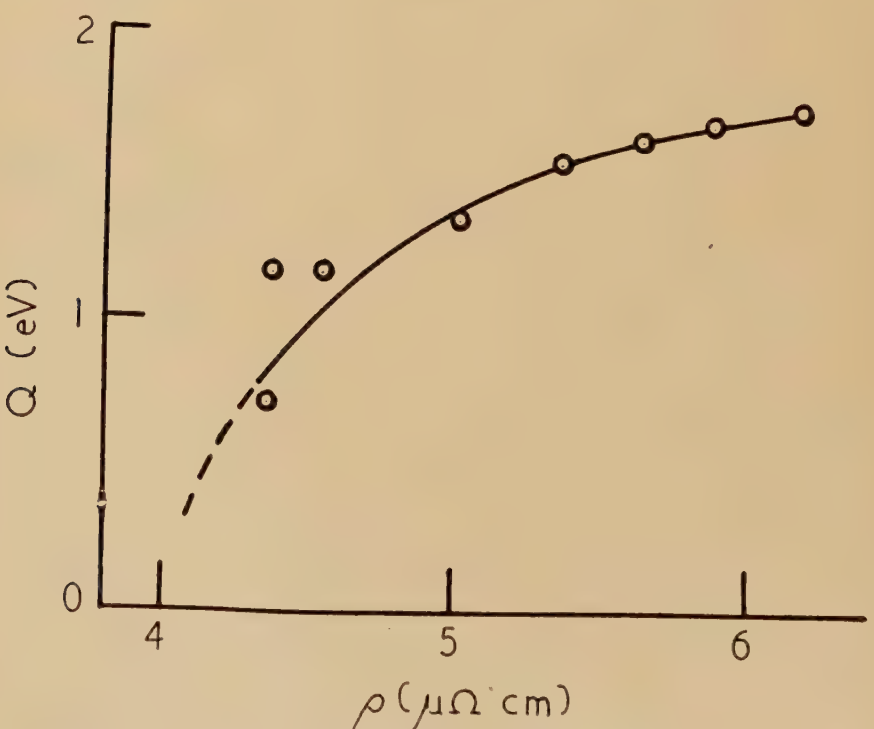

Q as a function of resistivity.

This has been tested in the following manner: A partially ordered specimen was allowed to relax towards a higher degree of order at 190°c and 210°c alternately, the gradients being measured at the temperature change points. By making the isotherms at each temperature sufficiently long the small effects due to the time required for the new equilibrium vacancy concentration to be establiished could be neglected. Intermediate heating periods were given at 230°c in order that a wide range in ρ could be covered in a reasonable time. Values of Q, so obtained, are plotted as a function of ρ in fig. 4.3. The expected trend is realized, the highest value of Q being about 1·7 ev. At the lower end, in the vicinity of $\rho \sim 4.5\ \mu\Omega$ cm, the results show a considerable scatter. This is discussed in § 5.

§ 5. The Vacancy Ordering Mechanism

The scatter in Q near equilibrium, just mentioned, initiated a more detailed study of the approach to equilibrium, this time at 230°c and 250°c, at which temperatures the ordering rates are conveniently higher.

Fig. 5.1

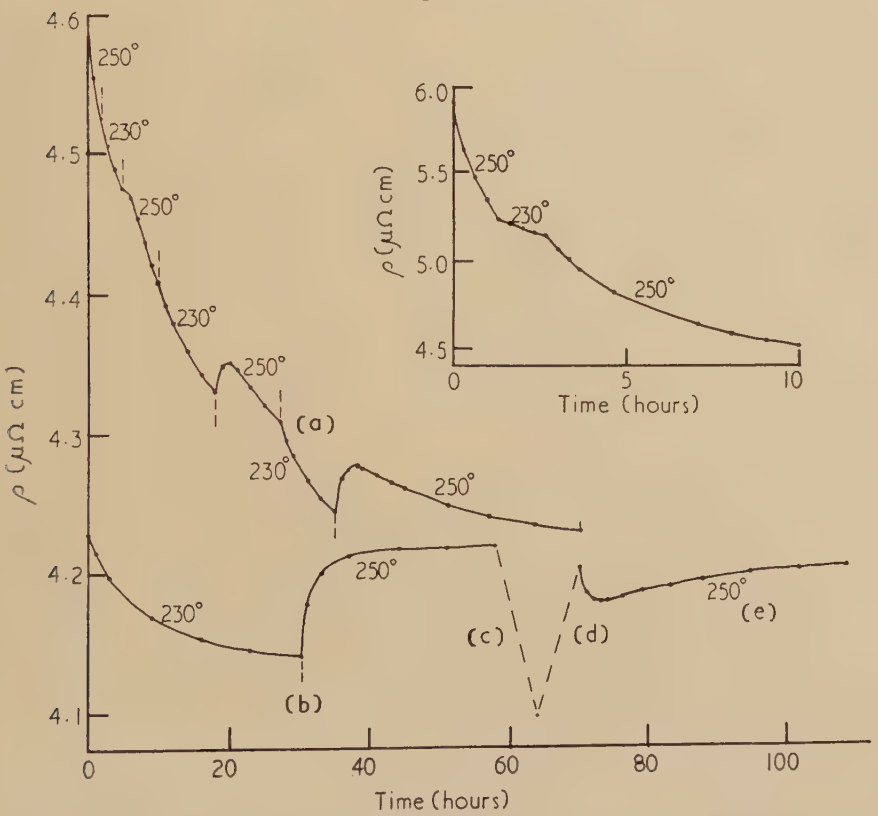

The approach to equilibrium at 250°c with alternate heatings at 230°c. The dashed markers on curves (*a*) and (*b*) indicate temperature change points.

The resistivity of a partially ordered specimen was followed as a function of time at these temperatures alternately. The behaviour in the early stages is shown inset in fig. 5.1. A measurement of Q at $\rho \sim 5{\cdot}2\,\mu\Omega$ cm gives a value of 1·4 ev in rough agreement with the results described above.

The interesting behaviour occurred as equilibrium at 250°c was approached, as illustrated by curve (*a*) of the main graph (which starts with the tail of the inset curve). It will be seen that, at the 230°c to 250°c change points, not only does the 250°c curve have a smaller gradient than the 230°c curve but, closer to equilibrium, this actually becomes positive before again going negative.

Fig. 5.2

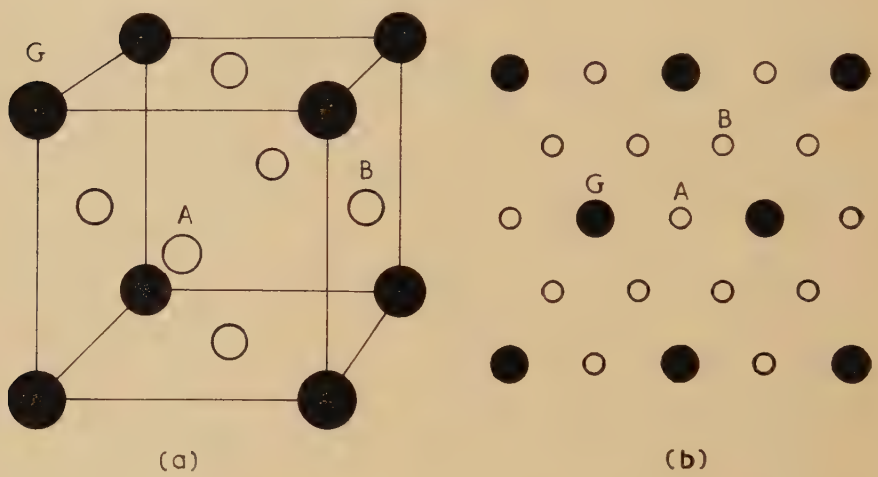

The perfectly ordered structure of Cu_3Au : (*a*) the unit cell, (*b*) the (111) plane.

To explain the phenomenon it is suggested that at least two types of wrong atom configurations were present, one of which was able to relax towards equilibrium more quickly than the other. These might be called, respectively, easy and hard types of disorder. At the 35 hour point, for example, the concentration of the easy type has been brought below the 250°c equilibrium value by heating at 230°c although this was not the case for the hard type. On returning to 250°c the easy type then relaxed upwards masking, for a while, the downward relaxation of the hard type.

The behaviour when very close to equilibrium at 250°c is shown by curve (*b*). This was obtained immediately after (*a*) but is returned to the origin for the sake of compactness. At 230°c relaxation of both types occurred with the result that on returning to 250°c both relaxed upwards and no peak occurred.

To test this explanation a heat treatment was devised which, it was hoped, would put the easy type above the 250°C equilibrium value and the hard type below, i.e. the reverse of the situation which had existed so far. On subsequent heating at 250°C the resistivity would then be expected to pass through a minimum. The heat treatment given consisted of 90 hours at 230°C, producing the drop shown dashed at (*c*), and 20 min. at 270°C, producing the increase shown dashed at (*d*). The aim was, first, to bring both below equilibrium at 250°C, and then to raise only the easy type above. On subsequent heating at 250°C the expected behaviour occurred as shown by curve (*e*). The effect was found to be quite sensitive to the time at 270°C, 10 min. being too short and 30 min. too long. This test also rules out the possibility of domain growth as the origin of the slower relaxation since the equilibrium domain size which would be implied has never been found.

Thus the scatter on the values of Q at $\rho \sim 4{\cdot}5\,\mu\Omega$ cm in the previous experiment are accounted for. The specimen must have been sufficiently near to equilibrium at 210°C for these effects to be significant.

A possible explanation of the easy and hard disorder is as follows: Consider the alloy in the perfectly ordered state as shown by the two diagrams of fig. 5.2. The simplest type of disorder is produced if the gold atom G is interchanged with the nearest neighbour copper atom A. The next simplest would be to interchange G with a next nearest neighbour B, and so on. Now consider how a moving vacancy might put these configurations right. The simplest type, the AG wrong pair, can be righted if a vacancy first arrives at the point G now occupied by the wrong copper atom. If it then interchanges with the gold atom, now at point A, and subsequently diffuses away (which it can do on copper sites only) the right configuration will result. For the wrong pair of type BG the process is more complicated. A vacancy has, first, to arrive at a point such as A and then interchange with the gold atom occupying point B. This now results in a wrong pair of the simpler type AG which can be righted either by a return of the vacancy to point G or by the arrival of a fresh vacancy if the first has diffused away. More complex wrong pairs would require correspondingly more stages in the righting process, each of which can be regarded as producing a wrong pair of simpler type. At equilibrium the concentration of the various types will be maintained by an equal and opposite transition between them. However, the rates of approach to equilibrium might well be different if the activation energies and other factors controlling the necessary atom vacancy interchanges are different.

A similar experiment to that just described was carried out at 290°C, at which temperature the ordering rates are much higher, to see if a third relaxation process could be distinguished, but none was found. The first two were again evident, this time lasting for periods of $\sim 0{\cdot}2$ and ~ 2 hours respectively; the resistivity then remained substantially constant for a further 20 hours. It may be that the majority of the disorder is due to only the two simplest types of wrong pair.

It is well known that, for an ordered alloy such as Cu_3Au, the electrical resistivity is not a unique function of the degree of order because of its dependence on both the domain size and the degree of order within the domains. The above observations show that even if the effect of domain size could be neglected ρ would still not be uniquely related to the degree of order. This has been further demonstrated in the following experiment:

A partially ordered specimen was prepared by two different heat treatments to about the same value of ρ and then bombarded after each with a fixed dose of γ-rays ($1{\cdot}4\times10^{16}\gamma$ cm ^{2}), and the resulting $\Delta\rho_b$, at 130°C, compared. The specimen was that used for the quenching experiments described in § 4, and the first treatment was taken as that for the 300°C quench and subsequent heating at 130°C; this resulted in $\rho=4{\cdot}78\,\mu\Omega$ cm (see the table). In this state the γ bombardment produced $\Delta\rho_b=1{\cdot}18\times10^{-2}$ $\mu\Omega$ cm. After heating the specimen for 2 hours at 370°C to recover the partially ordered state, the second treatment was given. This consisted of 10 hours at 230°C (producing $\rho=4{\cdot}97\mu\Omega$ cm) and 64 hours at 190°C (producing $\rho=4{\cdot}86\,\mu\Omega$ cm). After removing excess vacancies (a small effect after such a treatment), the bombardment gave $\Delta\rho_b=0{\cdot}69\times10^{-2}$ $\mu\Omega$ cm, which is considerably smaller. (Once again the two 130°C isotherms could be superimposed; i.e. the decay time of the excess vacancies was not altered.) The second treatment produced therefore, a state less sensitive to bombardment. It would appear that a lower concentration of easy disorder and higher concentration of hard disorder resulted.

This complexity of behaviour raises the problem of what exactly is meant by the activation energy for migration of vacancies E_m. According to the ordering mechanism here postulated there are several different types of hop which a vacancy may make, one of which is presumably the rate controlling process. Although this cannot be identified it is interesting to note that the decay time, and therefore (anticipating § 6) the number of such rate controlling hops before capture, is insensitive to the state of order.

§ 6. The Decay of Excess Vacancies at 130°C

From eqn. (3.1) the fall in resistivity at 130°C, due to excess vacancies, should be

$$\Delta\rho=\int_0^t\frac{d\rho}{dt}\,dt=\int_0^t v\nu\exp\left(-E_m/kT\right)(FW)dt.$$

Assuming that $F(W)\exp\left(-E_m/kT\right)$ can be taken as constant if $\Delta\rho$ is not too large, this may be written

$$\Delta\rho=\nu\exp\left(-E_m/kT\right)F(W)\int_0^t v\,dt.$$

The dependence of v on t is not known. One imagines, however, that the decay is due to the presence of vacancy capturing traps which might be

lattice imperfections, impurities, etc., or even interstitial atoms in the bombardment case. It will be supposed therefore (following Lomer and Cottrell 1955) that the vacancies make an average number $\bar{n}$ of hops before capture such that

$$\Delta\rho = \nu \exp(-E_m/kT)F(W)v_0\bar{t} \quad . \quad . \quad . \quad . \quad (6.1)$$

where v_0 is the initial vacancy concentration and $\bar{t}=\bar{n}\nu^{-1}\exp(E_m/kT)$ is the time required for $\bar{n}$ hops. It is the aim of the present section to find the factors controlling $\bar{n}$. In the experiment about to be described the time $t_{1/2}$ required to reach $\frac{1}{2}\Delta\rho$ at 130°C is taken as a measure of $\bar{t}$.

It was first thought that the domain boundaries might act as vacancy traps and, accordingly, an experiment to investigate the effect of domain size was carried out. In fig. 6.1. $\Delta\rho$ is plotted as a function of time at 370°C, the temperature used to grow the domains. After each period at 370°C the specimen was cooled to room temperature fairly quickly (~5 min), excess vacancies removed by heating at 160°C and 130°C and $\Delta\rho_b$ obtained (γ dose $=1{\cdot}5\times10^{16}\gamma$ cm^{-2}). In some cases it was then heated at 300°C for 2 hours and water quenched to obtain $\Delta\rho_q$. The value of the resistivity after each preparation is also plotted, indicating the growth of the domains. It will be seen that there is a small dependence on domain size in the bombardment case, but hardly any in the quench case. At the end of the experiment, the specimen was disordered by heating at 400°C when a partial repeat of the process gave similar results.

Fig. 6.1

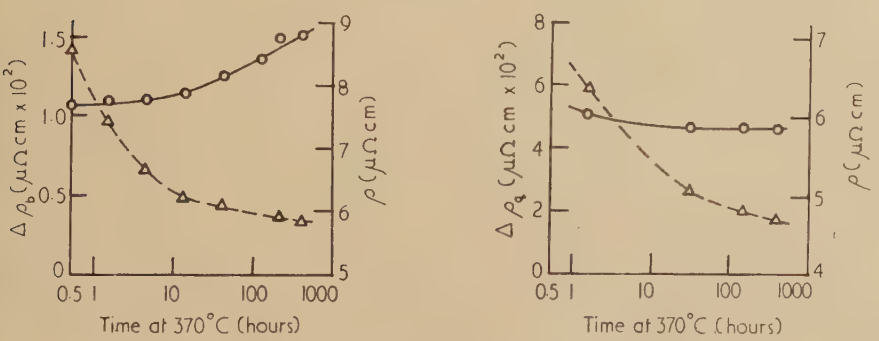

$\Delta\rho_b$, $\Delta\rho_q$ and ρ (dashed curves) as a function of time at 370°C.

The values of $t_{1/2}$ for the bombardment isotherms were found to increase slightly from about 50 min. to about 70 min. although, for the quench isotherms, they remained constant at about 100 min. Thus, taking $E_m=0{\cdot}9$ ev and $\nu=10^{13}$ sec^{-1}, the values of $\bar{n}$ were, for bombardment ($\bar{n}_b$), $1{\cdot}3\times10^5$ to $1{\cdot}9\times10^5$ and, for quenching ($\bar{n}_q$), $2{\cdot}7\times10^5$. The observation that $\bar{n}_q>\bar{n}_b$ appears to be characteristic; it was noticed in various exploratory experiments. An example afforded by the present

work comes from the quenching experiments described in § 4 in which $\bar{n}_b$ was $1{\cdot}6\times10^5$ and $\bar{n}_q$ $3{\cdot}8\times10^5$.

The effect of domain size is therefore not very great. It was discovered on the other hand, that the preliminary heat treatment had a strong influence on $\bar{n}$. As described in § 2, this consisted of 2 hours at 900°C in argon followed by a heat treatment at 600°C. The latter was found to be very important in that $\bar{n}$ could be increased by prolonging the treatment.

To investigate the effect further, a specimen was first prepared by heating at 900°C for 8 hours followed by cooling to room temperature in a few minutes (no change in weight $>0{\cdot}1\%$ occurred). The 600°C treatment was omitted but the ordering treatment, consisting of 5 days at 370°C (giving $\rho=6{\cdot}25\,\mu\Omega$ cm), was given. After the usual treatment to remove excess vacancies, it was bombarded with $1{\cdot}8\times10^{16}\,\gamma$ cm^{-2} and then heated at 130°C to obtain a bombardment isotherm. However, no fall in resistivity occurred. It was then heated at 320°C for 17 hours and quenched (giving $\rho=5{\cdot}35\,\mu\Omega$ cm) but again, on heating at 130°C, there was no further change in resistivity. A quench from ~370°C (giving $\rho=6{\cdot}70\,\mu\Omega$ cm), which, in specimens given the normal preparation, would have resulted in a large $\Delta\rho$ at 130°C, produced the same null effect. The values of ρ just quoted indicate the operation of the ordering mechanism at high temperature and yet no effect, due to excess vacancies, could be induced at 130°C. Ordering at high temperatures was verified by repeating part of the approach to equilibrium experiments at 250°C and 230°C described in § 5 ; although the ordering rates at a given ρ were somewhat smaller, the easy and hard relaxation processes were again evident.

This behaviour is explained if the heat treatment resulted in a value of $\bar{n}$ so small that the lifetimes of the vacancies, and consequently the ordering they produced at 130°C, were negligible. This would imply that a high concentration of vacancy traps was induced. Their presence would still allow ordering at high temperatures where the equilibrium concentration of vacancies in solution would be maintained.

The effect of the time at 600°C was next studied. The specimen, after being heated at 600°C for a certain time, was given a standard ordering treatment of 5 days at 370°C. Bombardment and quench isotherms (after 17 hours at 320°C) at 130°C were then taken. These, together with the null results just mentioned are plotted on a logarithmic time scale in fig. 6.2. It is apparent that $\Delta\rho$ was influenced strongly by the 600°C treatment, the effect being more pronounced in the case of the quench isotherms. A repeat of the 900°C treatment at the end of the experiment again put the specimen in the ' null ' state.

Values of $\bar{n}_b$ and $\bar{n}_q$ determined from these curves are plotted as a function of time at 600°C (log scale) in fig. 6.3. Once again $\bar{n}_q>\bar{n}_b$ although both must be very small at $t_{600}=0$. The limited data suggest that n_b saturates while $\bar{n}_q$ is still increasing.

It is suggested that the vacancy traps responsible for this behaviour are impurity atoms (not identified) which are relatively soluble at 900°C

and relatively insoluble at 600°C. Cooling the specimen fairly quickly from 900°C would then leave a supersaturated solution, the concentration

Fig. 6.2

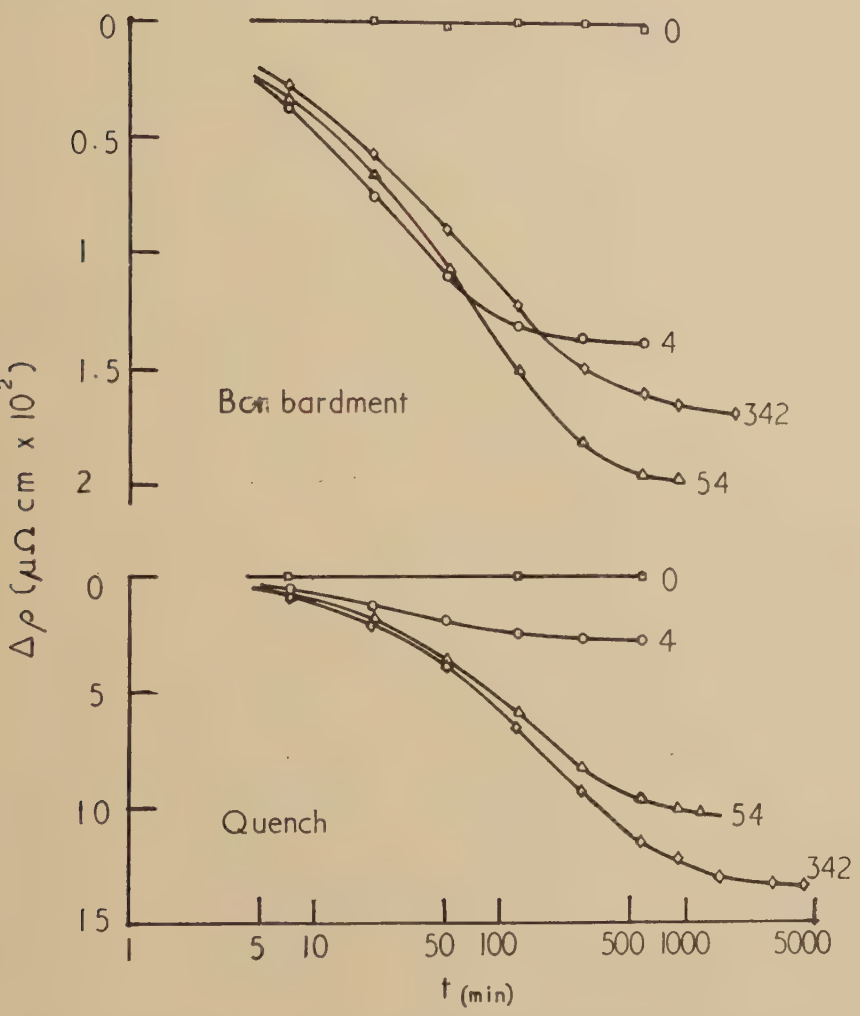

The effect of the duration of the 600°C treatment on the 130°C isotherms. The number against each curve refers to the time in hours at 600°C. The initial resistivities of the curves, in order of increasing t_{600}, were 6·25, 6·22, 5·96, 5·90 $\mu\Omega$ cm, for the bombardment set, and 5·35, 5·21, 5·19, 5·20 $\mu\Omega$ cm, for the quench set.

of which could be reduced in a reasonable time (presumably by diffusion) by heating in the neighbourhood of 600°C. A rough estimate of the

concentration at different stages of the experiment can be made in the following way :

For a random distribution of vacancies and impurity atoms the relation $\bar{n} \sim 1/ZC$ would be expected, where C is the impurity concentration and Z is the number of neighbouring sites in which a vacancy can be regarded as trapped. Taking $Z \sim 10$ gives $C \sim 1/10\bar{n}$ (the number of sites neighbouring a substitutional impurity is actually 12). Applying this to the experimental results, the concentration was reduced to $\sim 3 \times 10^{-7}$ by heating at 600°c for 342 hours. The concentration which would prevent

Fig. 6.3

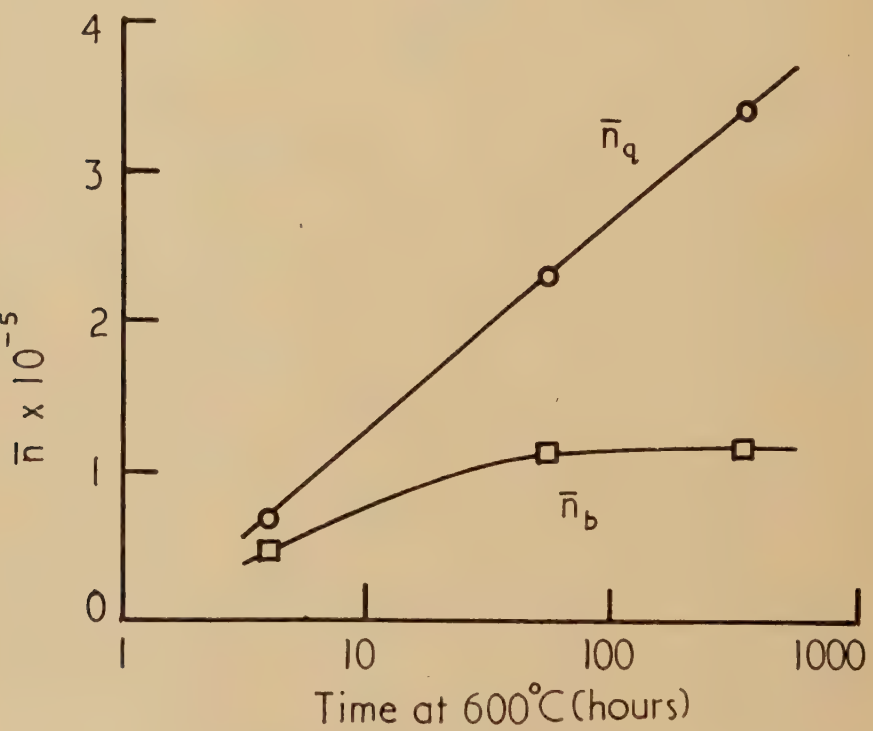

$\bar{n}_q$ and $\bar{n}_b$ as a function of time at 600°c.

the detection of ordering after quenching from 320°c may also be estimated. From eqn. (6.1) $\Delta\rho \propto \bar{l}$. This was roughly satisfied by the quench isotherms for which $\Delta\rho \sim 10^{-3} t_{1/2}$ ($\Delta\rho$ in $\mu\Omega$ cm and $t_{1/2}$ in minutes). Taking the limit of detectability for $\Delta\rho$ to be $5 \times 10^{-4}\,\mu\Omega$cm. this gives $t_{1/2} \sim \frac{1}{2}$ min. and hence $\bar{n}_q \sim 10^3$ and $C \sim 10^{-4}$. Such a concentration is consistent with the chemical analysis of the alloy.

To account for the smaller value and possible saturation of $\bar{n}_b$ it is necessary to have some extra trapping sites present after bombardment which are not present after quenching. These might well be interstitials.

According to the estimate made in the appendix, the bombardment would put in an interstitial concentration of $\sim 10^{-9}$. The maximum value of $\bar{n}_b$ reached was $\sim 10^5$, requiring z in this case, to be $\sim 10^4$. This rather large value is interpreted to indicate that interstitials are extremely effective in capturing vacancies.

§ 7. The Behaviour of Interstitials

Brinkman *et al.* (1954) concluded, from an experiment which they performed, that interstitials are more mobile than vacancies in Cu_3Au. Two specimens, one partially ordered and the other disordered, were given identical bombardments with 9 Mev protons at $-180°$C which produced a large increase in resistivity in the first and a smaller increase in the second. The temperature was then raised steadily to 130°C. In the region $-60°$C to 0°C about equal annealing occurred in both, removing almost all the extra resistance of the initially disordered specimen. Approaching 130°C, a further drop occurred in the initially partially ordered specimen, but none in the disordered one. The low temperature drop was assigned to the recombination of vacancies and interstitials through interstitial migration, and the high temperature drop to ordering through vacancy migration.

The authors pointed out that after the low temperature process was complete a small concentration of vacancies would remain if natural sinks for the interstitials existed; due to their presence, some of the interstitials would disappear without annihilating vacancies. This observation is here used to test their conclusions by a different type of experiment.

Suppose there is a concentration of sinks s for interstitials and let a bombardment be given during the course of which i_0 interstitials and v_0 vacancies are formed ($i_0=v_0$). Three interesting bombardment temperatures will be distinguished: (1) a low temperature at which both interstitials and vacancies are immobile, (2) a medium temperature at which only interstitials are mobile, (3) a high temperature at which both are mobile. If, after bombardment at each of the two lower temperatures, the specimen is raised to (3) ordering will occur. Due to the migration of interstitials and consequent annihilation of vacancies, the number of vacancies contributing to ordering will be different in each case. This number will now be determined as a function of dose for the three cases, assuming that the probabilities of capture of interstitials by sinks and vacancies are proportional to their respective concentrations.

(1) At the end of the bombardment the full concentration of interstitials (i_0) and vacancies (v_0) will be present. During the heating to the high temperature the relation between the change of the one and the change of the other will be

$$dv = \frac{\alpha v}{\alpha v + \beta s} di$$

where α and β are constants of proportionality. The final vacancy concentration v_f, when all the interstitials have gone, is obtained by integrating this expression, i.e.

$$\int_{i_0}^{0} di = \int_{v_0}^{v_f} \frac{\alpha v + \beta s}{\alpha v} dv$$

which gives

$$\frac{\alpha v_f}{\beta s} = \log \frac{v_0}{v_f}. \qquad \ldots\ldots\ldots \quad (7.1)$$

(2) In this case the interstitials are mobile immediately they are formed. Thus the relation between the growth of the vacancy concentration and the formation of interstitials is

$$dv = di\left(1 - \frac{\alpha v}{\alpha v + \beta s}\right).$$

Integrating to obtain v_f

$$\int_{0}^{i_0} di = \int_{0}^{v_f} \frac{\alpha v + \beta s}{\beta s} dv$$

which gives

$$\frac{\alpha v_f}{\beta s} = \left(1 + \frac{2\alpha v_0}{\beta s}\right)^{1/2} - 1. \qquad \ldots\ldots \quad (7.2)$$

(3) Here, both are mobile, the vacancies producing an amount of ordering dependent only on how far they get before capture. If the rate of production of displacements is small the vacancy concentration will also remain small, due to the limitation of their lifetimes by vacancy capturing traps (see § 6). Consequently the probability of vacancy annihilation by moving interstitials will be small. It will be assumed therefore that under these conditions effectively all the vacancies contribute to ordering, i.e.

$$v_f = v_0 \qquad \ldots\ldots\ldots \quad (7.3)$$

Plots of $\alpha v_f/\beta s$ against $\alpha v_0/\beta s$, for the three cases, are shown in fig. 7.1. Taking ordering at 130°c to be proportional to v_f, a plot of $\Delta\rho_b$ against dose should resemble these curves if two suitable lower temperatures are chosen. Such an experiment was carried out ; a partially ordered specimen was bombarded at 130°c, 0°c and −196°c. The bombardment rate was $1{\cdot}4\times10^{14}\,\gamma\,\mathrm{cm}^{-2}\,\mathrm{hour}^{-1}$, which was small enough to satisfy the condition mentioned under (3) (the half time of the vacancy decay was ~1 hour) and large enough for thermal ordering at 130°c to be negligible. The results obtained are plotted in fig. 7.2. The curvature of the 130°c plot is attributed mainly to the change in $F(W)$ occurring during the course of the experiment. Figure 7.3 shows a corrected version to take account of this. The correction, obtained from the deviation from linearity at 130°c, has been applied to all three curves.

Although the theoretical and experimental curves cannot be closely fitted together, which, perhaps, is not surprising in view of the elementary model assumed, the qualitative resemblance supports the hypothesis.

An estimate for s can be made by a very rough fitting, assuming the cross section for displacement to be $1{\cdot}5\times10^{-25}$ cm^2 (see appendix); this gives $s\sim2\times10^{-10}\alpha/\beta$.

Fig. 7.1

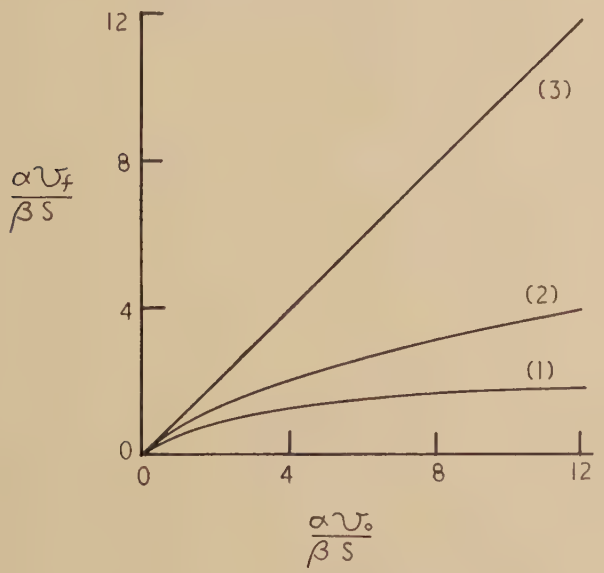

$\alpha v_f/\beta s$ as a function of $\alpha v_0/\beta s$ for the three temperatures (1), (2) and (3).

Fig. 7.2

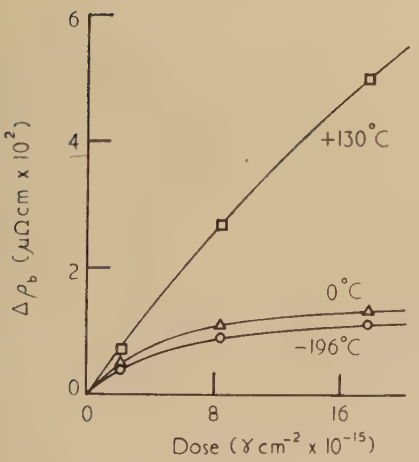

The ordering effect at 130°C as a function of γ-bombardment at the three temperatures indicated.

Fig. 7.3

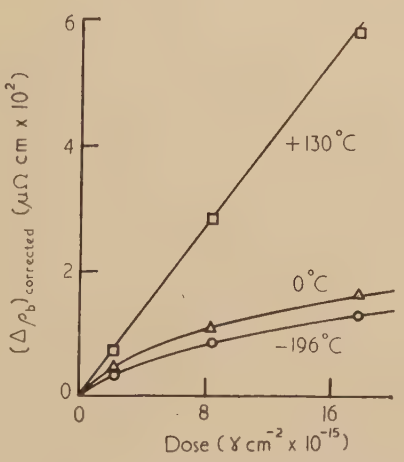

The corrected version of fig. 7.2.

According to the conclusions reached in § 6, interstititials are still present at 130°C. If this is so, some, at least, of the sinks might be better described as traps which anchor an interstitial without annihilating it. As pointed out by Lomer and Cottrell (1955), impurities might well act in this way. If a range of such traps exists, each with a different binding energy, s will be greater the lower the temperature. This may be an important factor in the immobilization of interstitials at low temperatures.

§ 8. Conclusion

The various experiments show that a vacancy ordering mechanism is a tenable hypothesis. The activation energies of formation and migration of vacancies, E_f and E_m, are about 1·0 ev and 0·9 ev respectively. The interaction between vacancies and wrong atoms is complex, leading to at least two relaxation periods in the ordering process which can be distinguished near equilibrium. A possible model, in terms of wrong atom configurations, to account for these has been given. The decay time of an excess vacancy concentration appears to be limited by the presence of vacancy capturing impurity atoms (not identified), the concentration of which can be varied by suitable heat treatment. Interstitials are more mobile than vacancies at a given temperature, but these too are probably trapped and can in turn contribute to the limitation of the vacancy decay time.

Acknowledgment

The author's thanks are due to Miss J. C. Matthews who obtained much of the data.

APPENDIX

The Displacement of Atoms by ^{60}Co *γ-rays*

The main interactions by which ^{60}Co γ-rays (mean energy$\sim$1·2 Mev) can displace atoms in Cu_3Au appear to involve the Compton and Photoelectric processes. These processes lead to energetic electrons which can produce displacements by elastic collisions with the nucleii. The displacement cross section σ_γ consists, therefore, of the product of two terms which are : (1) the cross section for producing an electron, (2) the probability that this will produce a displacement. An order of magnitude calculation, which assumes the threshold displacement energy E_d to have the usual value of 25 ev, gives $\sigma_\gamma \sim 10^{-25}$ cm^2.

Near the surface the density of displacements will, in general, be different to that in the interior ; electrons produced in the surface regions will have a chance of escape, although some compensation will occur due to incoming electrons produced in the surrounding material (usually mica). Thus, in effect, the cross section for producing displacements near the surface will depend on the environment. The effect was demonstrated with the aid of a thin specimen made from foil of thickness 0·005 cm. This was mounted in a polythene container and irradiated in an

approximately isotropic flux of γ-rays, first of all bare, and then with each surface covered by an additional Cu_3Au foil of thickness 0·007 cm. Although the irradiations were both equal, the subsequent $\Delta\rho_b$ at 130°C was about 18% greater after the second. The increase is attributed to a higher flux of incoming electrons in the presence of the extra foils, due to the appreciable production of photoelectrons not present in the polythene environment. It was estimated that about 30% more atoms were displaced (the dose was $1{\cdot}4\times10^{16}$ γ cm^{-2}).

The extra foils in the above experiment can be considered to have allowed the full production of vacancies in the specimen. Advantage was taken of the arrangement to measure σ_γ in terms of σ_1 the displacement cross section for 1 MEV electrons. An electron bombardment was given which produced the same effect as the second γ-bombardment above. From the ratio of the integrated fluxes it was found that $\sigma_\gamma\sim\sigma_1/200$. Accepting a previously estimated value of σ_1 to be 3×10^{-23} cm^2 (see P1) the value of $\sigma\gamma$ is therefore $\sim1{\cdot}5\times10^{-25}$ cm^2.

Although E_d has been taken to be 25 ev it was found, in fact, that displacements occur with lower recoil energies. Thus 0·3 MEV electrons, which can only give up to 13·5 ev to the copper atoms, produced a small effect. Using the thin specimen mentioned above, the ratio $\sigma_{0\cdot3}/\sigma_1$ was found to be $\sim10^{-3}$ (but this is an underestimate due to the small range of $\sim$0·006 cm of 0·3 MEV electrons in Cu_3Au). It may well be, as pointed out by Huntington (1954), that E_d has not a sharp value, the probability of displacement depending on the recoil direction with respect to the lattice as well as the recoil energy.

References

BRINKMAN, J. A., DIXON, C. E., and MEECHAN, C. J., 1954, *Acta Metallurgica*, **2**, 38.

DUGDALE, R. A., and GREEN, A., 1954, *Phil. Mag.*, **45**, 163.

HUNTINGTON, H. B., 1954, *Phys. Rev.*, **93**, 1414.

KINCHIN, G. H., and PEASE, R. S., 1955, *Rep. Prog. Phys.*, **18**, 1.

LOMER, W. M., and COTTRELL, A. H., 1955, *Phil. Mag.*, **46**, 711.

SEITZ, F., 1952, *Advances in Physics*, **1**, 43.

SIEGEL, S., 1951, *Phase Transformation in Solids* (London : John Wiley and Sons), p. 366.

SYKES, C., and JONES, F. W., 1936, *Proc. Roy. Soc.* A, **157**, 213 ; 1938, *Ibid.*, **166**, 376.

LVI. *Scattering of Cold Neutrons in Liquid Metals and the Entropy of Disorder*

By L. S. Kothari, K. S. Singwi and S. Visvanathan†
Atomic Energy Establishment, Bombay.

[Received September 21, 1955 and in revised form December 31, 1955]

Abstract

Introducing a varying degree of disorder in Mott's quasi-crystalline model of liquid metals, the change in the cold neutron scattering cross section on melting is calculated. Motts' calculations of the change in electric conductivity on melting have been repeated on the basis of this modified model using more recent data on the latent heat of fusion. It is shown that the change in the neutron scattering cross section in lead and the change in conductivity in sodium and potassium on melting can be explained if we assume that the entropy of disorder on melting is nearly $0{\cdot}5R$, R being the gas constant. That this value is of the right order of magnitude seems to be corroborated by self-diffusion data.

§ 1. Introduction

Recent theoretical work of Placzek (1954) and others (Squires 1952, Kothari and Singwi 1955) has been fairly successful in explaining the temperature dependence of the inelastic scattering cross section of cold‡ neutrons in polycrystalline solids. The present paper is an attempt to explain the cold neutron scattering at the melting point of a solid. This, obviously, involves a knowledge of the state of matter near the melting point for which no satisfactory theory exists so far. We have, therefore, to assume some model of the liquid state near the point of fusion.

Mott (1954) (hereafter referred to as I) in his attempt to explain the change in electrical conductivity of metals in going from the solid to the liquid state, assumed a quasi-crystalline structure of the liquid. In this model it is assumed that atoms continue to vibrate as in a solid, though with a lower characteristic frequency due to loosening of structure, about a mean position which moves about at random.

On the basis of the above model Mott obtained a reasonable agreement between theory and experiment. In the present paper, using a similar model, we calculate the change in the inelastic neutron scattering cross section in going from the solid to the liquid state. In contrast to the conductivity which mainly depends upon the Debye temperature and the

† Communicated by the Authors.

‡ The word ' cold ' is used here to denote neutrons of wavelength greater than that corresponding to the Bragg-cutoff.

density of electron states near the top of the Fermi distribution, both of which alter on melting, the situation for neutron scattering is much simpler in that it depends only on the former. It is difficult to calculate the density of states in the liquid state since the precise shape of Brillouin zones is not known.

The model that we have adopted for our calculations is that of Lennard-Jones and Devonshire (1939), based on the assumption that in the process of melting a number of new lattice positions (called β-sites) equal in number to the original sites (called α-sites) appear. The redistribution of the atoms between the old α-sites and the new β-sites involves an increase in the entropy. In other words, the entropy of disorder, the nature of which we wish to investigate, arises from the variety of ways in which the singly-occupied cells in the liquid can be arranged on a pseudo-lattice. This entropy is a complicated function of the order-parameter which in turn is a function of the force constants between the atoms. With our present state of knowledge it is difficult to calculate the exact value of the entropy of disorder.

Apart from its intrinsic interest, a study of the cold neutron scattering at the melting point of a solid may provide a somewhat reliable method of estimating the magnitude of the change in the entropy of disorder in going from the solid to the liquid state. The present paper is an attempt to estimate the magnitude of this entropy from the electron as well as the neutron scattering data at the melting point. Our results are of course based on the assumption of a quasi-crystalline model of the liquid state. We do not for a moment suggest that the true state of affairs at melting is what is given by this model. We, however, do suggest that it appears to be a reasonable working model.

§ 2. Mathematical Formulae

In deriving the expression for the Debye temperature Θ_L, in the liquid state, we proceed in a manner similar to that of I, where Θ_L is obtained by equating the chemical potentials μ_S and μ_L of the solid and liquid phases respectively, at the melting point T_M.

The chemical potentials $\mu_S(T_M)$ and $\mu_L(T_M)$ are respectively (see Fowler and Guggenheim, *Statistical Thermodynamics*, p. 329)

$$\mu_S(T_M) = -\chi_S{}^0 + 3kT_M \log_e [1-\exp(-h\nu_S/kT_M)] - kT_M \log_e J_S(T_M) + pV_S, \quad \ldots\ldots\ldots \quad (1\,a)$$

and

$$\mu_L(T_M) = -\chi_L{}^0 + 3kT_M \log_e [1-\exp(-h\nu_L/kT_M)] - kT_M \log_e J_L(T_M) + pV_L - \alpha kT_M, \quad \ldots\ldots\ldots \quad (1\,b)$$

where the subscripts L and S denote the liquid and solid phases respectively, L is the latent heat of fusion, k is the Boltzmann constant and other terms have their usual significance.

Formulae (1 *a*) and (1 *b*) are based on the Einstein approximation which is valid in our case since $T \gg \Theta$. The additional term αkT_M in

(1 *b*) represents the energy corresponding to the entropy of disorder in the liquid state arising from the number of ways in which the singly-occupied cells of the liquid can be arranged on a pseudo-lattice. In fact αk represents the entropy of disorder and is given by eqn. (1) of Appendix A, the derivation of which is given by Lennard-Jones and Devonshire (eqn. (12-B), 1939). We have here assumed α to be independent of temperature.

On equating $\mu_S(T_M)$ and $\mu_L(T_M)$ and neglecting the small differences between both the third and fourth terms of (1*a*) and (1*b*), we obtain the following formula for Θ_L,

$$\frac{L-\alpha kT_M}{3kT_M}=\log_e\frac{1-\exp\left(-\Theta_S/T_M\right)}{1-\exp\left(-\Theta_L/T_M\right)}, \qquad \ldots \quad (2)$$

where $L=\chi_S{}^0-\chi_L{}^0$, represents the latent heat of fusion.

Equation (2) differs from eqn. (1.1) of I in that the former contains an extra factor αkT_M. It is difficult to estimate the value of α in the absence of any proper theory of melting. We have, therefore, used in our calculations different values of α, ranging from 0 to 1 to see which value gives a reasonable agreement with experiment.

If we use Placzek's incoherent approximation the inelastic neutron scattering cross section is given by the formula

$$\sigma_{T_M}=\frac{3(S+s)}{Mk_1}\left\{\left(-\frac{1}{7}+\frac{2}{5}\frac{T_M}{\Theta_S}\right)+k_1{}^2\left(\frac{5}{3}\frac{T_M}{\Theta_S}-\frac{1}{2}\right)\right.$$
$$\left.+k_1{}^4\left(\frac{7}{4}\frac{T_M}{\Theta_S}-\frac{7}{24}\right)+k_1{}^6\left(\frac{3}{8}\frac{T_M}{\Theta_S}+\frac{3}{16}\right)\right\}, \qquad \ldots \quad (3)$$

(see eqns. (40) and (41), Kothari and Singwi 1955). In eqn. (3), S and s denote respectively, the coherent and the incoherent scattering cross sections per atom, M is the atomic mass expressed in terms of the neutron mass m_0 and k_1 is the wave number in dimensionless units corresponding to the neutron wave length λ and is given by

$$k_1=\left(\frac{\hbar^2}{2m_0k}\right)^{1/2}\frac{2\pi}{\Theta_S{}^{1/2}\lambda}. \qquad \ldots \quad (4)$$

We assume that the scattering cross section in the liquid state is also given by (3) and (4) with Θ_S replaced by Θ_L, and where Θ_L is given in terms of Θ_S by (2).

It may be pointed out here that though formula (3) takes care of all the multi-phonon processes which are important for temperatures of interest, its derivation is based on the assumption that atomic vibrations remain harmonic. The neglect of the contribution arising from anharmonic effects is a simplification. Since we are interested only in the difference of the scattering cross sections in the liquid and solid states at the melting point, the neglect of anharmonic contribution may not be serious.

In order to see whether the value of α as obtained from the neutron scattering data is consistent with that obtained from the change in electrical conductivity in going from the solid to the liquid state, we have repeated Mott's calculations, using recent values of the latent heat

of fusion and also taking into account the factor $\alpha k T_M$. Without repeating Mott's arguments we shall write the expression for the ratio of electrical conductivities as

$$\left(\frac{\eta_S}{\eta_L}\right)_{T_M} = \left(\frac{\Theta_S}{\Theta_L}\right)^2 \frac{[K(dE/dK)]_S^2}{[K(dE/dK)]_L^2}, \quad \ldots\ldots (5)$$

where the subscripts L and S have the same meaning as before, K denotes the wave number of an electron at the top of the Fermi distribution and E is the kinetic energy of such an electron. In writing eqn. (5) we have assumed with Mott (1934) that all other factors in the usual conductivity expression except those retained on the right-hand-side of (5) do not change appreciably on melting. Our model of the liquid state enables us to calculate Θ_L in terms of Θ_S, which is known. It, however, does not enable us to calculate $[K(dE/dK)]_L$ in terms of the corresponding quantity in the solid state, thus introducing considerable uncertainty in the calculation of η_L. For good conductors and especially for monovalent metals, using the same argument as given by Mott, we can write (5) with good approximation as

$$\left(\frac{\eta_S}{\eta_L}\right)_{T_M} = \frac{\Theta_S^2}{\Theta_L^2}. \quad \ldots\ldots\ldots (6)$$

The validity of (6) is doubtful for other metals.

§ 3. Results

Using eqns. (2), (3), (4) and (6) and different values of α we have calculated $(\eta_S/\eta_L)_{T_M}$ and $(\sigma_L - \sigma_S)/\sigma_S \times 100$ for various metals, and the results are shown in table 2.

Values of constants used in our calculations are given in table 1.

Table 1. Data for Various Metals

Element	Atomic weight	Melting point T_M °K	Latent heat of fusion in cal/gm	Debye Temp. (solid) Θ_S °K	$S+s$ (barns)	Wave number of neutrons in dimensionless units (eqn. (3))† k_1
Pb	207·2	600·4	5·86	88	11·6	0·3963 (8·3)
Cu	63·54	1356	42	310	7·8	0·2191 (8·0)
Al	26·97	932·7	94	410	1·5	0·1933 (8·0)
Mg	24·32	924	46·5	330	3·7	0·2827 (6·25)
Na	22·997	370·5	31·7	160	3·5	0·2939 (8·3)
K	39·096	335·3	15·7	99	2·0	0·3736 (8·3)

† Quantities in brackets give the corresponding wave lengths in Å units.

Table 2. Cold Neutron Scattering Cross Section and Electrical Conductivity at the Melting Point

Element	α	Debye Temp. in liquid state Θ_L°K	*Ratio of Electrical conductivities*		*Calculated neutron scattering cross section* σ (barns)		% change in scattering cross section
			$\left(\frac{\eta_S}{\eta_L}\right)_{\text{calc}}$	$\left(\frac{\eta_S}{\eta_L}\right)_{\text{obs}}$	Solid state	Liquid state	
Pb	0	61·24	2·065	2·07	1·98	2·95	49·06
	0·3	68·09	1·67			2·60	31·66
	0·5	73·91	1·42			2·37	20·00
	0·75	79·91	1·21			2·18	10·17
	1·00	87·36	1·015			1·98	1·01
Cu	0	215·3	2·07	2·07	3·31	4·41	33·13
	0·3	240·0	1·67			4·04	22·08
	0·5	258·2	1·44			3·81	15·20
	0·75	283·0	1·20			3·55	7·19
Mg	0	258·9	1·625		2·195	2·66	21·28
	0·3	290·9	1·29			2·39	9·07
	0·5	314·8	1·10			2·22	1·28
Al	0	237·8	2·97	1·64	0·79	1·22	54·53
	0·3	266·8	2·36			1·11	40·36
	0·5	288·3	2·02			1·07	35·18
	0·75	318·1	1·66			0·96	21·55
	1·00	351·6	1·36			0·885	11·91
Na	0	107·5	2·215	1·45	1·73	2·58	49·20
	0·3	120·8	1·75			2·29	32·35
	0·5	130·8	1·50			2·11	22·19
	0·75	144·7	1·22			1·91	10·43
K	0	69·78	2·01	1·55	0·85	1·25	47·87
	0·3	78·02	1·61			1·10	30·03
	0·5	84·16	1·38			1·01	19·36
	0·75	92·58	1·14			0·91	7·50

It will be seen that for $\alpha \approx 0{\cdot}5$ the calculated values of $(\eta_S/\eta_L)_{T_M}$ for Na, K and Al are in good agreement with experimental values, whereas for Pb and Cu $\alpha \approx 0$, gives a good agreement. Unfortunately, experimental data on the change of cold neutron scattering cross section at the melting point are lacking. However, preliminary results of Squires† on lead indicate a sharp increase of about 20% in the scattering cross section at the melting point. This would seem to indicate a value of α of about 0·5, as can be seen from table 2. On the other hand the conductivity data require α to be about 0.

§ 4. Discussion

The discrepancy between the two values of α in the case of lead is perhaps due to our assumption that the value of $[K(dE/dK)]^2_{T_M}$ is the same both for the solid and liquid phases. There is at present no possible way to decide this point quantitatively. We may, however, remark that a more reliable estimate of the value of α is obtained from thermal inelastic neutron scattering rather than from conductivity data, since the latter involve an uncertain change in $[K(dE/dK)]^2_{T_M}$.

The situation in the case of alkali metals is somewhat better. As we see from table 2, for Na and K the calculated values of $(\eta_S/\eta_L)_{T_M}$ are in good agreement with experimental values for $\alpha \approx 0{\cdot}5$. Now the free electron approximation is known to hold for these metals ; hence the change in conductivity on melting can be ascribed wholly to the change in their Debye temperatures. Unfortunately, no neutron scattering data are available for these metals to decide conclusively in favour of $\alpha \approx 0{\cdot}5$.

The conductivity data of Na and K and the neutron scattering data of Pb seem to indicate a value of $\alpha \approx 0{\cdot}5$ for these metals. This would mean that the change in the entropy of disorder on melting for these metals is nearly $\frac{1}{2}R$, R being the gas constant. The extra entropy is undoubtedly a manifestation of disorder in the liquid state and arises from the variety of ways in which the singly-occupied cells in the liquid can be arranged on a pseudo-lattice. It might be thought that this entropy of disorder in the liquid state could be explained by allowing the possibility of more than one atom to occupy the same cell. Recent calculations of Pople (1951) have shown, however, that these states give only a negligible contribution to the liquid partition function. The entropy arising from these states is called the communal entropy which does not become important until the critical point of the liquid.

We shall now use the order disorder theory of melting of Lennard-Jones and Devonshire (1939) to see whether the value of α as obtained from the conductivity and neutron scattering data is of the right order of magnitude. The relevant equations are given in Appendix A.

† We are grateful to Dr. Squires for sending to us his experimental results on lead before publication. Dr. Egglestaff informs us that he also observes a similar change.

In their theory the entropy of disorder and the average energy W required to take an atom from an α-site to a β-site are given in terms of an 'order parameter' Q. Taking the entropy of disorder to be $0{\cdot}5R$, corresponding to $\alpha \approx 0{\cdot}5$ and using eqns. (A.1) and (A.2), we find that at the melting point the values of W for Pb, Na and K are respectively, 6·2, 3·8 and 3·4 kcal per g mole. The α- and β-sites in the theory of Lennard-Jones and Devonshire have been introduced merely to obtain a convenient representation, capable of mathematical treatment. The arguments of the theory will equally apply to the general case of the transformation of a close-packed crystalline array to the more disorderly, open-packed arrangement in the liquid. It, therefore, seems quite reasonable to associate the average energy W with a part of the activation energy for self-diffusion in the liquid state.

The self-diffusion data in liquid lead at the melting point (see Appendix B) give for the activation energy a value of nearly 14 kcal per g mole. Self-diffusion in Pb is presumably determined by vacancies if the work of Huntington and Seitz (1942) on copper is taken as a basis since as in the case of copper the inner shells in lead are large. These authors have shown that in copper the energy of formation of a vacancy is of the order of the energy of migration. If we assume the same thing for lead, then the energy of formation of vacancies is nearly 7 kcal per g mole. This value is not far from 6·2 kcal per g mole as obtained by us. The agreement is more than what one would expect on the basis of our crude model.

In Appendix B we have estimated the activation energy for self-diffusion in liquid Na and K to be nearly 7 kcal per g mole. Huntington (1942) has shown that the energy required to form vacancies and that to form interstitial atoms are much more nearly the same for alkali metals than for copper. As a result it is not possible to decide between interstitial and vacancy diffusion in alkali metals. Whatever may be the real mechanism of self-diffusion in alkali metals, it is gratifying to see that values calculated by us are of the same order of magnitude as those given by self-diffusion data.

We, therefore, arrive at the conclusion that the conductivity data of Na and K and the neutron scattering data of Pb require that on melting the entropy of disorder for these metals is nearly $0{\cdot}5R$, and that this value is consistent with self-diffusion data. It would be highly desirable to have experimental data available for cold neutron scattering cross section in metals near the melting point.

In trying to explain the abrupt change in cold neutron scattering cross section at the melting point in lead, we have neglected the possibility of elastic scattering contributing in the liquid state. The neutrons used in Squires' experiment were filtered through graphite, which gives a cut-off at 6·7 Å, the mean wavelength being 8·3 Å. The cut-off in lead is at 5·7 Å. Now the observed change in volume on melting in this case is less than 5%, which would correspond to a change of utmost 2% in linear dimensions. Thus on our model, graphite filtered neutrons with a cut-off at 6·7 Å would not give rise to Bragg reflections in liquid lead.

Finally we would like to add that the scattering of cold neutrons in solids may provide a powerful method of investigating the absolute number of defects produced either by temperature or by irradiation.

References

Carpenter, L. G., and Steward, C. J., 1939, *Phil. Mag.*, **27,** 551.
Huntington, H. B., 1942, *Phys. Rev.*, **61,** 325.
Huntington, H. B., and Seitz, F., 1942, *Phys. Rev.*, **61,** 315.
Kothari, L. S., and Singwi, K. S., 1955, *Proc. Roy. Soc.* A, **231,** 293.
Lennard-Jones, J. E., and Devonshire, A. F., 1939, *Proc. Roy. Soc.* A, **170,** 464.
Mott, N. F., 1934, *Proc. Roy. Soc.* A, **146,** 465.
Placzek, G., 1954, *Phys. Rev.*, **93,** 895.
Pople, J. A., 1951, *Phil. Mag.*, **42,** 459.
Squires, G. L., 1952, *Proc. Roy. Soc.* A, **212,** 192.

APPENDIX A

In the theory of Lennard-Jones and Devonshire (1939) the entropy of disorder is given by

$$S=-2\,(1-Q)\log(1-Q)-2Q\log Q, \quad . \quad . \quad . \quad . \quad \text{(A.1)}$$

where the order parameter Q is defined by $Q=N_\alpha/N$, N_α being the number of atoms on α-sites and N is the total number of atoms. And the average energy W required to take an atom from an α-site to a β-site is

$$W=4kT\tanh^{-1}(2Q-1). \quad . \quad . \quad . \quad . \quad . \quad \text{(A.2)}$$

APPENDIX B

The coefficient of self-diffusion is given by the usual relation

$$D=D_0\exp(-E/RT) \quad . \quad . \quad . \quad . \quad . \quad . \quad \text{(B.1)}$$

where E is the activation energy per g mole. In the case of (solid) lead E is 28 kcal and D_0 is 5·1 cm²/sec. Using the measured value of $D=2{\cdot}55\times10^{-5}$ cm²/sec in liquid lead (Groh and Von Hevesy 1920, *Ann. der Physik*, **63,** 85) near the melting point, and assuming that the value of D_0 does not change appreciably in going from the solid to the liquid state, we get the energy of activation E in the liquid state to be 14·5 kcal.

In the case of alkali metals Na and K the activation energy E in the solid state from self-diffusion data is nearly 10 kcal and the value of D_0 is 0·32 cm²/sec (Norberg and Slichter 1951, *Phys. Rev.*, **83,** 1074, who quote private communication from Nachtrieb). Since in most metals in the liquid state the coefficient of diffusion D is of the order of 10^{-5} cm²/sec, we assume this value for Na and K and as before take the value of D_0 corresponding to that in the solid state to calculate the value of E in the liquid state. The calculation yields

Element	Na	K
E (kcal/g mole)	7·6	6·9

LVII. *Creep in Metal Crystals at Very Low Temperatures*

By N. F. Mott
Cavendish Laboratory, Cambridge†

[Received December 20, 1955]

Summary

A theory is given of creep in metallic single crystals at very low temperatures, which is based on the hypothesis that dislocations can pass through barriers, such as those provided by dislocations crossing the slip plane, owing to the quantum-mechanical tunnel effect. A detailed theory would depend on a knowledge of the atomic arrangements at the centre of a dislocation, which in this case does not exist, but a rough calculation shows that creep should be independent of temperature below about 10°K in cadmium.

In a recent paper in this journal Glen (1956) has described measurements of creep in single crystals of cadmium at the temperature of liquid helium, and has confirmed former observations of Meissner, Polanyi and Schmid (1930) that the effect exists. The purpose of this note is to attempt a theory of creep at low temperatures, based on the idea that a dislocation held up by a potential barrier, such as that which is formed when a screw dislocation cuts the plane in which it moves, can pass through it owing to the quantum-mechanical tunnel effect.

The model is that used to explain logarithmic creep (see, for example, Mott 1953). An (edge) dislocation is held up by a series of obstacles S_1, S_2, S_3 which may for instance be screw dislocations cutting the plane of the paper, so that the dislocation cannot move forwards without forming a jog. It is assumed that the stress σ acting on the dislocation is nearly as great as the stress σ_0 required to move it without the help of temperature. It is usually supposed (cf. Mott 1953), Cottrell 1952) that the activation energy to form a jog, and thus to pull a dislocation through a barrier, is then

$$J(1-\sigma/\sigma_0), \quad . \quad . \quad . \quad . \quad . \quad . \quad . \quad . \quad . \quad (1\,a)$$

where J is the jog energy. If one supposes, however, that the energy of the jog is a smooth function of displacement x along a line perpendicular to the dislocation, as in fig. 2, a better approximation would be

$$W_0(1-\sigma/\sigma_0)^{3/2} \quad . \quad . \quad . \quad . \quad . \quad . \quad . \quad . \quad (1\,b)$$

and the width of the barrier

$$w=a(1-\sigma/\sigma_0)^{1/2}. \quad . \quad . \quad . \quad . \quad . \quad . \quad . \quad . \quad (2)$$

---

† Communicated by the Author.

Fig. 1

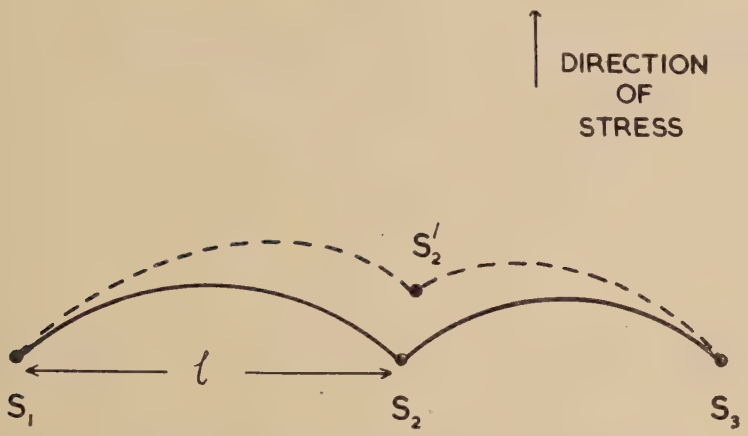

(*a*) Showing two stages in the movement of a dislocation line.

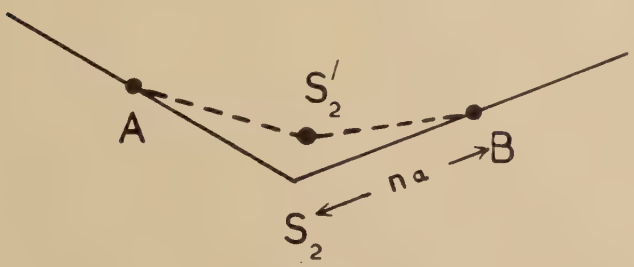

(*b*) Showing details of the movement past a screw.

Fig. 2

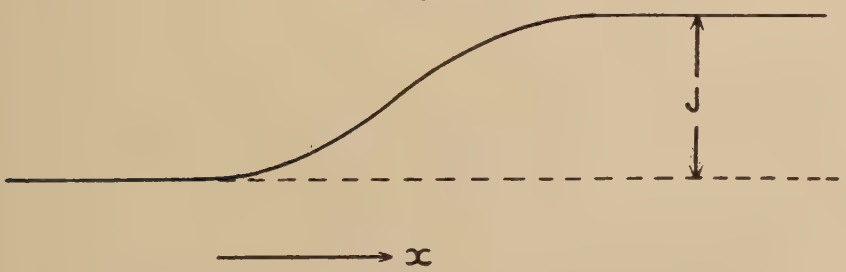

(*a*) is the potential energy of a jog as a function of displacement of the dislocation.

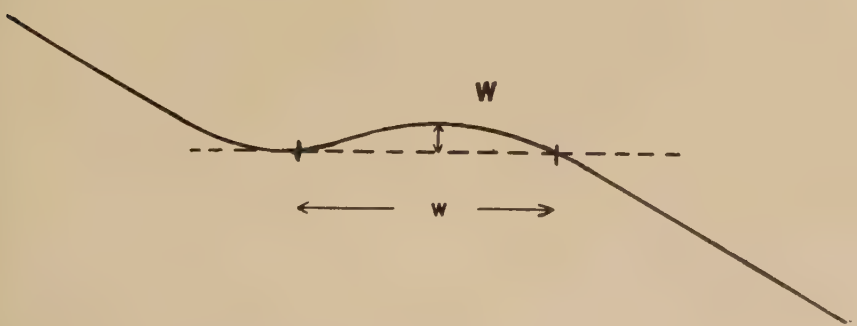

(*b*) is the same with the term σblx due to the stress added to it.

Here W_0 is of order a few electron volts and a of the order of the interatomic distance.

Expressions of this general form were first given by Mott and Nabarro (1948) for a different model, namely for dislocations held up by the stress field round a precipitate, but it seems to have escaped notice that they are of more general applicability. We doubt whether the change will greatly effect predictions already made except when σ is very near to σ_0, and hence at very low temperatures. We should under these conditions expect 'logarithmic' creep to satisfy the law (Mott 1953, p. 752)

$$(\text{strain})^{3/2}=\text{const. } kT \ln(\gamma t),$$

and hence the flow stress to depend on temperature according to a law of the type

$$\sigma=\sigma_0-AT^{3/2}.$$

In the problem to be considered here the possibility of the tunnel effect arises through the fact that, when σ approaches σ_0, the barrier becomes low *and* narrow. A moving dislocation is thought to have effective mass of order M, the atomic mass, per atomic plane cut by it. Tunnel effect will only be possible in processes in which a small length of dislocation moves. We thus suppose that, in creep by tunnel effect, a jog is formed by a process such as that shown in fig. 1 (*b*); the dislocation moves from the form AS_2B to AS'_2B, S_2B being a length equal to na so that the moving dislocation cuts $2n$ planes. The force acting at S'_2 is smaller than that acting at S_2. We suppose that the effective mean stress between S_2 and S'_2, points distant w apart, is

$$\sigma_{\text{eff}}=(1-w/na)\sigma. \qquad \ldots\ldots\ldots \quad (3)$$

We thus have an increased barrier height compared with (1 *b*)

$$W=W_0(1-\sigma_{\text{eff}}/\sigma_0)^{3/2} \qquad \ldots\ldots\ldots \quad (4)$$

and width compared with (2)

$$w=a(1-\sigma_{\text{eff}}/\sigma_0)^{1/2}. \qquad \ldots\ldots\ldots \quad (5)$$

The latter equation with (3) gives a quadratic for σ_{eff}; we have from (3) and (5)

$$\left(1-\frac{\sigma_{\text{eff}}}{\sigma}\right)=\frac{1}{n}\left(1-\frac{\sigma_{\text{eff}}}{\sigma_0}\right)^{1/2}.$$

To a rough approximation suppose n to be large enough to permit an expansion of σ_{eff} in ascending powers of $1/n$; we then find for the factor that occurs in (4) and (5)

$$1-\frac{\sigma_{\text{eff}}}{\sigma_0}=\eta+\frac{1}{n}\eta^{1/2},$$

where

$$\eta=1-\sigma/\sigma_0.$$

We now take the chance per unit time, to a sufficient approximation, that in fig. 1 (*b*) the dislocation moves by tunnel effect from the configuration AS_2B to AS'_2B to be

$$\nu \exp\left\{-2\left(\frac{4nMW}{\hbar^2}\right)^{1/2} w\right\}, \quad \ldots\ldots\ldots \quad (6)$$

this being the chance for a 'particle' of mass $2nM$ to penetrate a (rectangular) barrier of height W and breadth w.

ν is an atomic frequency of order 10^{12} sec^{-1} and whose exact value need not concern us. The dislocation is treated as a dynamical system with many degrees of freedom; penetration will occur for the mode of motion for which the value of n makes (6) a maximum. The expression (6) is a maximum when n is chosen to give a minimum value of

$$(nW)^{1/2}w$$

and hence of

$$n^{1/2}(1-\sigma_{\text{eff}}/\sigma_0)^{5/4}=n^{1/2}(\eta+\eta^{1/2}/n)^{5/4}.$$

Since η is small it is clear that this minimum value is reached when $n=1/\eta^{1/2}$, so that (6) becomes

$$\nu \exp\left\{-2\alpha \sqrt{\left(\frac{2MW_0}{\hbar^2}\right)a\eta}\right\}$$

where α is a constant of order unity.

The creep strain ϵ will be given by a law of the type

$$\epsilon=A \ln \gamma t$$

where the constant A is independent of the temperature and given by

$$A=\text{const.}/a\sqrt{(2MW_0/\hbar^2)}$$

and the constant is of order unity.

We shall compare the creep rate with that due to thermal activation. According to the analysis given above, the chance per unit time for a thermally activated movement will be

$$\nu \exp\{-W_0\eta^{3/2}/kT\}. \quad \ldots\ldots\ldots \quad (7)$$

Creep by tunnel effect will thus be more rapid than by thermal activation if

$$2\sqrt{\left(\frac{2MW_0}{\hbar^2}\right)a} < \frac{W_0}{kT}\eta^{1/2}.$$

A reasonable assumption is that $2mW_0a^2/\hbar^2 \sim 1$, where m is the mass of the electron; this would imply that W_0 is about 1 ev. W_0 should be of the order of the jog energy, but without a detailed knowledge of the curve shown in fig. 2 we cannot evaluate it directly. The critical temperature above which thermal activation becomes important is then given by

$$kT/W_0 \sim \tfrac{1}{2}\sqrt{(m/M)}\eta^{1/2}.$$

Since the creep rate is observable, the quantity (7) should be of the order of the inverse of a few seconds, so that $W_0\eta^{3/2}/kT$ will be of the order 30.

Some re-arrangement then gives, eliminating η

$$\frac{kT}{W_0} \sim \left(\frac{m}{M}\right)^{3/4} \left(\frac{1}{2}\right)^{3/2} (30)^{1/2}.$$

If $m/M \sim 0{\cdot}5 \times 10^{-5}$ and $W_0 \sim 1$ ev, this gives temperatures of the order of a degree Kelvin. The various approximations introduced clearly make this result uncertain by several multiples of two ; it at any rate predicts creep independent of temperature in the liquid helium range.

References

Cottrell, A. H., 1952, *J. Mech Phys. Solids*, **1**, 53.
Glen, J. W., 1956, *Phil. Mag.*, in the press.
Meissner, W., Polanyi, M., and Scbmid, W. E., 1930, *Z. Phys.*, **66**, 477.
Mott, N. F., 1953, *Phil. Mag.*, **44**, 742.
Mott, N. F., and Nabarro, F. R. N., 1948, *Report of the Bristol Conference on the Strength of Solids* (London : Physical Society), p. 1.

LVIII. *The Lifetime of the* 200 kev *Excited State of* ^{19}F

By C. M. P. Johnson
Cavendish Laboratory, Cambridge†

[Received December 22, 1955]

Experiments to determine the magnetic moment of the 200 kev excited state of ^{19}F (see Phillips and Jones 1956 and Lehmann, Leveque and Fiehrer 1955, and Treacy 1955) have made it necessary to know the lifetime of the state more accurately than previously determined (Jones, Phillips Johnson and Wilkinson 1954, and Thirion, Barnes and Lauritsen 1954).

The experimental arrangement used was similar to that of Bell, Graham and Petch (1952) as shown in fig. 1. The counters were sodium iodide crystals 2 in. × 2 in. × 1 in. in size, optically coupled to EMI 6262 photomultipliers. The collectors of these were connected to limiters for the fast coincidence circuit, and proportional pulses were taken from the twelfth dynodes. The resolving time of the fast coincidence unit was 45 millimicroseconds in one series of runs, and 80 millimicroseconds in another. The proportional pulses from the counters were fed to single channel kick sorters, set for the counter A to accept the photopeak of a 1·35 Mev gamma ray, and the counter B the photopeak of a 200 kev gamma ray. The outputs of the single channel kicksorters, and of the fast coincidence unit, were connected to a triple coincidence circuit of resolving time about one microsecond. This ensures that each counter counts only one gamma ray.

The sources of ^{19}F used were discs of teflon irradiated for one minute with fast neutrons from the cyclotron, giving ^{19}O which decays to ^{19}F with a 30 second half life. The discs were placed between the two crystals after irradiation, and the coincidence rate recorded for different lengths of delay cable inserted between counter A and the coincidence unit. Coincidence counts were taken for the same number of single counts from the low energy counter, so that the number of decay processes in each run was the same. The runs were started when the activity of the source had reached a standard value, so that the number of random coincidences was the same for each value of decay, and any dead time effects in the singles scaler were eliminated. The number of random coincidences was determined by putting the delay between counter B and the coincidence unit, and was found to be 4 for each run, so that the ratio of real to random coincidences was never less than sixteen, even for the largest value of delay.

---

† Communicated by the Author.

Fig. 1

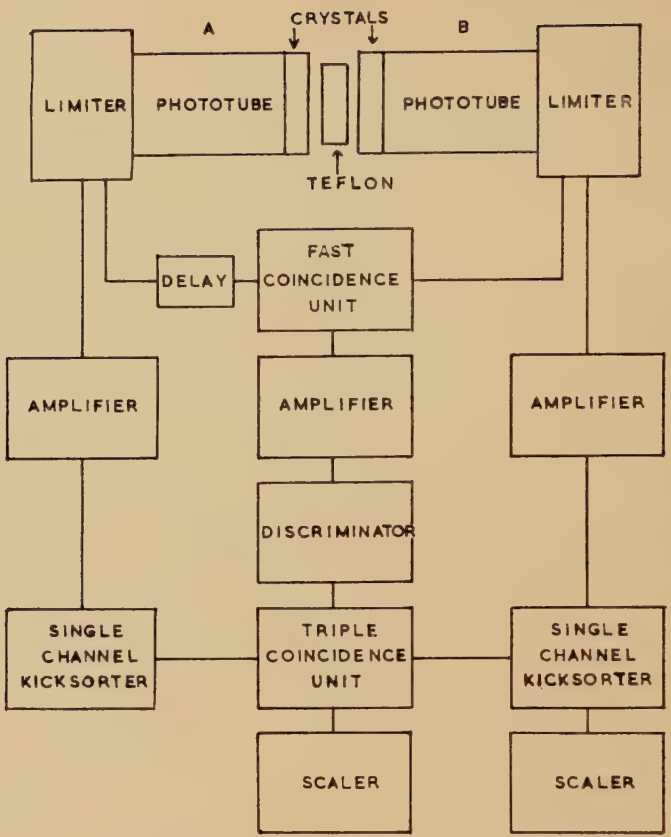

Schematic diagram of the apparatus.

Fig. 2

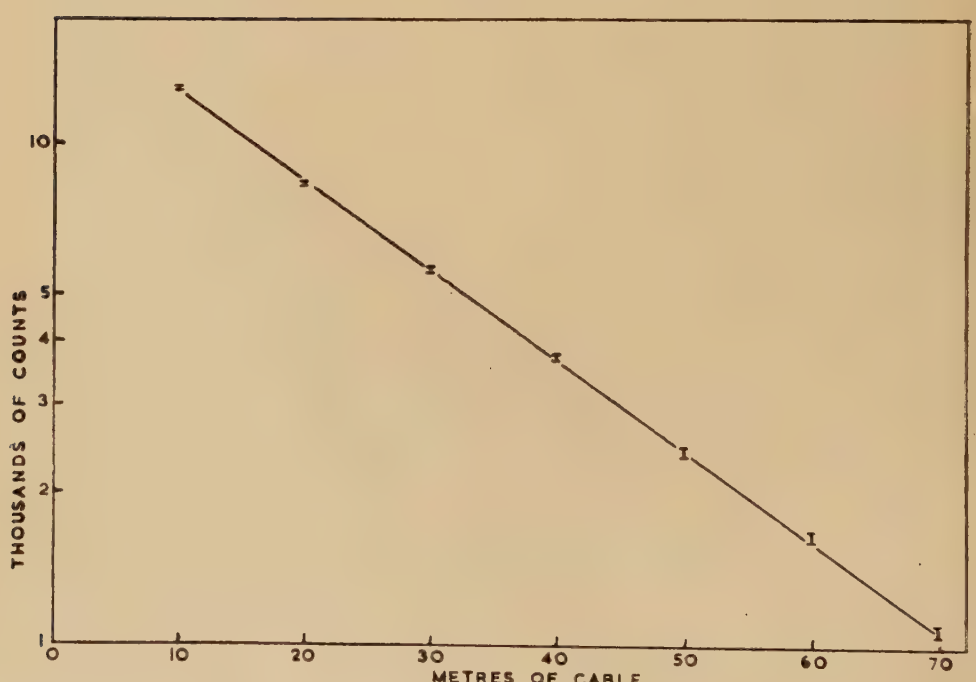

Delay curve.

The effect of attenuation in the delay cable was investigated by plotting prompt resolution curves using a ^{22}Na source first with no additional delay, and then with 40 metres of cable in each counter lead. A small decrease in the effective resolving time was observed, hence a fairly long resolving time was used so that the effect of this on the lifetime will be very small. This was confirmed by the fact that there was no significant difference in lifetime from the runs with the two values of resolving time.

The delay cable was calibrated by measuring the resonant frequencies of the three lengths of cable used with an accurate crystal calibrated wavemeter. This introduced a correction of 2% to the lifetime since the cables were cut to length assuming the manufacturer's value of dielectric constant to be correct. A semilogarithmic plot of the sum of all the runs, with randoms subtracted but not corrected for cable error, is shown in fig. 2. The coincidence rate for zero delay was not used as there may be spurious prompt coincidences due to the decay of ^{16}N or detection of beta–gamma coincidences.

The slope of the line was calculated by the method of least squares to be $(0{\cdot}812 \pm 0{\cdot}0087) \times 10^7$ sec^{-1}, (probable error) giving, after correction for cable error and allowing for the small uncertainty due to attenuation, a value of the mean life of $(1{\cdot}25 \pm 0{\cdot}025) \times 10^{-7}$ sec. This agrees well with other determintaions, (Fiehrer *et al.*, private communication, Thirion *et al.* 1954) and with the matrix element calculated from the shell model by Elliott and Flowers (1955).

The author is grateful to the Department of Scientific and Industrial Research for a maintenance grant.

References

Bell, R. E., Graham, R. L., and Petch, H. E., 1952, *Canad. J. Phys.*, **30**, 35.
Elliott, J. P., and Flowers, B. H., 1955, *Proc. Roy. Soc.* A, **229**, 536.
Jones, G. A., Phillips, W. R., Johnson, C. M. P., and Wilkinson, D. H., 1954, *Phys. Rev.*, **96**, 547.
Lehmann, P., Leveque, A., and Fiehrer, M., 1955, *Comptes Rendus*, **241**, 700.
Phillips, W. R., and Jones, G. A., 1956, *Phil. Mag.*, June.
Thirion, J., Barnes, C. A., and Lauritsen, C. C., 1954. *Phys. Rev.*, **94**, 1076.
Treacy, P., 1955, *Nature, Lond.*, **176**, 923.

LIX. *The Magnetic Moment of the* 200 kev *Excited State of* ^{19}F

By W. R. Phillips and G. A. Jones
Cavendish Laboratory, Cambridge†

[Received December 22, 1955]

Summary

We have measured the magnetic moment of the 200 kev excited state of ^{19}F by observing the influence of an external magnetic field on the directional properties of a γ–γ cascade through this state. The cascade follows the β-decay of ^{19}O produced by neutron bombardment of HF. The result, $\mu = +3{\cdot}50 \pm 0{\cdot}24$ n.m., assumes that no time-dependent quadrupole interaction is present in the source ; the effect of the possible presence of such an interaction is discussed.

§ 1. Introduction

The interaction of the magnetic moment of an excited nucleus with an external magnetic field may alter the angular correlation of radiation proceeding through the excited state. Observation of the change may then be used to determine the magnetic moment of the excited nucleus and such measurements have been performed, e.g. Aeppli *et al.* (1952), Raboy and Krohn (1954). For the change in correlation to be observable with present techniques the lifetime of the excited state must lie within the region 10^{-9} to 10^{-6} sec.

We have measured the magnetic moment of the 200 kev excited state of ^{19}F by observing the change in correlation with magnetic field of the γ–γ cascade proceeding through this level after the β-decay of ^{19}O (Jones *et al.* (1954). The mean lifetime of this state has been determined as $(1{\cdot}25 \pm 0{\cdot}03) \times 10^{-7}$ sec (Johnson 1956), and its spin is 5/2.

Liquid sources of hydrofluoric acid were irradiated with neutrons from the Cavendish cyclotron to produce the ^{19}O. The lifetime of 30 sec allowed removal from the vicinity of the cyclotron to make the observations. The measurements have been analysed on the assumption that there is no perturbing influence in the intermediate state other than that of the external magnetic field, but the effect of such interactions it discussed.

During the course of this work, similar measurements, utilizing different reactions involving this state, have been carried out at Saclay (Lehmann *et al.* 1955) and at Canberra (Treacy 1955), with results in excellent agreement with our own.

† Communicated by the Authors.

§ 2. Theory

The interactions of magnetic and electric fields on the magnetic and electric moments of the nucleus induce transitions between the magnetic substates in the intermediate state, defined with respect to an arbitrary axis. The resulting time-dependence of the population of the substates implies a time-dependent angular correlation of the emitted radiation. In general if $W_0(\theta)=1+\Sigma_\nu A_\nu P_\nu(\theta)$ is the unperturbed correlation, then the perturbed correlation is given by $W(\theta)=\Sigma_\nu A_\nu G_\nu P_\nu(\theta)$ where the coefficients G_ν, of magnitude less than unity, are given for several cases of interest by Abragam and Pound (1953). For the second γ-ray emitted at time t after the first, the delayed correlation is

$$W_d(\theta)=1+\Sigma_\nu A_\nu G_\nu(t) P_\nu(\theta). \quad . \quad . \quad . \quad . \quad . \quad . \quad (1)$$

In the case that the only interaction present is that of the magnetic moment μ with an external magnetic field H it may be shown that

$$W_d(\theta, H)=1/\tau\, e^{-t/\tau}\, W_0(\theta \pm \omega t) \quad . \quad . \quad . \quad . \quad . \quad . \quad (2)$$

if coincidences are observed 'one way only' (i.e. one detector has zero efficiency for one of the γ-rays) as in the present experiment. τ is the mean lifetime of the intermediate state and ω is the Larmor frequency of precession, i.e., $\omega=\mu H/I\hbar=g\mu_\nu H/\hbar$ where g is the gyromagnetic ratio and I the spin of the excited state.

If the coincidence resolving time is very much greater than the lifetime of the state than the average correlation is observed :

$$W(\theta, H)=\int_0^\infty W_d(t)\, dt.$$

For $W_0(\theta)=1+A_2 \cos^2\theta$ this leads to

$$\frac{W(180°, H)}{W(90°, H)}=\frac{1+b_2+4\omega^2\tau^2}{1-b_2+4\omega^2\tau^2} \quad . \quad . \quad . \quad . \quad . \quad . \quad (3)$$

where

$$b_2=\frac{A_2}{2+A_2}.$$

Thus a series of measurements of this ratio at different values of H gives $|g|$, whilst observation of $W(\theta, H)$ for a particular H gives the sign of g. Because of poor yield, this was the method used to determine g, rather than the more elegant observation of W_d (e.g. Steffen and Zobel 1955).

§ 3. Decay of ^{19}O

The features of the decay scheme of ^{19}O pertinent to the discussion are shown in fig. 1. The 200 kev state is known to be (5/2+) (Jones *et al.* 1954, Sherr *et al.* 1954). We assign the characteristics (3/2+) to the 1·59 mev state from measurements, with liquid HF source, of the unperturbed γ_1–γ_2 correlation, which is adequately represented by the function $W_0(\theta)=1-(0{\cdot}272\pm 0{\cdot}027)\cos^2\theta$, after correction for geometry. Of the three possibilities, (3/2+), (5/2+) and (7/2+), consistent with the decay

scheme, (3/2+) gives exactly this correlation for a pure M1 transition for γ_1; (7/2+) can be made to fit the data only by assuming a 3% admixture of E2 in γ_1, i.e. about 300 times more than for single particle transitions. The most recent survey of radiative transitions in light nuclei (Wilkinson 1956) indicates that such an admixture, though not very probable, cannot be ruled out. We prefer the assignment (3/2+) because shell model calculations on this nucleus (Elliott and Flowers 1955) predict a (3/2+) state near 1·6 MeV with a strong M1 transition to the 200 keV state. The spin assignment does not affect the interpretation of the experiment, but is of interest in assessing possible perturbing effects in the source.

§ 4. Choice of Suitable Source

In the previous note on the ^{19}O decay it was observed that, using teflon sources the observed anisotropy was two-thirds the value expected for γ_1 a pure M1 transition to a (3/2+) state. Further measurements showed that in fact the anisotropy was initially the same as that observed with HF sources but changed on neutron bombardment of the teflon, decreasing to about one-fifth the initial value. The structural disorder caused by the neutrons thus introduces a large perturbing effect, and the final anisotropy is consistent with the 'hard core' correlation remaining in the source when a static electric quadrupole interation is present.

Using 40% by weight hydrofluoric acid as source the only expected interaction is that of the electric quadrupole moment with randomly fluctuating electric field gradients. For such an interaction Abragam and Pound (1953) show that the coefficients $G_\nu(t)$ in eqn. (1) have the values $\exp(-\lambda_\nu t)$. λ_2 is proportional to the correlation time τ_c of the HF solution, which is a measure of the time the environments of a molecule in the liquid are in a given configuration. τ_c is roughly proportional to the viscosity of the liquid and as $\eta \sim 1{\cdot}5$ cpoise in our case, we expect λ_2 to be very small.

§ 5. Experimental Method

The γ-detectors were NaI (Tl) crystals, 3·7 cm dia. × 3·7 cm long for the 1·37 MeV radiation and 2 cm × 2 cm × 1 cm for that of 200 keV. To assist magnetic screening, 6 in. long perspex light-pipes removed the accompanying photomultipliers type EMI 6262 from near the magnet. Perspex absorbers, to remove β-radiation, were placed over the detecting crystals, and, to prevent the possibility of spurious coincidences by γ-scattering from one crystal to the other, the high energy detector was screened, front and sides, with 4 mm of lead.

The electromagnet was designed with the object of minimizing the occurrence and effect of spurious coincidences arising from the large flux of β-rays stemming from the source and in coincidence with γ_1 and γ_2. To this end the pole pieces were long and tapered (3 in. dia. to 1 in. dia. over 6 in.), and the yoke and coils were removed far from the

region of detection. In addition the pole-faces were capped with graphite discs, 1 cm thick, to reduce the intensity of bremsstrahlung ; the remaining gap of 2 cm was sufficient to accommodate the large sources, in cylindrical polythene containers of inner dimensions 1 cm dia. $\times$ 1·5 cm. The variation of H over the gap was only 3% at 1000 gauss and less than 1% over the dimensions of the source.

Fig. 1

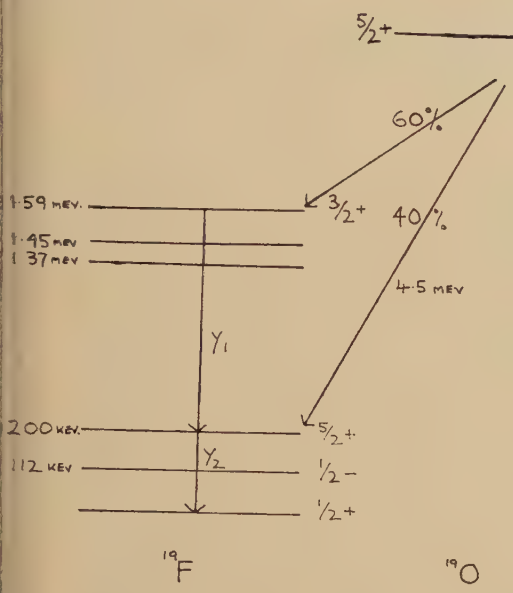

Decay scheme of ^{19}O, relevant to the experiment.

Fig. 2

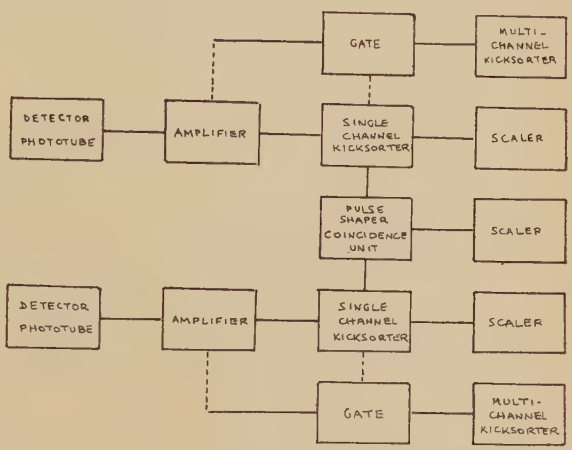

Schematic diagram of electronic apparatus used.

A block diagram of the electronic apparatus is shown in fig. 2. The detecting ' windows ' of the single channel kicksorters were set respectively to straddle the photopeak of γ_2 and to cover the range 600–1400 kev of the spectrum of γ_1. The efficiencies of γ-detection were maintained constant by frequent monitoring of the relative positions of ' window ' and peak using a multi-channel kicksorter in conjunction with a gate circuit. The mean value of the coincidence resolving time, determined throughout the experiment, was $2\tau_0 = 0{\cdot}7 \pm 0{\cdot}01$ μsec.

It was found that the reaction ^{19}F(n, α)^{16}N produced an intense source of 7-sec ^{16}N, but that a waiting period of 1 minute between irradiation and measurement eliminated the possiblity of significant effects from this decay since γ-cascades are not produced (see Ajzenberg and Lauritsen 1955) for γ-transitions in ^{16}O.

The total number of coincidences observed divided by the total number of, say γ_2 single counts at the various angles is a measure of the correlation

function provided that the efficiency of the γ_1-counter does not change. In our case the γ_2-counter was moveable and the efficiency of detection of γ_1 was kept constant by monitoring with the multichannel kicksorter. If N_c is the number of coincidences observed, after subtraction of randoms, for a total of N counts in the low energy detector, after subtracting the background, then $R(H)$ is a measure of the correlation at field H where

$$R(H)=\frac{W(180°, H)}{W(90°, H)}=\left(\frac{N_c}{N}\right)_{180°}\Big/\left(\frac{N_c}{N}\right)_{90°}.$$

The random coincidences were estimated from the single counting rates and the resolving time, allowing for the decay of the source ; they never exceeded 5% of the total number of coincidences. The values of $R(H)$ for different values of H were measured in addition to the zero-field ratio.

§ 6. Results

Before the results obtained can be analysed in terms of eqn. (2) the following corrections must be considered :—

(1) Geometry corrections ; eqn. (2) refers to a point to point correlation. Krohn and Raboy (1955) have shown that the geometry correction is independent of field, but only for circular detectors of constant efficiency over their surface. It is not expected that the small departure from these conditions in our case will seriously affect this conclusion, so the geometry correction is simple.

(2) The effect of finite resolving time ; eqn. (2) is derived for infinite resolving time. We have estimated that, for values of H of interest, the correction required is never more than $\frac{1}{2}$%, so we have neglected it, but included its effects in determing the probable error of our result.

(3) The effect of spurious coincidences produced by the presence of the magnet. The zero-field ratio $R(0)$ was greater than the value observed on removal of the pole-pieces by an amount corresponding to a 10% isotropic contribution of coincidences from secondary effects in the pole-pieces, and this istoropic contribution must be subtracted out from the experimentally observed ratios $R(H)$. Since all the ratios $R(H)$ contain information on the ratio $R(0)$, we have attempted to arrive at a correction based on all the observations rather than merely on the ratio of $R(0)$ with and without the pole-pieces.

The method of analysis was as follows. A value was assigned to $R(0)$, in a range consistent with the experimental measurement, and the 'magnet correction' therefore determined. A least squares fit for the corrected $R(H)$ to eqn. (3) was made in the parameters b_2 and $\omega\tau$ and this was compared at $H=0$ with the corrected $R(0)$, namely the experimental measurement without pole-pieces. Over a range of values of $R(0)$, the least squares fit was consistent at $H=0$ with the corrected $R(0)$ and the curve corresponding to the centre of this range was taken as the best

Fig. 3

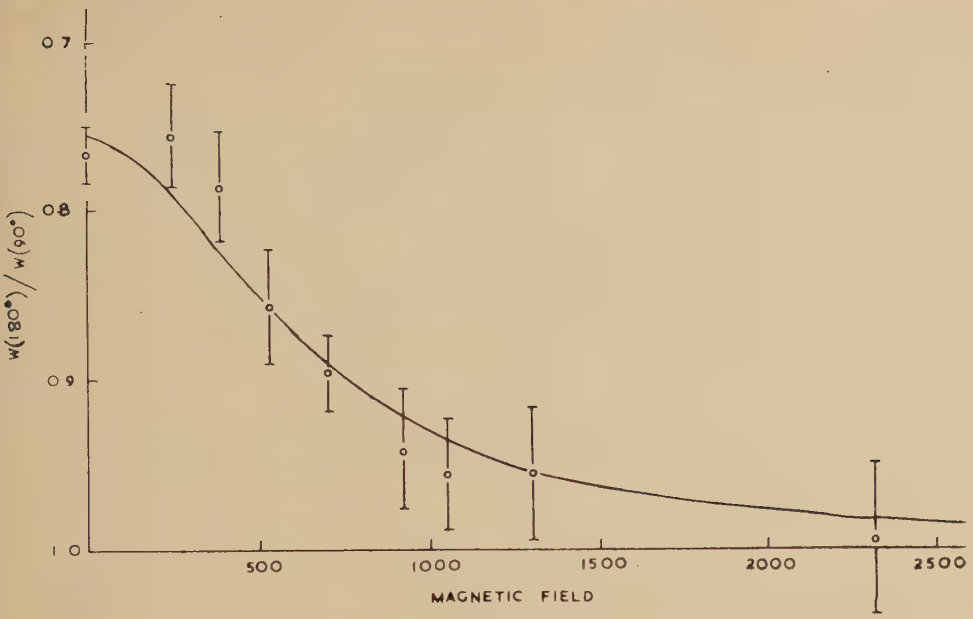

Experimental values of $R(H)$ versus H, corrected for magnet scattering in manner outlined in text. Errors on points correspond to number of counts observed. Full line represents curve for 3·50 n.m.

Fig. 4

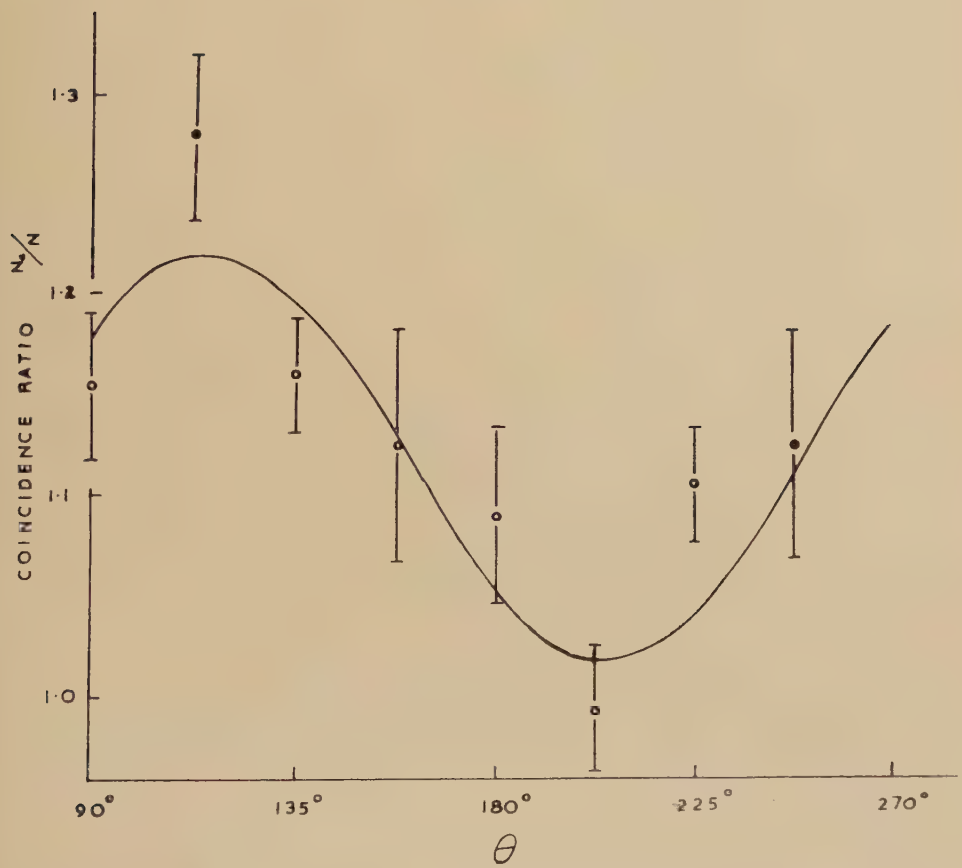

Angular correlation observed at $H = 700$ gauss. Errors on points correspond to number of counts observed, and points are uncorrected for magnet scattering. Full line represents curve for $\mu = +3{\cdot}50$ n.m. on an arbitrary scale.

possible fit, with the appropriate $\omega\tau$ as the best experimental determination. This curve is shown in fig. 3, together with the corerected $R(H)$; the errors on the points are probable errors based on counting statistics. The value of $g\tau$ calculated from this curve is $g\tau = 1{\cdot}74 \times 10^{-7}$, which, for $\tau = 1{\cdot}25 \times 10^{-7}$, gives $|g| = 1{\cdot}40 \pm 0{\cdot}09$.

The sign of g was determined by observing $W(\theta, H)$ for $H = 700$ gauss The correlation is shown in fig. 4. The direction of precession is that corresponding to positive μ, so, since the spin $I = 5/2$, we have

$$\mu = +3{\cdot}50 \pm 0{\cdot}24 \text{ n.m.}$$

The errors quoted are probable errors and include errors arising from uncertainty in b_2. spread of experimental points about the curve of best fit, and uncertainty in τ and H.

§ 7. Discussion

The analysis of the results in terms of eqn. (2) assumes that there is no time-dependent quadrupole interaction present in the source. Such interaction would decrease the anisotropy of the correlation, so an E2 component would be needed in γ_1 to offset this and the agreement between measurement and a pure radiation pattern reduced merely to chance. We have calculated the effect of an interaction, of strength $\lambda_2 = 1{\cdot}83 \times 10^6 \text{ sec}^{-1}$, such that the true anisotropy is 20% greater than that measured at $H = 0$, and find that g would be increased by 25%, while the necessary introduction of $\frac{1}{4}$% of E2 in γ_1 is probably not unreasonable. Thus the effect of quadrupole interaction in the source is obviously of importance. So far, because of poor yield, we have not attempted delayed correlation experiments which would indicate the magnitude of such an effect.

Now the calculations of Elliott and Flowers (1955), which have enjoyed considerable success in this mass region, predict that the M1 transition from the 1·59 Mev to the 200 kev levels should be near single-particle strength, so to produce the degree of mixing required above, the E2 strength would have to be very much greater than that of a single particle. In addition their predicted value of μ for the 200 kev state is $+3{\cdot}35$ (± 5%) n.m. (cf. the single $d_{5/2}$ particle of the Schmidt model gives $\mu = +4{\cdot}793$ n.m.) which is in excellent agreement with our measured value on the assumption of no quadrupole interaction. On balance, it seems reasonable to infer that the simplest interpretation of our results is correct, that the calculations of Elliott and Flowers on the states of ^{19}F are still in accord with measurements, and that $\mu = +3{\cdot}50 \pm 0{\cdot}24$ n.m. is a true measure of the magnetic moment of the 200 kev state of ^{19}F.

Acknowledgments

We are indebted to E. G. T. Morley for operating the Cavendish cyclotron and one of us (W. R. P.) wishes to thank the D.S.I.R. for a maintenance grant during the course of this research.

References

Aeppli, H., Albers-Schönberg, H., Frauenfelder, H., and Scherrer, P., 1952, *Helv. Phys. Acta*, **25**, 339.
Abragam, A., and Pound, R. V., 1953, *Phys. Rev.*, **92**, 832.
Ajzenberg, F., and Lauritsen, T., 1955, *Rev. Mod. Phys.*, **27**, 77.
Elliott, J. P., and Flowers, B. H., 1955, *Proc. Roy. Soc.* A, **229**, 536.
Johnson, C. M. P., 1956, *Phil. Mag.*, in the press.
Jones, G. A., Phillips, W. R., Johnson, C. M. P., and Wilkinson, D. H. 1954, *Phys. Rev.*, **96**, 547.
Krohn, V. E., and Raboy, S., 1955, *Phys. Rev.*, **97**, 1017.
Lehmann, P., Leveque, A., and Fiehrer, M., 1955, *Comp. Rend.*, **241**, 700.
Raboy, S., and Krohn, V. E., 1954, *Phys. Rev.*, **95**, 1689.
Sherr, R., Li, C. W., and Christy, R. F., 1954, *Phys. Rev.*, **94**, 1076.
Steffen, R. M., and Zobel, W., 1955, *Phys. Rev.*, **97**, 1188.
Treacy, P. B., 1955, *Nature, Lond.*, **176**, 923.
Wilkinson, D. H., 1956, *Phil. Mag.*, in the press.

LX. CORRESPONDENCE

Release of Stored Energy and Changes in Line Shape During Annealing of Deformed Nickel

By D. Michell
Division of Tribophysics, C.S.I.R.O., University of Melbourne, Australia†

[Received December 28, 1955]

Previous work on the broadening of the lines in the x-ray diffraction patterns of deformed metals has, in general, been restricted to a comparison of the patterns for the heavily deformed and the fully annealed states. However, Wilson and Thomassen (1934) investigated the x-ray line breadth and other properties for a number of deformed metals after annealing at various temperatures. For nickel, the recovery of line breadth occurred in two stages. Further, Clarebrough, Hargreaves and West (1955, 1956) have shown that the energy stored in deformed nickel is released in at least two stages during annealing and that there are corresponding changes in electrical resistivity, density and hardness. It seemed desirable to correlate these changes with changes of line shape during annealing. As the first stage of this programme, the energy stored in deformed nickel powder has been measured and line shapes determined on the same powder at various stages of annealing. The nickel used was identical with that used by Clarebrough, Hargreaves and West.

The deformed nickel powder was produced by surface grinding followed by sieving through a 350 mesh per inch sieve. Specimens for the measurement of stored energy and of the diffraction pattern were prepared by pressing this powder into suitable holders without a binder. The measurement of the stored energy and the manner of its release were determined by the calorimetric method of Clarebrough, Hargreaves, Michell and West (1952) using a heating rate of 6°c/min. The x-ray diffraction pattern between 30° and 130° in 2θ was determined at room temperature with a Geiger counter spectrometer (monochromatic Cu Kα radiation) for the one specimen, as deformed and after heating at 6°c/min to a number of temperatures up to 870°c.

The results of the stored energy measurements are shown in fig. 1. Curve (*a*) shows the rate of release of energy and curve (*b*) the energy remaining in the specimen, both as functions of the temperature. Interpreted in the manner of Clarebrough, Hargreaves and West (1955) for solid nickel, region A corresponds to recovery and region C to recrystallization. An intermediate region present in solid specimens is either absent in the filings or completely masked by the broad region C. The low

† Communicated by Professor N. F. Mott, F.R.S.

temperature at which the peak, region C, begins suggests that the maximum deformation present in the powder is greater than that in solid specimens of nickel deformed to fracture, while the large range of temperature over which this region occurs indicates that a wide range of deformations is present.

Fig. 1

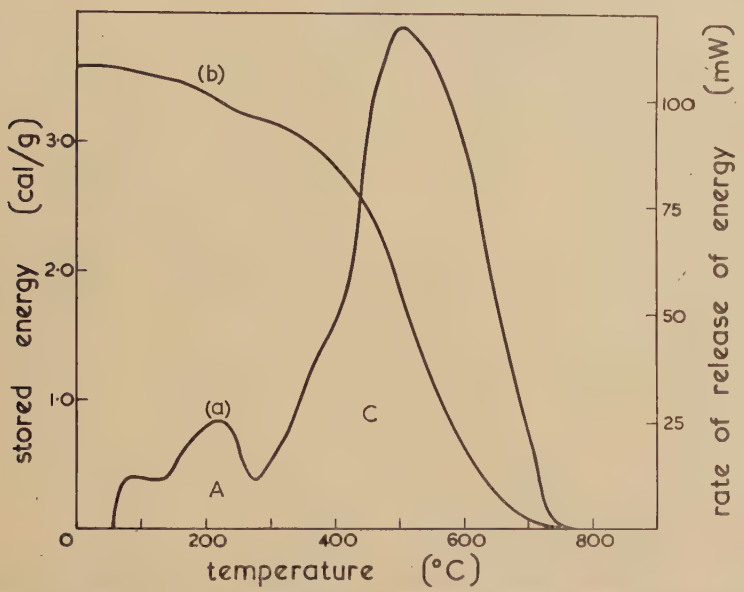

Release of energy from deformed nickel powder during annealing as a function of temperature.
(*a*) Rate of Release of energy. (*b*) Energy still stored in specimen.

The significant features of the diffraction patterns may be summarized as follows :

(1) the background intensity remained constant during annealing ;

(2) the integrated intensities of the 222 and 400 lines remained constant during annealing, while those of the 111 and 200 lines decreased by about 7% over the temperature range 400–870°c ;

(3) the tails of all diffraction lines remained practically unaltered up to 400°c, although the peak intensities of the lines increased ;

(4) from the measurements of line positions no evidence was found for stacking faults or changes in lattice parameter.

The line shapes have been analysed by various methods (Hall 1949, Warren and Averbach 1950, 1952, Williamson and Smallman 1954). In each case the broadening has been attributed partly to strain and partly to particle size effects. Values of strain and ' apparent particle size ' have been calculated as functions of temperature by each of the three methods. The results obtained by applying the Warren and Averbach method of Fourier analysis to the 111 and 222 reflections are shown in fig. 2. The

results for other reflections and other methods are qualitatively similar. Although the numerical values depend markedly on the method of analysis used, the decrease in strain without change in ' apparent particle size ' on annealing to 400°c and the further decrease in strain with an increase in ' apparent particle size ' on annealing to 870°c are obtained by all methods of analysis.

Fig. 2

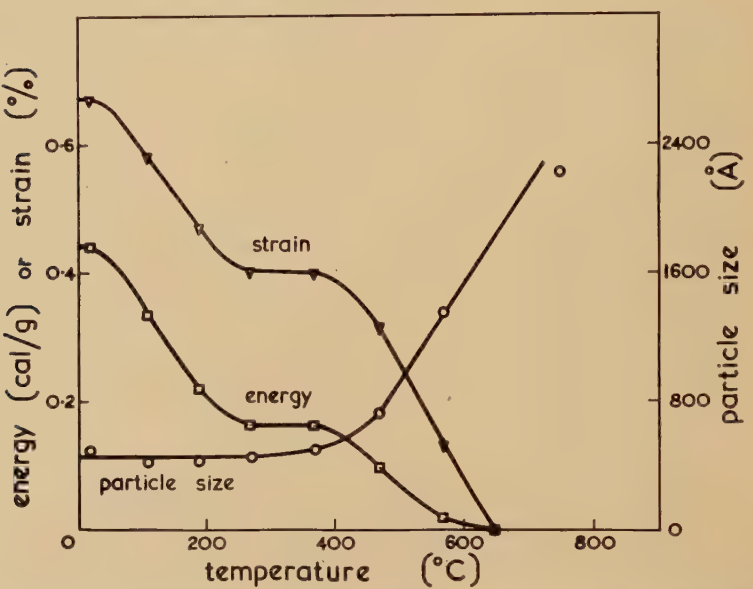

Results of the Fourier analysis of the shape of the 111 and 222 lines from deformed nickel powder.

The energies calculated from the strains derived by the three methods of analysis are all considerably lower than the measured value of stored energy of 3·6 cal/g. The values calculated using the mean strain from the Warren and Averbach analysis for the 111 and 222 reflections are indicated in fig. 2.

Gay, Hirsch and Kelly (1954) have suggested that a deformed metal consists of particles of comparatively low strain surrounded by heavily deformed regions. If the ' apparent particle size ' obtained from our analyses can be identified with the size of their particles, the decrease in lattice strain without change in ' apparent particle size ' at temperatures below 400°c is consistent with their model for recovery. In addition, the experimental observations (1) and (2) above indicate that the diffracted intensity from the heavily deformed regions goes predominantly into the tails of the lines. Thus observation (3), which is independent of the analyses, is also consistent with the Gay, Hirsch and Kelly model for recovery.

The stored energy measurements indicate that recrystallization commences at approximately 400°c. In agreement with this, as the

temperature of annealing is raised above 400°C, the intensity in the tails of the X-ray lines decreases rapidly, the calculated lattice strains decrease and the 'apparent particle sizes' increase. The decrease in integrated intensity of the 111 and 200 lines is probably due to an increase in extinction resulting from an increase in both particle size and crystal perfection.

A full account of this work will be published shortly.

References

Clarebrough, L. M., Hargreaves, M. E., Michell, D., and West, G. W., 1952, *Proc. Roy. Soc.* A, **215**, 507.

Clarebrough, L. M., Hargreaves, M. E., and West, G. W., 1955, *Proc. Roy. Soc.* A, **232**, 252; 1956, *Phil. Mag.* (in press).

Gay, P., Hirsch, P. B., and Kelly, A., 1954, *Acta Cryst.*, **7**, 41.

Hall, W. H., 1949, *Proc. Phys. Soc.* A, **62**, 741.

Warren, B. E., and Averbach, B. L., 1950, *J. Appl. Phys.*, **21**, 595; 1952, *Ibid.*, **23**, 497.

Williamson, G. K., and Smallman, R. E., 1954, *Acta Cryst.*, **7**, 574.

Wilson, J. E., and Thomassen, L., 1934, *Trans. A.S.M.*, **22**, 769.

The Spin and Magnetic Moment of ^{116*}In

By P. B. Nutter

A.S.R.E., Portsmouth, Hants.

[Received December 9, 1955]

A conventional (Davies, Nagle and Zacharias 1949) atomic-beam apparatus using magnetic resonance was employed to study the spin and magnetic moment of the ^{116}In isomer of 52 min half-life. Transitions of the $\Delta F=0$, $\Delta m=\pm 1$ type between the magnetic sub-states of the $p_{1/2}$ atomic ground state were observed in a weak magnetic field and from them the nuclear spin was found to be 5. Measurements in a stronger field indicated a hyperfine structure splitting (Goodman and Wexler 1955) of $\Delta\nu=8670\pm 170$ Mc/s and positive magnetic moment, the value of which was calculated (Fermi 1930) as $4{\cdot}21\pm 0{\cdot}08$ nuclear magnetons.

Indium metal was irradiated in the Harwell pile (BEPO); when it was placed in the oven it had a specific activity of about 2 curies/g mostly due to ^{116*}In. To detect the beam, the atoms were ionized on the surface of the usual oxidized tungsten strip and then collected alternately on two similar targets. The radio-frequency power which caused the transitions was switched on and off in a regular one minute cycle as the target potentials were changed. Measuring the ratio of the activities accumulated on the targets after runs of about 20 minutes allowed us to determine resonances and eliminate slow drifts of beam intensity and source decay. The magnetic field was monitored continuously by observing resonances due to a stable Indium isotope through measuring the ion current.

In order to compare the result with the shell model (Mayer 1950) the magnetic moments were calculated for possible configurations, assuming no configuration mixing.

The magnetic moments were calculated on the basis of j–j coupling of the odd nucleons. The value used for the magnetic moment of the $g_{9/2}$ proton in these calculations was that found in the nuclei ^{113}In and ^{115}In. Experimental values for the $s_{1/2}$, $d_{3/2}$ and $d_{5/2}$ neutrons were also available, but for the $g_{7/2}$ and $h_{11/2}$ neutrons magnetic moments were estimated assuming the intrinsic magnetic moment to be depressed, as indicated by Bloch (1951). The configurations $g_{9/2}s_{1/2}$, $g_{9/2}d_{5/2}$ and $g_{9/2}\,g_{7/2}$ are seen to give moments in reasonable agreement with experiment.

Configuration	$g_{9/2}s_{1/2}$	$g_{9/2}d_{3/2}$	$g_{9/2}d_{5/2}$	$g_{9/2}g_{7/2}$	$g_{9/2}h_{11/2}$
Calculated magnetic moment	+4·49	+5·58	+4·26	+4·30	+1·37

The author is indebted to D.S.I.R. for the provision of a maintenance award throughout the course of this work and also wishes to thank Mr. West of A.E.R.E. for his help in connection with the provision of active material for the experiment.

Further thanks are extended to Dr. K. F. Smith, Mr. R. S. Title and Mr. G. H. Rees for their assistance during the experiments and especially to the former for many previous discussions.

References

Bloch, F., 1951, *Phys. Rev.*, **83**, 839.

Davies, L., Nagle, D. E., and Zacharias, J. R., 1949, *Phys. Rev.*, **76**, 1068.

Fermi, E., 1930, *Z. Phys.*, **60**, 320.

Goodman, L. S., and Wexler, S., 1955, unpublished. The author is indebted to Drs. Goodman and Wexler for communicating the results of their experiments at Argonne before publication.

Mayer, M. G., 1950, *Phys. Rev.*, **78**, 16.

The Absorption of Sound in Liquid Helium below 1°K

By J. A. Newell† and J. Wilks
Clarendon Laboratory, Oxford

[Received March 28, 1956]

Measurements using a pulse technique are in progress to determine the absorption of sound in liquid helium as a function of pressure, and a brief summary of the results between 1·2°K and the lambda point has been given (Newell 1955 a). At temperatures below 1·2°K there is a large maximum in the absorption and the figure shows our results in this region for sound of a frequency of 14·4 Mc/s. (As the absorption depends on the density of the liquid ρ, and the frequency ν and velocity c of the sound which all vary with pressure, our results are given as the coefficient of absorption divided by the normalizing factor $2\pi^2\nu^2/\rho c^3$.) Although

† Present address : I.C.I., ' Terylene ' Council, Harrogate.

these results have the same general form as those obtained by Chase and Herlin (1954, 1955) under the vapour pressure at 12·1 Mc/s, there is the significant difference that their maximum shows two peaks whereas we observe only one. These authors remark that the presence of two peaks gives good support to a theory of the absorption due to Khalatnikov (1950, 1952) ; each being associated with one of the two relaxation times involved in the theory.

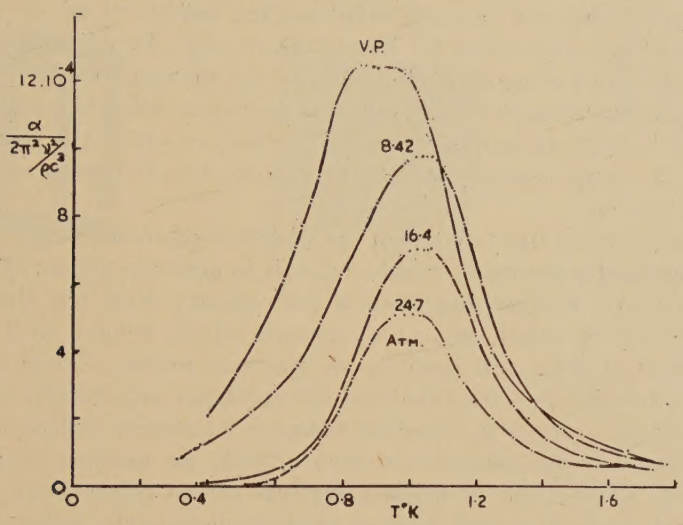

The coefficient of absorption of sound of 14·4 Mc/s in liquid helium at pressures ranging from the vapour pressure to 24·7 atmospheres. (As explained in the text, the coefficient of absorption is normalized by the factor $2\pi^2\nu^2/\rho c^3$.)

One might attempt to resolve the discrepancy between the experimental results by recalling that on Khalatnikov's theory the relaxation times vary with temperature, and therefore the position of the peaks will depend on the frequency of the sound. The two relaxation times vary with temperature at different rates, and at a certain temperature become equal in magnitude; thus if the absorption were measured at the frequency corresponding to this particular relaxation time one might expect to see only one peak. The difference between the frequency used in our experiments (14·4 Mc/s) and in those of Chase and Herlin (12·1 Mc/s) is too small to account for the observed difference in absorption, but we decided that a final elucidation of this point would have to await the conclusion of measurements now in progress (with Dr. K. Dransfeld) at a frequency of 6 Mc/s. However, a recent note (Whitney 1955) suggests that the double peak of Chase and Herlin is spurious and it therefore seems worthwhile to publish our data on this point. It is to be noted that the present results are in better accord with the theory, for while Chase and Herlin claim that the two peaks give evidence of two relaxation times, Khalatnikov's expression for the absorption does in fact lead to only one peak (Arkhipov 1954, Newell 1955 b).

Our results may be more profitably discussed when the present measurements at different frequencies are completed and we have somewhat more information on the temperature dependence of the relaxation times. However, several points appear to be well established. (1) The peak is rather wide and at temperatures below that of the maximum the absorption is much higher than the theoretical values. This may well be due to relaxation effects associated either with the first viscosity or with the scattering of phonons through small angles, neither of which processes have been fully considered by Khalatnikov. (2) As we will discuss at a later date, the variation of the height of the maximum with pressure is in quite good agreement with the theory, bearing in mind the approximate nature of some of the constants. (3) The way in which the temperature at which the peak occurs varies with pressure does not seem to correlate with the theory.

Finally we would like to confirm the observations of Whitney regarding the care needed when using quartz crystals to generate pulses of sound in liquid helium. Helium has such a low density that the damping it produces is very small, and even crystals which behave well in other liquids tend to ring and oscillate in spurious modes. Thus the pulse shape can become very irregular and the radiation pattern be so distorted that too large a decay is observed between successive reflections of the same pulse. As an example of such effects, we mention that in one experiment with a pair of aligned crystals acting respectively as transmitter and receiver, a very marked improvement of the pulse shape was obtained by inserting a diaphragm between them. Moreover, although the crystals were 16 mm in diameter, the presence of even a 4 mm diaphragm did not reduce the size of the signal.

References

Arkipov, R. G., 1954, *Dokl. Akad. Nauk. S.S.S.R.*, **98**, 747.

Chase, C. E., and Herlin, M. A., 1954, *Phys. Rev.*, **95**, 565 ; 1955, *Ibid.*, **97**, 1447.

Khalatnikov, I. M., 1950, *Z. Eksper. Teor. Fiz.*, **20**, 243 ; 1952, *Ibid.*, **23**, 21.

Newell, J. A., 1955 a, *Conference de Physiques des Basses Temperatures* (Paris : Institut International du Froid), p. 80 ; 1956 b, *Thesis*, Oxford.

Whitney, W. M., 1955, *M.I.T. Research Laboratory of Electronics, Quarterly Progress Report*, Oct. 1955, p. 21.

ERRATUM

The Creep of Cadmium Crystals at Liquid Helium Temperatures, by J. W. Glen, 1956, *Phil. Mag.*, **1**, 407.

In the table the units under the headings t_1 and t_2 should, in both cases, read (min) not (sec).

[*The Editors do not hold themselves responsible for the views expressed by their correspondents.*]